# The Role of Core binding factor beta subunit (Cbfb) in AML-ETO Transformation Activity and Haematopoietic Stem cells (HSCs)

Mobarki, Abdullah Ahmed Y

*Awarding institution:*
King's College London

# The Role of Core binding factor beta subunit (Cbfb) in AML-ETO Transformation Activity and Haematopoietic Stem cells (HSCs).

**Abdullah Ahmed Mobarki**

**A thesis submitted for the Degree of Doctor of Philosophy**

**Department of Haematological Medicine**

**School of Medicine**

**King's College London**

**2016**

# Declaration

I hereby declare that this thesis is my own work and has not been submitted to any institution for any award. Where other sources of information have been used, they have been acknowledged.

**Abdullah Mobarki**

**October/2015**

# Acknowledgement

First and foremost, eternal thanks to God on the bounties and blessings that facilitated completion of this PhD.

Then, I would like to thank my supervisor Professor Eric So and His lovely PA Erica for their help, encouragement, advices, and support throughout my PhD. Thanks Eric for believing in me and giving me this great opportunity to work with you in this scientific field.

Also, I would like to say thank you to my second supervisor professor Farzin Farzaneh, my previous postgraduate coordinator professor Nicholas Thomas and the current one Dr. Alan Ramsay for their encouragement and useful advices.

Special thanks to my daily supervisor Dr Bernd Zeisig for his help, support and patience on the face of my countless questions and also to his lovely family.

I can't forget our lab manager Miss Amanda Wilson as without her help nothing would be possible from ordering the reagents to the *in vivo* injections. Thank you very much for your help.

Many thanks indeed to my previous and current lab mates from whom I got the knowledge especially Dr. Clemence Virely (you're an angel), Mr. Winston Roy, Dr. Michael Cheung, Dr. Maria Teresa, Dr. Kar Lok Kong, Dr. Jackie, Dr. Priscilla Lau, Dr. Magdalena Zarowiecki, Dr. Lu Zhao, Dr. Tsz Kan Fung, Dr. Jayant Rane, Dr. Maria Mallardo, Miss Clear Lynn, Mr. Henry Lekgetho, Mr. Anthony Eiliazadeh and Dr. Teerapoong. Thanks guys for your help and I wish you all the best.

**Acknowledgement**

I don't know what I have to say to my father! Thanks for forcing me to continue my PhD despite your sickness. Believe me I wouldn't do it if you didn't force me and it wasn't that easy for me as my heart was and still bleeding and it will take time to recover.

I would like to say sorry to the greatest person I have ever seen (my mum). I know it wasn't that easy for you and you missed me a lot, but I promise we will spend the rest of our lives together. Thank you very much mum, sisters, brothers and friends for your love, help, support and prayers.

Special thanks to my wife (Marim) for her love, encouragement and patience throughout my studies in the UK. Sorry, I didn't find any more words to explain my thankfulness to you, so I will let my heart speaks…….

Also, I would like to say to my daughter (Taleen) you are the best stem cell result I have ever got and thanks for showing me the beauty of this life. I can't wait to meet my son (Ahmed) who was in a hurry and decided not to wait for me and came earlier than I thought.

I can't express my thankfulness to Jazan University for the financial support.

Finally, I want to say thank you to everyone who deserve to be thanked and I did not mention his/her name. God bless you all.

# Abstract

Core binding factors are heterodimeric transcription factors composed of two subunits, alpha and beta. In mammals, the alpha subunit is encoded by three genes, AML1, 2, 3 (also known as RUNX1, 2,3), whereas only one gene encodes the beta subunit CBFB. AML1 and CBFB have a pivotal role during embryonic haematopoiesis as both Aml1 and Cbfb Knock-out mice lacked definitive haematopoiesis and died at 12.5 dpc. In addition, these two genes are the most frequent targets for chromosomal translocations in leukaemia generating AML1-ETO (AE) fusion and CBFB-SMMHC fusion, respectively. Although, Cbfb enhances the binding affinity of AML1 to DNA, its role in AE-mediated transformation remains unclear. Recent studies by others and our group using Cbfb-interaction defective AE mutants in different experimental settings have yielded conflicting results (Kwok, Zeisig et al. 2009; Roudaia, Cheney et al. 2009). Definition of Cbfb requirement is important for understanding the biology of the disease and also for designing better cancer therapeutics.

Thus in my PhD project, we aim to clearly define the role of Cbfb in AE-mediated leukaemogenesis and also to investigate the effect of Cbfb deletion on the development of HSCs. To achieve the proposed aims, we used Cbfb conditional knockout mouse model (Cbfbfl/fl Rosa 26 Cre ER) where only an alternatively spliced form of Cbfb that is incapable of interacting with AE will be expressed. Our in vitro data showed that deletion of Cbfb resulted in a reduction of the 3$^{rd}$ round colonies, but does not completely impair AE-mediated transformation of the primary mouse hematopoietic cells. In addition, the Cbfb-interaction defective AE

mutant Y113A/T161A was able to transform all the sorted distinct haematopoietic cell populations including LSK stem cell-enriched populations, common myeloid progenitors (CMP) and granulocyte and myeloid progenitors (GMP). To investigate the role of Cbfb in leukaemogenesis, I employed an AML mouse model generated by expression of AML1-ETO9a (AE9a) into fetal liver cells. In contrast to MN1-mediated leukaemogenesis, Cbfb was crucial for both the leukaemia development as well as its maintenance. To study the role of Cbfb in normal haematopoiesis, we conditionally deleted Cbfb at the adult stage and analysed its impact on normal haematopoietic development. Our data showed when Cbfb was ablated in the whole animal or only in the haematopoietic system, haematopoietic stem/progenitor populations were significantly compromised. In addition, Cbfb KO cells were incapable of reconstituting secondary recipient mice. Strikingly, no haematopoietic defect was observed when Cbfb was ablated only from the microenvironment. The data showed an important function of Cbfb in maintaining normal haematopoiesis in a cell-autonomous manner. Together, these results reveal an important function of Cbfb in both normal and malignant haematopoiesis. On-going effort on RNA/ChIP-sequencing and future functional validation of candidate downstream targets will further shed light into the underlying mechanisms for the function of Cbfb, and development of novel therapeutic strategies for AE9a leukaemia and HSC transplant.

# Table of Contents

# List of figures

# List of Tables

# Abbreviations

| | |
|---|---|
| AE | AML-ETO |
| AGM | Aorta-Gonad-Mesonephros |
| AML | Acute myeloid leukaemia |
| BD | Binding Domain |
| BM | Bone marrow |
| BSU | Biological Services Unit |
| CBF | Core binding factor |
| CBFB | Core Binding Factor Beta |
| CEBPα | CCAAT/enhancer binding protein alpha |
| CFU | Colony forming unit |
| CLP | Common lymphoid progenitors |
| CML | Chronic myeloid leukaemia |
| CMP | Common myeloid progenitors |
| Cre | Cre recombinase/Causes recombination |
| DMEM | Dulbecco's Modified Eagle Medium |
| DMSO | Dimethyl sulfoxide |
| DNA | Deoxyribonucleic acid |
| dNTP | Deoxyribonucleotide triphosphates |
| EDTA | Ethylenediaminetetraacetic acid |
| ELDA | Extreme Limiting Dilution Analysis |
| ER | Estrogen receptor |
| ES | Embryonic stem |
| ETO | Eight twenty one |
| FACS | Fluorescence-activated cell sorting |
| Flt3 | FMS-related tyrosine kinase 3 |
| GAPDH | Glyceraldehyde 3-phosphate dehydrogenase |
| GFP | Green fluorescent protein |
| GM | Granulocyte macrophage |
| GM-CSF | Granulocyte-macrophage colony-stimulating factor |
| GMP | Granulocyte and myeloid progenitors |
| HA | Human influenza hemagglutinin |
| HABD | High affinity binding domain |
| HE | Hematoxylin and eosin |
| HGB | Haemoglobin |
| HPC-1 | Haematopoietic progenitor cell-1 |
| HPC-2 | Haematopoietic progenitor cell-2 |

| | |
|---|---|
| HR | Hit and Run |
| HSC | Haematopoietic stem cells |
| IP | Immunoprecipitation |
| LDA | Limiting dilution assays |
| LMPP | Lymphoid-primed multi-potent progenitors |
| LSC | Leukaemia stem cells |
| LSK | Lin-Sca1+Kit+ |
| M-CSF | Macrophage colony stimulating factor |
| MEP | Megakaryocyte/erythroid progenitor |
| MFI | Mean fluorescence intensity |
| MLL | Mixed lineage leukaemia |
| MN1 | Meningioma1 |
| MPP | Multipotent progenitor |
| MSCV | Murine stem cell virus |
| MTA | Methylcellulose transformation assay |
| NHR | Nervy homology regions |
| NMTS | Nuclear matrix targeting signal |
| NOD | Non-obese diabetic |
| NRAS | Neuroblastoma RAS viral oncogene homolog |
| PAS | Para-aortic splanchnopleura |
| PB | Peripheral blood |
| PBS | Phosphate buffer saline |
| PCR | Polymerase chain reaction |
| PI | Propidium iodine |
| PLT | Platelet |
| qRT-PCR | Quantitative reverse transcriptase polymerase chain reaction |
| RBC | Red blood cells |
| RHD | Runt homology domain |
| RNA | Ribonucleic acid |
| RPMI | Roswell park memorial institute |
| RT | Reverse transcriptase |
| RTTA | Retroviral transduction and transformation assay |
| RUNX | Runt-related transcription factor |
| SCF | Stem cell factor |
| SCID | Severe combined immunodeficiency |
| SCL | Stem-cell leukaemia |
| shRNA | Small hairpin RNA/short hairpin RNA |
| SLAM | Signalling lymphocytic activation molecule |
| SM | Suspension medium |
| SP | Single positive |

| | |
|---|---|
| TAM | Tamoxifen |
| VSV-G | Vesicular stomatitis virus glycoprotein epitope |
| WB | Western blot |
| WBC | White blood cell |
| WT | Wild type |
| YFP | Yellow fluorescent protein |

# 1 Introduction

## 1.1 Haematopoiesis

Stem cells are distinguished from other cells in having the unique ability to maintain long-term self-renewal, and also to differentiate into multiple cell types (Metcalf 2007). These cells can be broadly classified into two main categories: embryonic stem cell, and adult or tissue specific stem cells. Establishment and maintenance of the haematopoietic system relies on adult stem cells called haematopoietic stem cells (HSCs). In fact, the haematopoietic system is probably one of the most highly regenerative tissues as around $10^{12}$ cells are generated daily in the adult human bone marrow (BM). Despite the complexity of haematopoiesis, it is considered as one of the best understood developmental system. In 1909, Alexander Maximow postulated that blood is organized as a cellular hierarchy with a single cells at its apex looking like a lymphocyte (Doulatov, Notta et al. 2012). Four decades later, this hypothesis was proven by an functional rescue experiment where the haematopoietic system was completely reconstituted in irradiated mice by transplantation of cells isolated from healthy donors (Lorenz, Uphoff et al. 1951). However, this experiment did not distinguish if the haematopoiesis is arising from a single stem cell or from different lineage specific stem cells. Till and colleagues were able to demonstrate the clonal nature of spleen colonies that derived from transplanted mouse BM. The data showed that when a single colony carries a recognizable chromosomal marker, majority of the cells carry the same marker suggesting the existence of multipotent HSCs (Till and Mc 1961; Becker, Mc et al. 1963). In general, the production of blood can be divided into two main stages:

embryonic and adult haematopoiesis in which different embryonic and adult organs play crucial roles to maintain and regulate this process.

### 1.1.1 Embryonic haematopoiesis

In mammals, the initial wave of blood cell production takes place in the yolk sac, which generates transitory haematopoietic cells such as primitive erythrocytes and some myeloid cells. This type of blood formation is called primitive haematopoiesis and its main function is to facilitate tissue oxygenation of the growing embryo (Orkin and Zon 2008; Medvinsky, Rybtsov et al. 2011). During mouse embryonic development, primitive haematopoiesis occurs between day E7 and E7.5 in the yolk sac, and by day E9.5 Aorta-Gonad-Mesonephros (AGM) has higher numbers of CFU-S than the yolk sac (Medvinsky, Samoylina et al. 1993). Although by E8 the heart starts beating, massive movement of the yolk sac erythroid cells into the embryo's body is observed only at E10 due to lack of a complete development of primitive vascular system (McGrath, Koniski et al. 2003). The second wave of blood formation is called definitive haematopoiesis, in which definitive haematopoietic stem cells (dHSCs) give rise to all mature blood cells (Medvinsky, Rybtsov et al. 2011). At day E10.5, HSCs isolated from AGM possessed long-term reconstitution ability into irradiated adult mice (Medvinsky and Dzierzak 1996). Approximately one dHSC was isolated from the 11.5 AGM, placenta and yolk sac, and by E12 the total number of mouse dHSCs was increased dramatically and around 80% was found in the fetal liver (Kumaravelu, Hook et al. 2002; Gekas, Dieterlen-Lievre et al. 2005)(figure1.1).

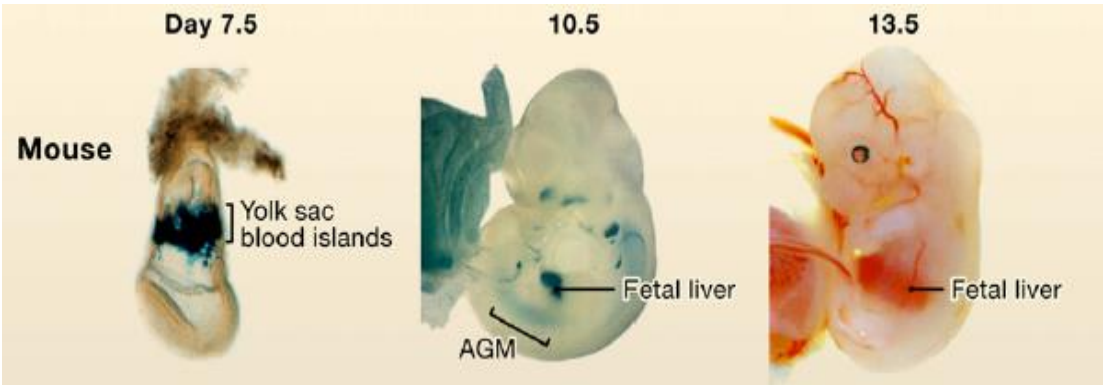


Figure 1-1 The main sites of mouse embryonic haematopoiesis.

The figure was adopted from Orkin et al. (Orkin and Zon 2008) and illustrates the main sites of mouse embryonic haematopoiesis. Yolk sac blood islands are visualized by LacZ staining of transgenic embryo expression *GATA-1*- driven *LacZ*. AGM and fetal liver are stained by LacZ in *Runx1-LacZ* knockin mice.

### 1.1.2 Adult Haematopoiesis

In adult, BM represents the main site of haematopoiesis and provides the proper environment for the maintenance and differentiation of HSCs. However, some blood cells are maturated at sites other than BM such as T and B cells at the thymus and spleen, respectively. Today, cell surface antibodies and multicolour flow cytometry analysis have shown that haematopoiesis is a developmental hierarchy system with HSC at the top and differentiated cells on the bottom. The Weissman model proposes that long term HSCs (LT-HSC) are at the top of the hierarchy, which possess life-long self-renewal as well as multi-lineage differentiation potential. These cells are phenotypically defined as $LIN^{-}IL\text{-}7R\alpha^{-}$ $SCA1^{+}KIT^{+}FLT3^{-}Thy1^{low}CD34^{-}$ and are present at a low frequency in the BM (figure 1.2 A) (Osawa, Hanada et al. 1996; Adolfsson, Borge et al. 2001; Weissman, Anderson et al. 2001). LT-HSCs give rise to limited self-renewal cells called short-term HSCs ($LIN^{-}IL\text{-}7R\alpha^{-}$ $SCA1^{+}KIT^{+}FLT3^{low}Thy1^{low}CD34^{+}$) (Morrison, Uchida et al.

1995; Christensen and Weissman 2001). Multipotent progenitors (MPP: $LIN^{-}IL^{-}7R\alpha^{-}SCA1^{+}KIT^{+}FLT3^{low-hi}Thy1^{-}CD34^{+}$) represent the next distinct populations, which are able to differentiate into all blood cell lineages. Signalling lymphocytic activation molecule (SLAM) family markers were also used to enhance the purification of mouse HSCs. Within the LSK ($LIN^{-}SCA1^{+}KIT^{+}$) population, LT-HSCs were highly purified as $CD150^{+}CD48^{-}$ cells while MPPs were $CD150^{-}CD48^{-}$ (Forsberg, Prohaska et al. 2005; Kiel, Yilmaz et al. 2005; Kiel, Yilmaz et al. 2008; Oguro, Ding et al. 2013). Recently, it has been shown that the LSK populations can be subdivided into four fractions according to their CD150 and CD48 expressions: HSC ($CD150^{+}CD48^{-}$), MPP ($CD150^{-}CD48^{-}$), haematopoietic progenitor cell-1 (HPC-1) ($CD150^{-}CD48^{+}$) and haematopoietic progenitor cell-2 (HPC-2) ($CD150^{+}CD48^{+}$) (Oguro, Ding et al. 2013). Common lymphoid progenitors (CLP: $LIN^{-}IL\text{-}7R\alpha^{+}SCA1^{lo}KIT^{lo}$) are considered as the first lymphoid progenitor that lost all myeloid differentiation potential and have the capability to form all the lymphoid cells (Kondo, Weissman et al. 1997). The Weissman model also proposes that all myeloid and erythroid cells arise from a group of progenitors called common myeloid progenitors (CMP: $LIN^{-}SCA1^{-}KIT^{+}CD34^{+}FcγRIIFcγRIII^{lo}$). CMPs differentiate into more specified progenitors such as megakaryocyte/erythroid progenitor (MEP: $LIN^{-}SCA1^{-}KIT^{+}CD34^{-}FcγRIIFcγRIII^{lo}$) and granulocyte/monocyte progenitor (GMP: $LIN^{-}SCA1^{-}KIT^{+}CD34^{+}FcγRIIFcγRIII^{hi}$)(Akashi, Traver et al. 2000). However, this view has been challenged by Jacobsen and colleagues who proposed that MEP can also be a direct progeny of ST-HSC which lacks FLT3 expression and do not go through CMP stage. In addition, their model demonstrated that MEPs are separated from lymphoid-primed multi-potent progenitors (LMPPs), which represent the shared precursors of

both lymphoid and myeloid lineages (figure 1.2 B)(Adolfsson, Mansson et al. 2005; Yang, Bryder et al. 2005).

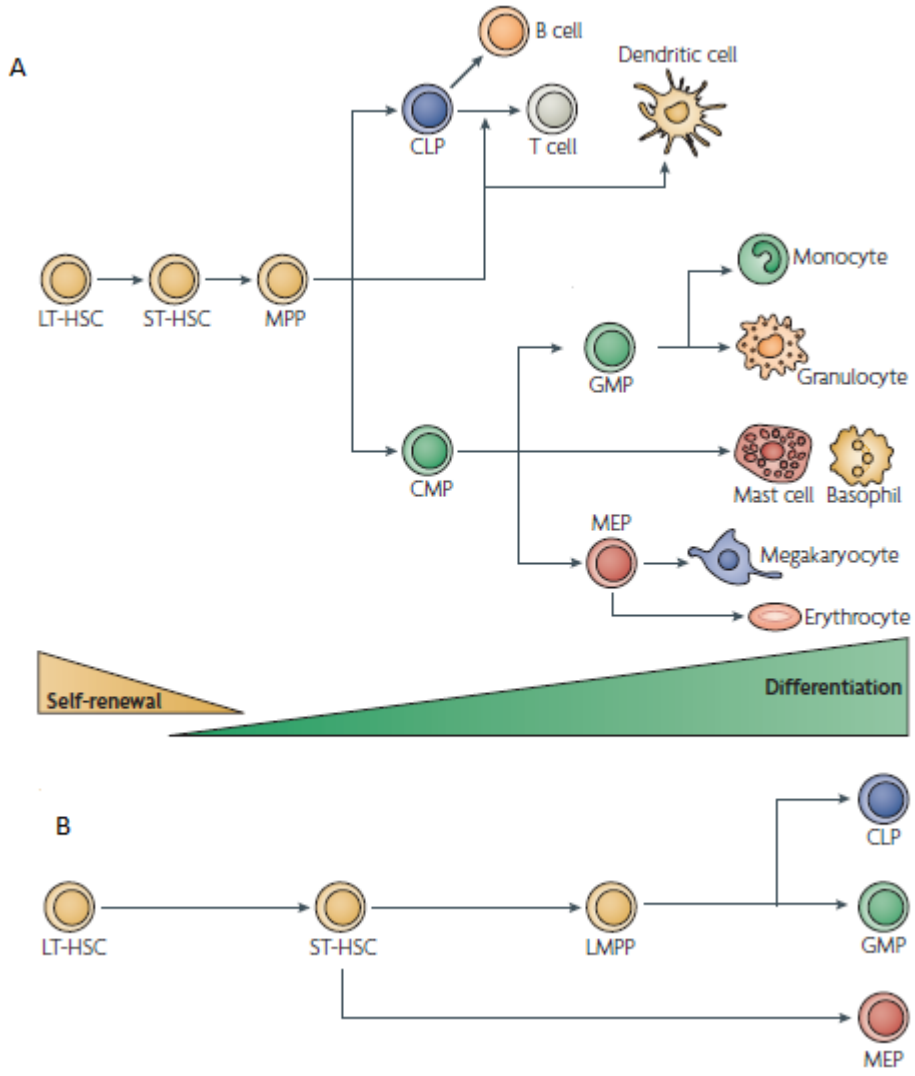


Figure 1-2 The current concept of adult haematopoiesis

The figure adopted from Rosenbauer et al. (Rosenbauer and Tenen 2007) and Illustrates the current concept of adult haematopoiesis. (A): A diagram represents the model established by the Weissman's group. LT-HSC: Long term haematopoietic stem cell; ST-HSC: short term haematopoietic stem cells; MPP: multipotent progenitor; CLP: common lymphoid progenitor; CMP: common myeloid progenitor; GMP: granulocyte/monocyte progenitor; MEP: megakaryocyte/erythroid progenitor. (B) A diagram represents the revised model by the Jacobsen's group. LMPP: lymphoid-primed multipotent progenitor.

### 1.1.3 Transcription Factors in Haematopoietic Development

Transcription factors have been defined as proteins that are able to bind to specific DNA sequences of a gene and regulate its transcription either positively or negatively (Latchman 1997). Several transcription factors have been found to play crucial roles during embryonic and adult haematopoiesis. For instance, generation of fetal liver HSC from the mesoderm requires stem-cell leukaemia factor (SCL) and runt-related transcription factor1 (RUNX1/AML1) (Shivdasani, Mayer et al. 1995; Okuda, van Deursen et al. 1996). However, a much milder impact on maintenance and self-renewal of adult HSCs was observed when SCL was conditionally inactivated in these cells suggesting that some transcription factors which are essential during embryonic haematopoiesis may be not required at the adult stage (Mikkola, Klintman et al. 2003). Furthermore, the formation of myeloid cells is maintained by different transcription factors such as PU1, growth-factor independent 1 (GFI1), CCAAT/enhancer binding protein-α (C/EBPα) and interferon-regulatory factor 8 (IRF8)(figure 1.3) (Holtschke, Lohler et al. 1996; Yamanaka, Barlow et al. 1997; Hock, Hamblen et al. 2003; Dakic, Metcalf et al. 2005). Whereas PU1 expression is essential for CMP formation, it seems that C/EBPα is totally dispensable as mice deficient for this gene have normal number of CMPs but lacked GMPs and all subsequent lineages (Zhang, Zhang et al. 1997). In zebrafish, myeloid and erythroid/megakaryocytic/eosinophil differentiations have been found to be promoted by PU1 and GATA1, respectively. The two proteins are physically interacting and affect each other's function as inhibition of GATA1 expression resulted in haematopoietic shift to the myeloid fate, whereas the opposite affect

was observed upon inhibition of PU1 (Galloway, Wingert et al. 2005; Rhodes, Hagen et al. 2005).

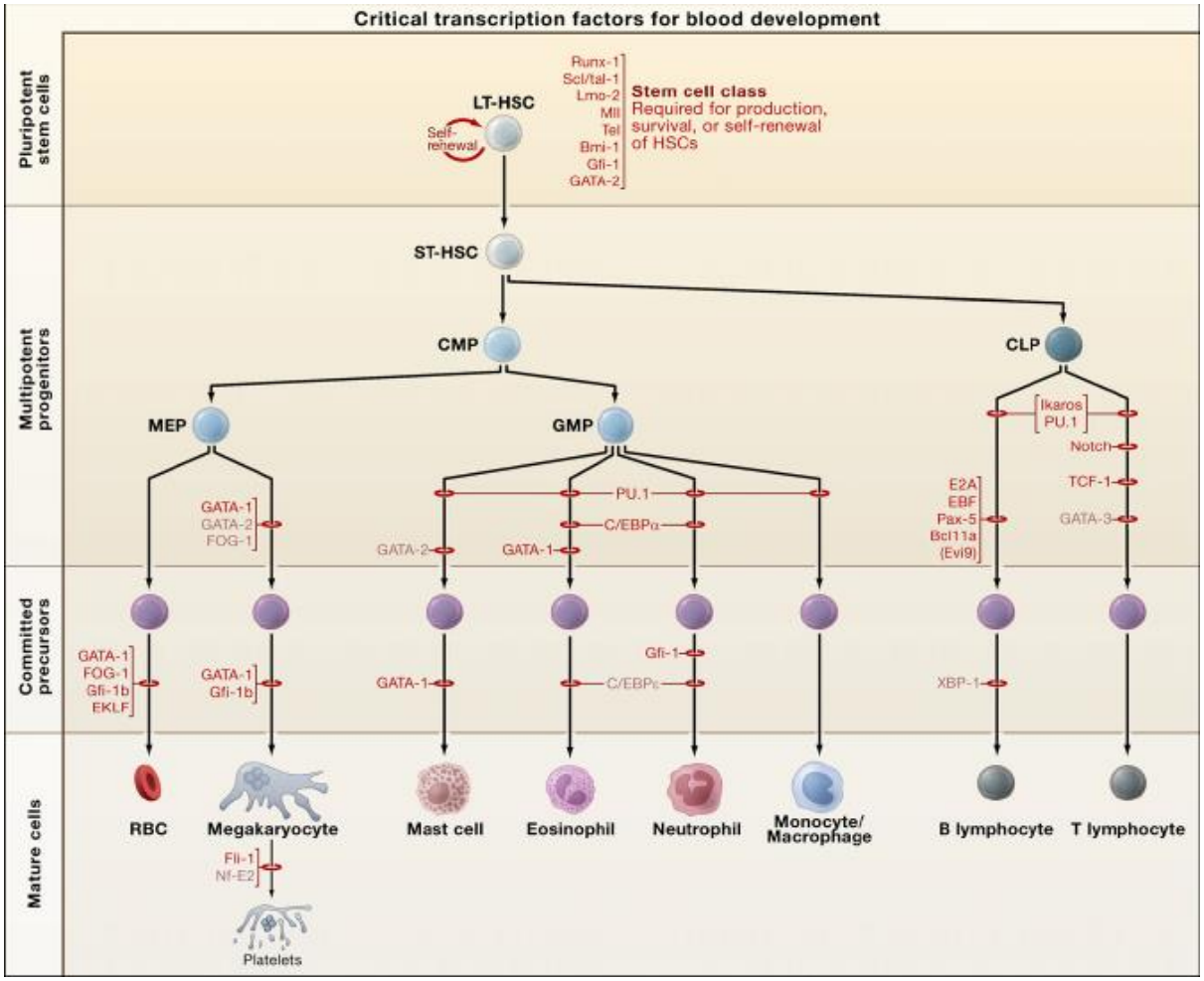


Figure 1-3 The requirement of some transcription factors during haematopoiesis.

The figure adopted from Orkin et al (Orkin and Zon 2008)and illustrates the requirement of some transcription factors during haematopoiesis.

## 1.2 Core binding factor

Core binding factor (CBF) is a heterodimeric transcription factor complex composed of two subunits, alpha and beta. In mammals, the alpha subunit is encoded by three genes, AML1, 2, 3, which are also known as RUNX1, 2, 3, whereas only one gene encodes the beta subunit CBFB. The alpha subunit represents the DNA binding element of the complex and its binding affinity is significantly increased in the presence of the beta subunit (Hart and Foroni 2002; de Bruijn and Speck 2004; Link, Chou et al. 2010). This complex performs a crucial role during haematopoiesis through regulation of different haematopoietic target genes such as granulocyte-macrophage colony stimulating factor (GM-CSF) (Takahashi, Satake et al. 1995), interleukin 3 (IL-3)(Shoemaker, Hromas et al. 1990), colony stimulating factor 1 (CSF1/M-CSF)(Zhang, Fujioka et al. 1994) and T-cell antigen receptors (TCRs)(Redondo, Pfohl et al. 1992). Moreover, knock-out studies have shown that both AML1 and CBFβ are essential for definitive haematopoiesis and mice lacking these genes died at E12.5 with nearly identical phenotypes suggesting that both subunits are required and collaborate to maintain a common function at least during fetal haematopoiesis (Sasaki, Yagi et al. 1996; Wang, Stacy et al. 1996; Wang, Stacy et al. 1996). Furthermore, the two genes are among the most frequent targets of chromosomal translocations in leukaemia such as t(8;21), t(12;21), Inv(16)(p13;q22) and t(16;16)(p13;q22).

### 1.2.1 CBF alpha and beta subunits

#### *1.2.1.1 AML1 (RUNX1)*

Acute myeloid leukaemia 1 (AML1), also known as CBF alpha2, Polyomavirus enhancer binding protein 2 alpha (PEBP2alphaB) and runt-related transcription factor 1 (RUNX1), was first cloned using DNA isolated from a t(8;21) leukemic patient (Miyoshi, Shimizu et al. 1991). In human, the RUNX1 gene is located on chromosome 21 and can be transcribed from two alternatives promoters (distal (P1) and proximal (P2)). Consequently, different isoforms of RUNX1 can be synthesized by alternative splicing (figure 1.4)(Blyth, Cameron et al. 2005; Lam and Zhang 2012). In general, there are three main protein isoforms of RUNX1, (RUNX1a, RUNX1b, and RUNX1c) which are all characterized by the presence of 128 amino acids runt homology domain (RHD) at their N-terminal region. This domain is responsible for both DNA binding and heterodimer formation with the beta subunit. In addition, this domain interacts with several proteins such as ETS family, C/EBP alpha GATA1 and SMAD3 (figure 1.5). RUNX1 contains 31 amino acids at the C- terminal end called a nuclear matrix targeting signal (NMTS), which is responsible for transcriptional activation. On the other hand, a VWRPY motif at the C-terminus mediates its Groucho/TLE-dependent transcriptional repressor activity (figure 1.5). Messenger RNAs (mRNAs) from both RUNX1a and RUNX1b are transcribed from the proximal (P2) promoter encoding for 250 and 453 amino acids proteins, respectively. Although, they are transcribed from the same promoter, their c-terminal regions are different in which the transactivation domain is missing in the RUNX1a protein. RUNX1c represents the longest isoform as its transcript is transcribed from the distal (P1) promoter (figure 1.4).

Interestingly, various RUNX1 isoforms seem to play specific roles during haematopoiesis based on the site of transcription. For instance, knock-in studies using reporter genes for P2 (hCD4) and P1 (GFP) promoters in embryonic stem cell (ES) have shown that P2 promoter may play a crucial role for initiation of definitive haematopoiesis from hemogenic endothelium while the P1 promoter might be active in more mature progenitor cells. Moreover, Runx1 P1 null mice, in which sequences for P1 promoter and exon1 were replaced with $neo^r$ cassette, were born alive with reduction in PB white blood and platelet cells, whereas offspring with severe reduction in P2 activity died shortly after birth (Sroczynska, Lancrin et al. 2009; Bee, Swiers et al. 2010). Furthermore, RUNX1a was found abundantly expressed in CD34+ progenitors in human cord blood and over expression of this isoform using retroviral approach into mouse primitive haematopoietic cells has potentiated their engraftment ability (Tsuzuki, Hong et al. 2007). However, another study showed that RUNX1 over-expressed murine bone morrow mononuclear cells were able to induce lymphoblastic leukaemia into lethally irradiated mice (Liu, Zhang et al. 2009), suggesting that elevated RUNX1 increases engraftment abilities and may lead to haematopoietic malignancies.

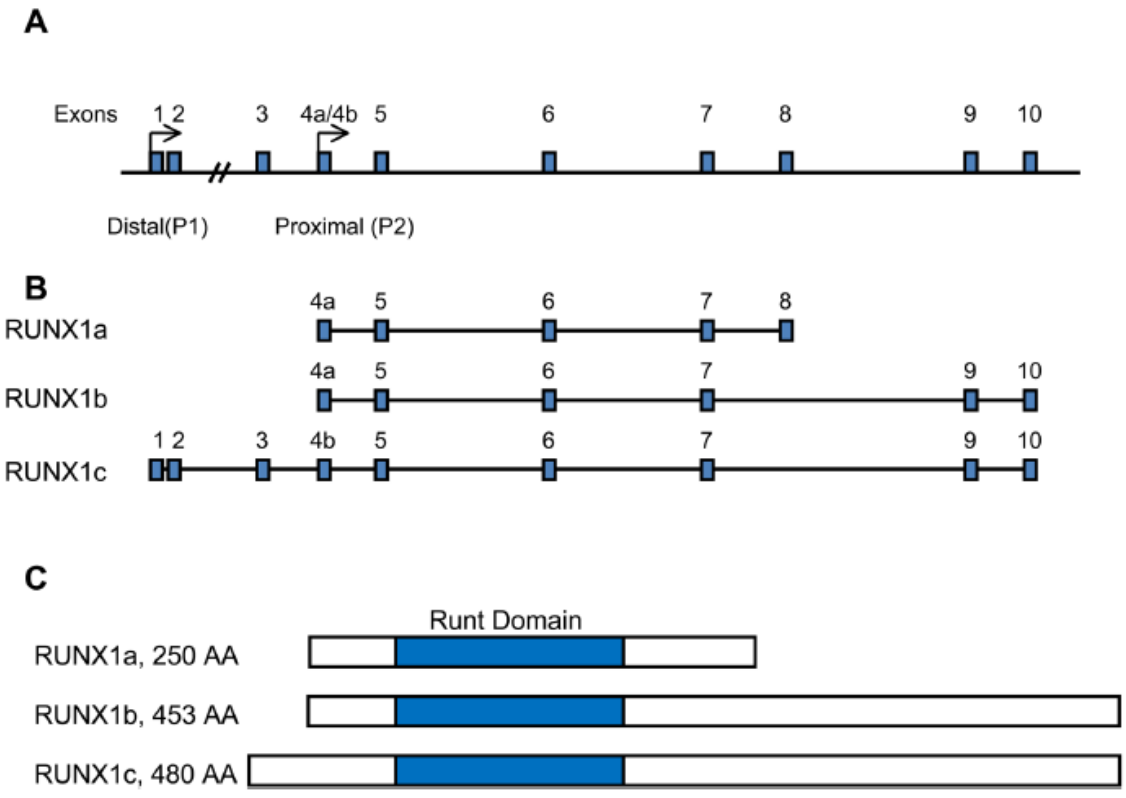


Figure 1-4 The RUNX1 (AML1) isoforms

The figure adopted from Lam et al (Lam and Zhang 2012) and shows RUNX1 isoforms. (A) The genomic locus of RUNX1 on chromosome 21 with the location of the proximal and distal promotors. (B) The three main transcriptional isoforms of RUNX1. (C) The three main proteins of RUNX1.

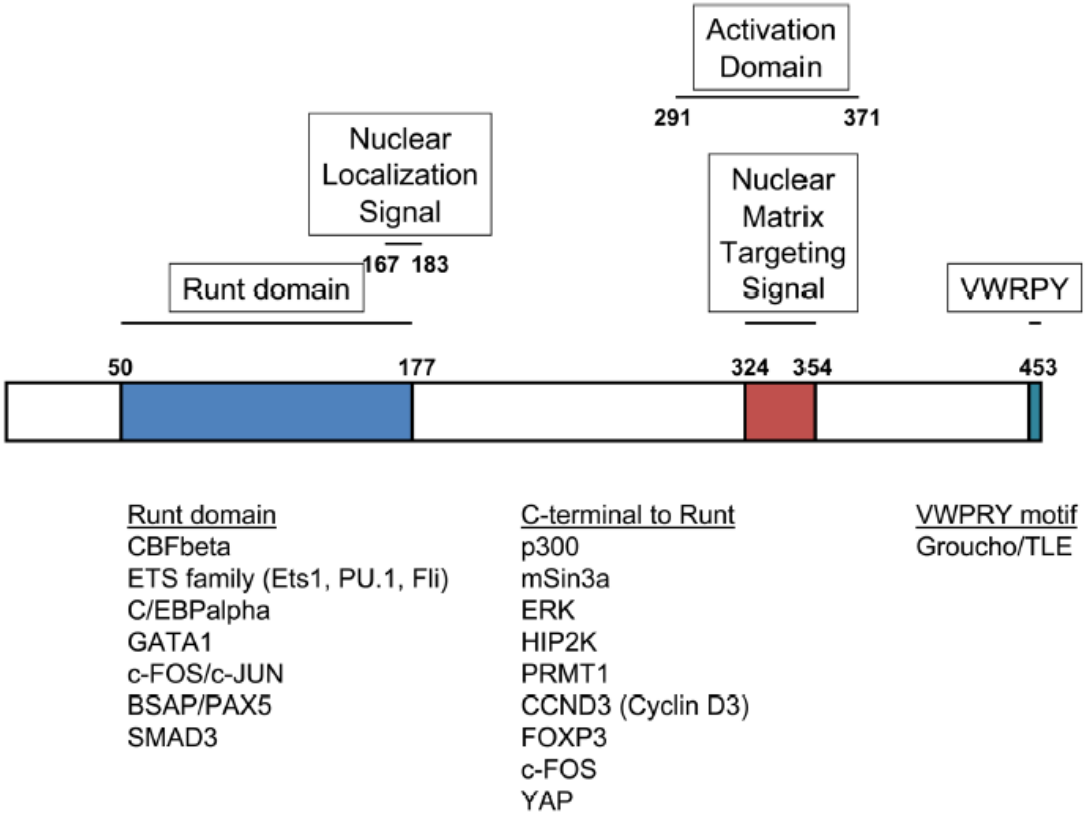


Figure 1-5 The RUNX1 (AML1b) domains

The figure adopted from Lam et al (Lam and Zhang 2012) and shows RUNX1 domains in AML1b and their interaction partners.

### *1.2.1.2 CBFB*

Core Binding Factor Beta subunit (CBFB), also known as Polyomavirus Enhancer-Binding Protein 2 Beta Subunit (PEBP2B), is the beta subunit of the core binding factor heterodimeric complex. This complex regulates several genes specific to haematopoiesis (RUNX1) and osteogenesis (RUNX2). Although, the beta subunit is a non-DNA binding regulatory element, it enhances the affinity of Runt domain for DNA binding (Tang, Crute et al. 2000; Yan, Liu et al. 2004; Li, Lukasik et al. 2006). In human, CBFB gene is located on chromosome 16 and two mRNA variants differed in their carboxyl terminus are generated by alternative splicing. Two proteins isoforms, one and two, of CBFB were detected in human encoding 187 and 182 amino acids, respectively. The two proteins contain the alpha subunit heterodimerization domain which spans exons one, two, three, four and three amino acids from exon five (1-135 amino acids, figure 1.6), however the functional difference between these two isoforms remains unclear. In murine, there are four isoforms of Cbfb that encode proteins, CBFβ (p22) and CBFβ (P21.5) that containing 187 and 182 amino acids, respectively. These two proteins were able to heterodimerize efficiently with the alpha subunit (CBFα) *in vitro* (Ogawa, Inuzuka et al. 1993; Wang, Wang et al. 1993; Miller, Stacy et al. 2001). The third isoform is CBFβ (p18) that lacks amino acids encoded in exon 5 resulting in a truncated protein (155 amino acids). The fourth isoform is CBFβ (p17.6) that lacks amino acid encoded in exon 3 and fails to bind with CBFα (Wang, Wang et al. 1993; Kagoshima, Akamatsu et al. 1996). Although CBFβ on its own does not bind to the DNA, the interaction between CBFβ and the runt domain of the AML protein stabilizes the association of this complex (Kim, Sieweke et al. 1999). Moreover, the N-terminal 141 amino-acid fragment of CBFβ protein was able to

rescue definitive haematopoiesis in CBFβ-deficient embryonic stem cells suggesting the importance of the heterodimerization domain for the in vivo function(Miller, Stacy et al. 2001).

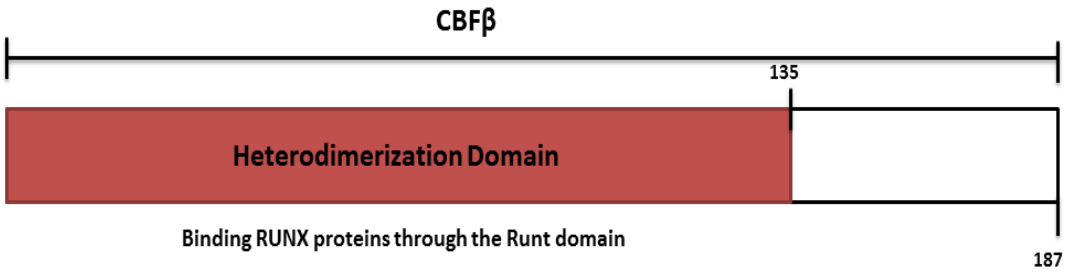


Figure 1-6 A diagram showing the heterodimerization domain of CBFβ protein

The figure shows the structure of CBFβ protein and its heterodimerization domain which is essential for binding of RUNX proteins through their Runt domains.

### 1.2.2 Expression Patterns of CBF

Runx1 was found to be expressed at different sites and cells during embryogenesis and adult haematopoiesis. North *et al* (North, Gu et al. 1999) showed that Runx1 expression was detected in the endothelial cells of different embryonic haematopoietic sites such as the yolk sac, the para-aortic splanchnopleura (PAS), the aorta-gonad mesonephros (AGM), and the vitelline and umbilical arteries. All the bone morrow haematopoietic stem and progenitors cells including the long term repopulating HSCs, colony forming units-spleen (CFU-S) and most of colony forming unit- cultures (CFU-Cs) express Runx1. Although, dendritic cells and mature macrophages expressed Runx1, this expression was rapidly declined in terminal differentiated cells such as erythrocytes and granulocytes (Basecke, Feuring-Buske et al. 2002; Lorsbach, Moore et al. 2004; North, Stacy et al. 2004). In T-cell development, most of cells in the double negatives stages (DN1 ($CD44^+CD25^-$), DN2 ($CD44^+CD25^+$), DN3 ($CD44^-CD25^+$)) expressed Runx1 protein whereas cells at the DN4 ($CD44^-CD25^-$) stage showed a reduced expression level. Both double positive (DP) (CD4/CD8) cells and single positive (SP) cells expressed Runx1 mRNA as well as the protein. The $B220^+$ bone morrow cells differentially expressed Runx1 based on their maturation status as the highest percentage of Runx1+ cells was found in the pre-pro-B-cell population whereas the lowest percentage was in the pre-B-cell population (Basecke, Feuring-Buske et al. 2002; Lorsbach, Moore et al. 2004; North, Stacy et al. 2004).

Kundu and colleagues were able to study the expression of Cbfb at the single-cell level using a knock-in approach in which Cbfb coding sequences are fused

to those of GFP (Kundu, Chen et al. 2002). Cbfb was expressed in all of the major embryonic sites of haematopoiesis (yolk sac, liver, AGM) as well as the adult one (BM, lymph node, spleen, thymus). In addition, Cbfb was detected in $Lin^-$ $c\text{-}kit^+$ bone morrow population, which is enriched for haematopoietic stem and progenitor cells as well as in CFU-Cs, megakaryocytes, monocytes and granulocytes. Similarly to Runx1, Cbfb expression rapidly declines in the definitive erythroid as the $Ter119^+$ cells show no expression. All T-cell populations were found to express a uniform level of Cbfb. In B-cell development, the highest level of Cbfb was found similarly to Runx1 in pre-pro-B cells while the pre-B cells showed low expression (Kundu, Chen et al. 2002; Taniuchi, Osato et al. 2002).

### 1.2.3 Structure and Interaction

The interaction between Runx1 and CBFβ is considered as a pivotal step for their normal functions as well as for their roles in haematopoiesis. Warren and his group gained important insight into this interaction by co-expressing human protein fragments of RUNX1 (residues 50-183) and CBFβ (residues 2-135) in E. coli. The overall structure showed that the runt domain of RUNX1 forms 12 stranded β barrels, whereas the CBFβ subunit was composed of both α/β structures (Warren, Bravo et al. 2000). The α/β structures of CBFβ are consisting of six-stranded β-sheets packed on one another surrounded by four peripheral α-helices (Huang, Peng et al. 1999; Warren, Bravo et al. 2000; Zhang, Lukasik et al. 2003) (figure 1.7). Moreover, the complex was arranged as six runt domains with four CBFβ subunits as two dimers of runt domain-CBFβ heterodimers and a homo-dimer runt domain. In addition to the DNA binding enhancement of the runt domain upon the

interaction, CBFb was found to be fundamental for protecting RUNX1 from ubiquitin-proteasome degradation (Huang, Shigesada et al. 2001).

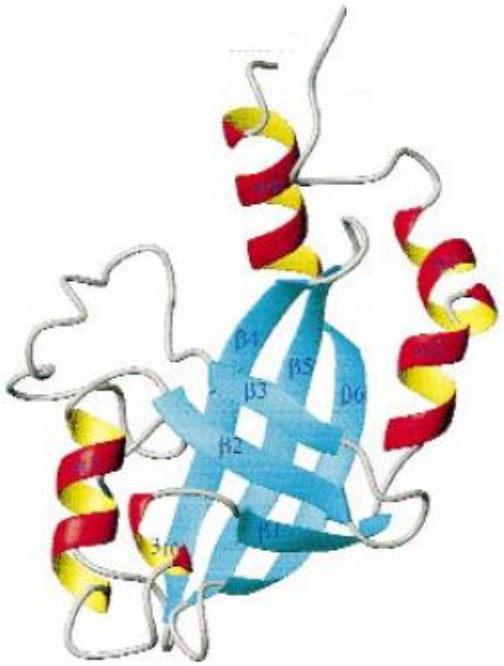

Figure 1-7 A diagram showing the α-helices and β-strands of CBFβ protein

The figure adopted from Huang et al (Huang, Peng et al. 1999) shows a ribbon representation of CBFβ (141). Red and yellow colours represent the α-helices whereas the β-strands are illustrated by cyan.

### 1.2.4 Role of CBF in Haematopoiesis

#### *1.2.4.1 Embryonic Haematopoiesis*

Three studies by Wang et al 1996, Sasaki et al 1996, and Niki et al 1997 (Sasaki, Yagi et al. 1996; Wang, Stacy et al. 1996; Niki, Okada et al. 1997) were carried out to investigate the role of Cbfb in embryogenesis and also to study its impact on haematopoiesis. In spite of the failing attempt to disrupt exons 4 and 5 of the Cbfb gene in Wang's study, they were able to create a hypomorphic Cbfb allele by replacing the 5' half of exon 5 with $neo^r$ gene. Similar strategy was considered in Sasaki's work in which they were able to replace exon 5 with a $neo^r$ gene. Mice heterozygous for this mutation were inbred and their progeny were analysed. Cbfb homozygous mutant embryos were able to express only a truncated protein which was weakly associated with the alpha subunit. Live offspring homozygous for this mutation were not obtained and all embryos died at E12.5 due to haemorrhage in the central nervous system and impairment in the fetal liver haematopoiesis. Niki and his colleagues were able to disrupt the Cbfb gene through replacing the first exon with $neo^r$ gene, and as a result neither transcripts nor proteins of Cbfb gene were synthesised. All the data demonstrated that fetal liver haematopoiesis was severely disrupted and this finding was confirmed by liver sections stain, methylcellulose colony forming assay and RT-PCR. Liver sections from E12.5 WT and heterozygous Cbfb mutated embryos showed abundance of haematopoietic progenitors, nucleated and non-nucleated erythrocyte inside the sinusoidal cavities. In contrast, the homozygous mutated Cbfb embryos contained very few erythroid and myeloid progenitors and lack mature erythrocytes. Moreover, in contrast to WT Cbfb controls, no differentiation of definitive erythroid, myeloid and mix colonies

from cells isolated from yolk sacs and livers of the homozygous mutated Cbfb embryos could be observed. Furthermore, RT-PCR data showed yolk sac cells isolated from the mutated embryos lacked expression of key genes, which are essential for definitive haematopoiesis such as c-myb, gata2 and flt3. The results of these three studies are very similar to the Runx1 knock out data (Okuda, van Deursen et al. 1996; Wang, Stacy et al. 1996; Okada, Watanabe et al. 1998) suggesting that the full length Cbfb transcript may perform a crucial function, which is missing in the truncated protein.

#### *1.2.4.2 Adult Haematopoiesis*

In contrast to the crucial role of Runx1 during embryogenesis, several studies have demonstrated that Runx1 was not essential for adult haematopoiesis as the conditionally deleted Runx1 mice were viable (Ichikawa, Asai et al. 2004; Growney, Shigematsu et al. 2005; Motoda, Osato et al. 2007; Ichikawa, Goyama et al. 2008; Schindler, Van Buren et al. 2009; Jacob, Osato et al. 2010; Cai, Gaudet et al. 2011). However, there were a number of haematopoietic abnormalities which were observed during analysis of the Runx1 deficient mice. For instance, the numbers of LSK cells were elevated in the bone morrow of Runx1 deleted Mx1-cre mice. Moreover, these mice had defects in B cell development as there was around 20% reduction in the percentage of mature B cells (CD19+ B220+) with severe reduction in pre-B and pro-B cells. T-cell development was also affected upon deletion of Runx1 by three fold reduction in DN3, DN4 and around 40% reduction in the percentage of DP cells(Ichikawa, Asai et al. 2004). Although, the number of *in vitro* CFU-Meg was elevated, the deleted mice showed severe impairment of

platelet production and megakaryocyte differentiation, suggesting the requirement of Runx1 for megakaryocyte maturation (Ichikawa, Asai et al. 2004; Growney, Shigematsu et al. 2005). It seems Runx1 is not critical for the terminal maturation of granulocyte and monocyte as mice lacked its expression had morphologically normal mature myeloid cells. Interestingly, Runx1 deficient mice had a mild myeloid expansion in their haematopoietic tissues in addition to a myeloproliferative phenotype, which is consistent with the identification of RUNX1 mutations in human myeloid malignancies (Bejar, Stevenson et al. 2011). Histological examinations of both spleen and liver of the Runx1 deleted mice showed extramedullary haematopoiesis, however spontaneous leukaemia was not observed in these mice (Growney, Shigematsu et al. 2005).

The role of Runx1 in HSC function is not clear as different groups have reported opposing effects of Runx1 deletion on the numbers of LT-HSC (Ichikawa, Goyama et al. 2008; Schindler, Van Buren et al. 2009; Cai, Gaudet et al. 2011). Using the Hoechst 33342 side population gating strategy, Ichikawa et al showed that the Runx1 deficient bone morrow had more quiescent HSCs and concluded their study by demonstrating the negative impact of Runx1 on quiescent HSCs (Ichikawa, Goyama et al. 2008). On the other hand, Schindler et al used SLAM markers to analyse the Runx1 deleted mice and they observed a significant reduction in LT-HSCs (Schindler, Van Buren et al. 2009).

Although two different Runx1 mouse models were used in these studies, it seems that the number of phenotypic and functional LT-HSCs depends on the criteria as well as the markers used to define them. In fact, this was demonstrated

by Cai et al who used both SLAM and CD34- flt3- LSK markers to study the effect of Runx1 deletion on adult haematopoiesis. In contrast to the severe reduction in SLAM-marked phenotypic LT-HSCs, they found a 2 fold increase on LT-HSCs upon using CD34- Flt3- LSK markers (Cai, Gaudet et al. 2011). Unexpectedly, the mean fluorescence intensity (MFI) of CD150 and CD48 in the Runx1 deleted LSK flt3- cells were significantly higher, despite the fact that their Slamf1 (CD150) and CD48 mRNA levels were low or unchanged, respectively. In fact, these data forced them to stain the analysed cells using all the markers (SLAM, CD34, flt3, LSK) and they found the CD34 FLt3 LSK-marked phenotypic LT-HSCs were shifted upwards on the CD48 axis and did not fall within the CD48- gate. These results suggest that upon Runx1 deletion several commonly used LT-HSC markers are dysregulated, therefore their reliability for defining of phenotypic HSCs may be challenged.

At the start of my PhD, the role of Cbfb in adult haematopoiesis remains poorly understood especially in the myeloid compartments. Therefore, this PhD was also aimed to investigate the role of Cbfb in adult haematopoiesis using conditionally knockout mice. Talebian et al (Talebian, Li et al. 2007) studied the role of Cbfb in haematopoiesis using a hypomorphic Cbfb allelic series, in which they were able to reduce the level of Cbfb by 3 to 6- folds. This reduction caused abnormalities in megakaryocytes, granulocytes and bone development. T-cell development was severely impaired as the mature thymocytes were virtually absent when Cbfb was reduced by 6-folds. Moreover, differentiation blocks were observed during the early T-lineage progenitors in particular within the DN1 and DN2 subsets. Furthermore, the $Cbfb^{f/f}$:Lck mice showed approximately 2-folds

reduction at the DN stage with severe impairment of mature thymocytes. In contrast, a moderate reduction of mature thymocytes was observed in $Cbfb^{f/f}$:Cd4 mice (Naoe, Setoguchi et al. 2007). These data suggest that the level as well as the spatial deletion of Cbfb may play a critical role during adult haematopoiesis.

### 1.2.5 Role in Solid tumours

Recently, the next-generation sequencing and SNP array analysis have shown that both RUNX1 and its heterodimeric partner, CBFB, were mutated in breast cancer (Banerji, Cibulskis et al. 2012; Ellis, Ding et al. 2012). In addition, RUNX1 deletion was also observed in oesophagus cancer (Dulak, Schumacher et al. 2012). CBFβ was found to be expressed in the metastatic breast cancer cell line (MDA-MB-231) and targeting its expression using siRNA or shRNA resulted in less invasive cells (Mendoza-Villanueva, Deng et al. 2010). Moreover, the growth of two prostate cell lines (PPCI and PC-3) and the SKOV-3 ovarian cell line was significantly inhibited upon knockdown of CBFβ (Davis, Rogers et al. 2010). Thus, it seems that CBFβ contributes to the invasive capability of these cell lines and targeting its expression may represent a promising therapeutic strategy for some human malignant cancers.

### 1.2.6 Role in Leukaemia

The RUNX1 and CBFB genes are the most frequent targets for chromosomal translocations in leukaemia generating AML1-ETO (AE) fusion and CBFβ-SMMHC fusion in t(8;21) and inv(16) AMLs, respectively.

#### *1.2.6.1 AML1-ETO*

AML1-ETO (also known as RUNX1-ETO, RUNX1-RUNX1T1 and RUNX1-MTG8) is one of the most frequent chromosomal translocation in human leukaemia and is found in 5-10% of AML (Zeisig, Kulasekararaj et al. 2012). This translocation joints together sequence of RUNX1 on chromosome 21 with that of ETO on chromosome 8, t(8,21). Its breakpoints occur in intron 5 of RUNX1 gene and in either intron 1a or 1b of the ETO gene. The common form of AML1-ETO fusion protein consists of 752 amino acids containing the N-terminal of AML1 protein, in which the runt domain is included, and almost the entire transcriptional repressive ETO protein (Tighe and Calabi 1994; Tighe and Calabi 1995; Zhang, Strissel et al. 2002). As shown in figure 1.8, four Nervy homology regions (NHR) are characterizing the ETO part, which share the Drosophila Nervy protein.

These NHRs are responsible for the interaction of ETO with other proteins. For instance, NHR1 interacts with E proteins and inhibits their ability to recruit some co-activator molecules such as p300/CBP (Zhang, Kalkum et al. 2004) . NHR2 and NHR4 interact with co-repressors like mSin3a, NCoR/SMRT and HDACs (Lutterbach, Westendorf et al. 1998; Wang, Hoshino et al. 1998; Zhang, Hug et al. 2001).

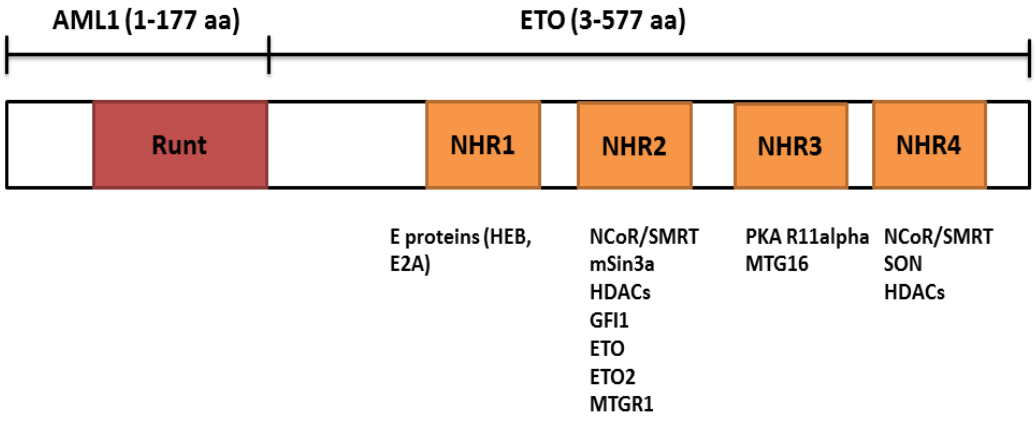


Figure 1-8 The structure of AML1-ETO and its interaction partners.

The figure modified from Lam et al (Lam and Zhang 2012) which illustrates structure of AML1-ETO and its interaction partners.

Multiple isoforms of AML1-ETO were detected in AML patient samples, most of them contained the full length (752 amino acids). Interestingly, AML1-ETO truncated isoform, which has 552 amino acids, was able to induce leukaemia rapidly in mice, suggesting the C-terminal of the full length may act as an inhibitor for the leukaemogenesis of this protein (Yan, Burel et al. 2004) as full length AML1-ETO cannot induce leukemia in mice. Also, another AML1-ETO transcript, which included an extra exon (9a), was detected in AML patients (figure 1.9). Contrasting to the full length, this transcript was also able to induce leukaemia in a mouse model (Yan, Kanbe et al. 2006).

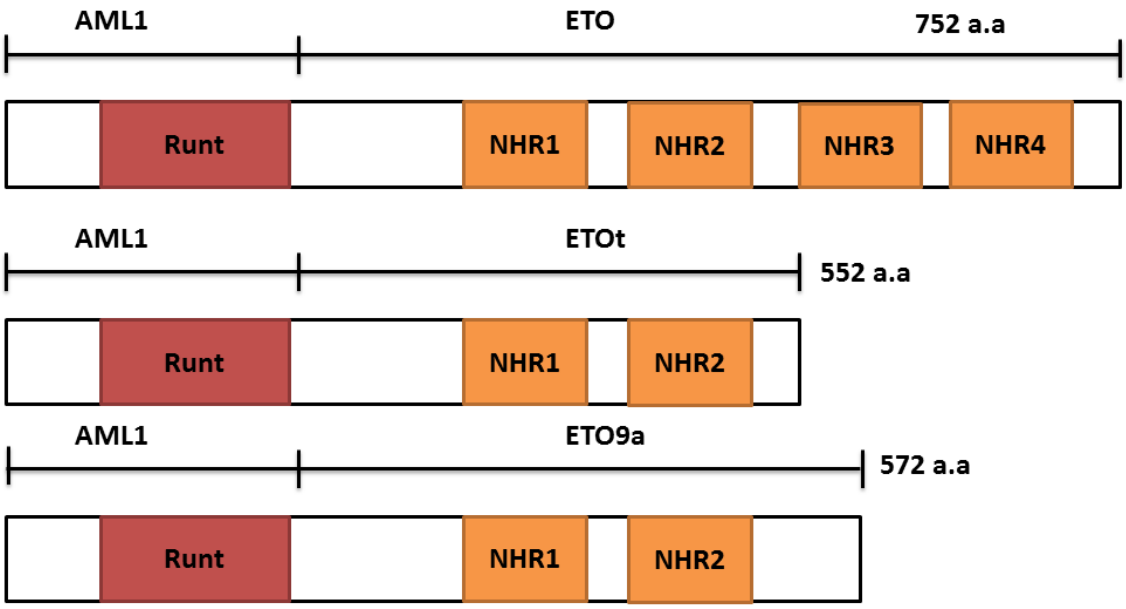


Figure 1-9 Structures of the main three AML1-ETO isoforms.

Several models have been used to investigate the impact of AML1-ETO on haematopoiesis. For instance, inducible expression of AML1-ETO in a transgenic zebrafish model recapitulated some phenotypes seen in AML patients such as accumulation of blasts cells and disruption of normal haematopoiesis (Yeh, Munson et al. 2008). Zhang and colleagues developed the first mouse model using a Knock-in approach, in which the AML1-ETO fusion gene was inserted into the AML1 locus (Yergeau, Hetherington et al. 1997; Okuda, Cai et al. 1998). Heterozygous AML1-ETO mice died embryonically with phenotypes most similar to that revealed by AML1 and Cbfβ KO mice. Although AML1 KO mice entirely lacked definitive haematopoiesis, yolk sac and fetal liver cells isolated from the heterozygous AML1-ETO embryos were able to differentiate into macrophage and dysplastic myeloid cells, respectively (Yergeau, Hetherington et al. 1997; Okuda, Cai et al. 1998). In addition, transgenic AML1-ETO mice under the control of several promoters such as

MRP8 and a tetracycline-responsive element have been also generated; however these mice were healthy and displayed a normal haematopoiesis and failed to develop leukaemia (Rhoades, Hetherington et al. 2000) without induction of additional mutations by treating these mice with N-ethyl-N-nitrosourea resulted in AML (Yuan, Zhou et al. 2001). Similar results were observed by another group after using conditional AML1-ETO Knock-in mice and Mx1-Cre inducible system (Higuchi, O'Brien et al. 2002).

Retroviral transduction and transformation assay was conducted to investigate the effect of AML-ETO on normal haematopoiesis. Although immature blast cells and inhibition of myeloid differentiation were observed, spontaneous AML development did not occur (de Guzman, Warren et al. 2002; Schwieger, Lohler et al. 2002). Xenograft models, in which human CD34+ cells were transduced with AML1-ETO and transplanted in to NOD/SCID mice, had demonstrated that AML1-ETO alone was able to enhance self-renewal but incapable to induce leukaemia (Mulloy, Cammenga et al. 2003; Basecke, Schwieger et al. 2005). These data reveal that the AML1-ETO may have additional properties, which promote leukaemogenesis, rather than simply acting as a dominant negative regulator of AML1 target genes.

## 1.3 Leukaemia stem cells (LSCs)

Decades ago, it was postulated cancers might be originated from subset of cells that have stemness properties (Makino 1959; Hamburger and Salmon 1977; Salmon, Hamburger et al. 1978). However, this has not been fully characterized until recent years with the advance in FACS analysis and transplantation models. The presence of LSC was firstly demonstrated in acute myeloid leukaemia (AML), in which the existence of a small number of phenotypically distinctive leukemic cells is responsible for generating the disease in xenograft models. For instance, Bonnet and Dick demonstrated that a small fraction of primitive cells (Lin-CD34+CD38-) was able to induce the disease in NOD/SCID mice with a phenotype similar to the one observed in patients. In addition, these cells were also able to induce AML in secondary recipients, demonstrating their self-renewal ability. On the other hand, mature cells (Lin-CD34+CD38+ or CD34-) failed to transfer the disease. Therefore they concluded their study by suggesting that the target of leukeamic transformation is normal primitive cells rather that progenitor cells (Bonnet and Dick 1997). However, several studies later on showed that some progenitor cells can be transformed by some oncogenes and also were able to induce AML in mice. Using RTTA, So et al. clearly demonstrated that MLL-GAS7 can transform multipotent haematopoietic progenitors leading to the induction of mixed lineage leukaemia in mice, but not CMP or CLP progenitors (So, Karsunky et al. 2003). Cozzio and colleagues were able to demonstrate that MLL-ENL can transform CMP and GMP *in vitro* and these cells induced leukaemia *in vivo* with latencies similar to

the MLL-ENL HSC transformed cells (Cozzio, Passegue et al. 2003). Recently, Heuser et al demonstrated that CMP cells were able to be transformed by MN1 and also to generate leukaemia *in vivo*, whereas GMP cells were unable (Heuser, Yun et al. 2011).

It has been demonstrated that LSCs may home in the microenvironment of the BM where they will maintain quiescent at G0 stage (Guan, Gerhard et al. 2003; Ishikawa, Yoshida et al. 2007). Consequently, chemotherapy treatment that targets highly dividing cells (bulk disease) has a minimum impact in eliminating the LSCs which causes the relapse. Indeed, developing better curative therapies for leukaemia requires not just full understanding of the LSCs properties, but also their main differences with the bulk population and the normal HSCs.

## 1.4 Objectives

AML1 and CBFB are the most frequent targets for chromosomal translocations in acute myeloid leukaemia generating AML1-ETO (AE) fusion and CBFβ-SMHCC fusion, respectively. Although, Cbfb enhances the binding affinity of AML1 to DNA, its role in AE-mediated transformation remains unclear. Recent studies by others (Park, Speck et al. 2009; Roudaia, Cheney et al. 2009) and our group (Kwok, Zeisig et al. 2009; Kwok, Zeisig et al. 2010) using Cbfb-interaction defective AE mutants in different experimental settings have yielded conflicting results. The role of Cbfb in AE-mediated leukaemogenesis remains unclear. In addition, while AML1 and Cbfb have a pivotal role during embryonic haematopoiesis, the function of Cbfb in adult haematopoiesis is still not fully understood. Definition of Cbfb requirement is important for understanding the biology of the disease and also for designing better cancer therapeutics, in particular when inhibitors targeting Cbfb/AML1 interaction is being developed for this purpose (Gorczynski, Grembecka et al. 2007; Cunningham, Finckbeiner et al. 2012). Thus in my PhD project, we aim to clearly define the role of Cbfb AE-mediated leukaemogenesis and also in the development of normal HSCs.

The main aims of the PhD project are the following:

1- To define the role of Cbfb in AE in vitro transformation activity using primary bone marrow cells derived from mice carrying conditionally deleted Cbfb alleles.
2- To investigate the role of Cbfb in AE-mediated transformation in different haematopoietic stem/progenitors cells isolated from Cbfbf/fRosa26Cre ER.

3- To define the role of Cbfb in AE leukaemogenesis using fetal liver cells isolated from Cbfbf/fRosa26Cre ER.

4- Establishing an *in vivo* AEs leukaemia models that allow us to study the impact of Cbfb deletion on initiation and maintaining this disease.

5- To define the molecular function and downstream target of Cbfb involved in leukaemic transformation.

6- To investigate the role of Cbfb in development of normal adult HSCs by targeting Cbfb in whole mouse versus only in the haematopoietic cells or the stromal environments.

# 2 Materials and methods

## 2.1 Mice

Cbfb flox mouse in a mixed background was a kind gift from Dr. Ichiro Taniuchi and the targeting strategy for generating this mouse is illustrated in figure 2.1. The strategy was characterized by placing a floxed neomycin resistance cassette next to exon 5 and a loxP site to the other flanking intron. After introducing this mutation into embryonic stem cells, a transient expression of Cre recombinase was carried out to remove the neomycin resistance cassette. Thus, exon 5 of this transgenic mouse was flanked by loxP sites (figure2.1 (Naoe, Setoguchi et al. 2007)). At the beginning, $Cbf\beta^{flox}$ mouse was crossed with Rosa 26 YFP mouse to generate $Cbf\beta^{fl/fl}$ Rosa 26 $^{YFP/wt}$ mouse and also backcrossed with C57BL/6 to generate a $Cbf\beta^{flox}$ mouse in a pure background. In addition to this mouse strain, $Cbf\beta^{fl/fl}$ Rosa 26 Cre ER mice were generated by breeding $Cbf\beta^{flox}$ pure C57BL/6 background mice with heterozygous Rosa 26 Cre ER mice.

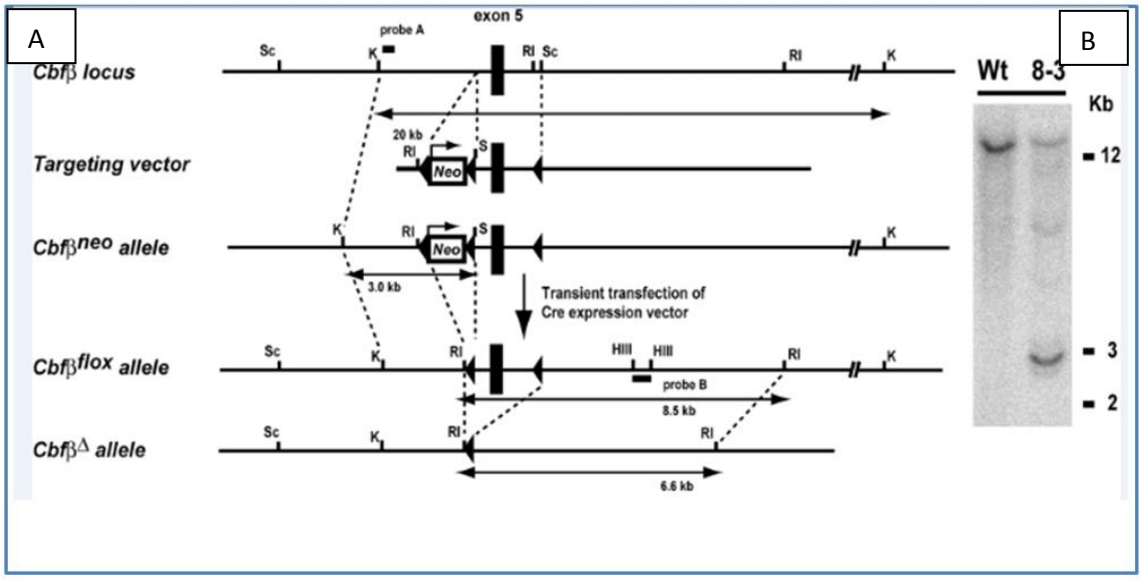

Figure 2-1 Targeting strategy for generating Cbfb flox mouse

(A) shows structures of the wild type cbfb, targeting vector and the targeted Cbfb neo loci. Black boxes and triangles indicate exons and loxP sequences, respectively. Bg, BgIII; K, KpnI; RI, EcoR1, HIII, HindIII; S, SaII; Sc, Sac1. (B) Southern bot of embryonic stem cell clones (Naoe, Setoguchi et al. 2007).

## 2.2 Genotyping

Genomic DNA (gDNA) was isolated from ear biopsies of 5-week-old mice using Hotshot buffer. The ear samples were lysed in a hotshot lysis buffer containing (25mM NaOH and 0.2mM EDTA) for 20-30 minutes at 95$^{o}$C and neutralized by adding equal amount of host shot neutralizing buffer (40mM Tric-HCL). Cbfb floxed, deleted and wild-type alleles were detected by multiplex PCR with the following primers: G2, 5'-CCTCCTCATTCTAACAGGAATC-'3; G3, 5'-GGTTAGGAGTCATTGTGATC AC-'3; and G6, 5'-CATTGGATTGGCGTTACTGG-'3 (figure 2.2). PCR amplifications were carried out in a 20-µl reaction volume contained 1X Dream Green buffer supplemented with 2.5 mM $MgCl_2$ (Fermentas), 0.25 mM dNTP mix (Roche), 1µM from each primer and 0.5 unit of Dream Taq$^{TM}$ Green DNA polymerase (fermentas). Thirty cycles of amplification were performed using the following PCR conditions: Hot start for 4 minutes at 94$^{o}$C, denaturating for 30 seconds at 94$^{o}$C, annealing for 30 seconds at 54$^{0}$C, elongation at 72$^{o}$C for 30 seconds, and final elongation for 7 minutes at 72$^{o}$C. Genotyping of Cbfβ$^{fl/fl}$ Rosa 26 $^{YFP/wt}$ and Cbfβ$^{fl/fl}$ Rosa 26 Cre ER mice were carried out similarly to the floxed one using different primers as shown in table 2.1.

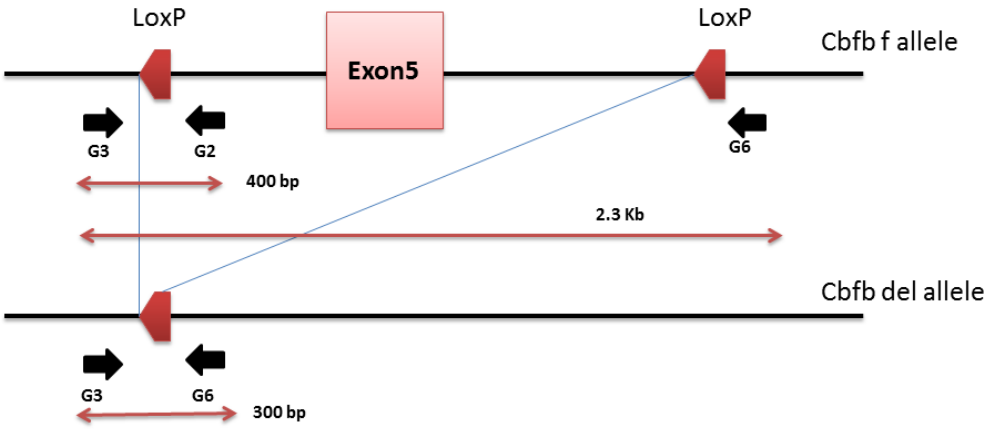


Figure 2-2 Locations of Cbfb primers (G2, G3 and G6).

This diagram shows locations of Cbfb primers which were used for genotyping (Flox band: 400bp, KO band: 300bp and WT band: 275bp).

Table 2-1 Primer sequences for genotyping of Cbfβfl/fl Rosa 26 YFP/wt and Cbfβfl/fl Rosa 26 Cre ER mice.

| Mouse | Primers (5'-3') | Annealing Temperature |
|---|---|---|
| **Cbfbf/f Rosa 26 YFP/WT** | 5'-AAGACCGCGAAGAGTTTGTC-3',<br>5'-AAAGTCGCTCTGAGTTGTTAT-3',<br>5'-GGAGCGGGAGAAATGGATATG-3' | 60°C |
| **Cbfbf/f Rosa 26 Cre ER** | 5'-CGTACTGCGGTGGGAGAAT-3'<br><br>5'-TGCATGATCTCCGGTATTGA-3' | 60°C |

## 2.3 Cloning

The retroviral plasmids (MSCV, Clontech) expressing different transcription factors such as AML1-ETO, AML1-ETO9a, MLL-AF9, MN1, hit and run cre were obtained from the clone database of our leukaemia and stem cell biology group (Kwok, Zeisig et al. 2009; Kwok, Zeisig et al. 2010; Yeung, Esposito et al. 2010; Smith, Yeung et al. 2011). Cbfb and exon 5-deleted Cbfb were cloned into pSG5 vectors by isolating cDNAs from WT and deleted Cbfb cells, respectively. The cDNAs were amplified using primers having EcoRI and BamHI sites (F:

5'AAATTTGAATTCATGCCGCGCGTCGTCCCGGA3',R: 5'AAATTTGGATCCTTAACGAAGTTTGAGATCATCACG 3')

(figure 2.3). Then, the digested cDNAs were cloned between the EcoRI and BamHI sites of the pSG5 vector.

Similar strategy was performed to tag both the WT cbfb as well as the spliced isoform with HA tag and to clone them into pMSCV puro vector. Firstly, the cDNA templates were amplified using primers have Bgl II, HA sequences and EcoR1 sites(F:5'AAATTTAGATCTATGTACCCATACGATGTTCCAGATTACGCTCCGCGCGTCGTCCCG3',R:5'AAATTTGAATTCT TAACGAAGTTTGAGATCATCACCG 3'). Then, the digested cDNAs were cloned between the Bgl II and EcoR1 sites of the pMSCV vector. All the DNA plasmids were prepared using Qiagen/Fermantas kits according to the manufacturer's instructions.

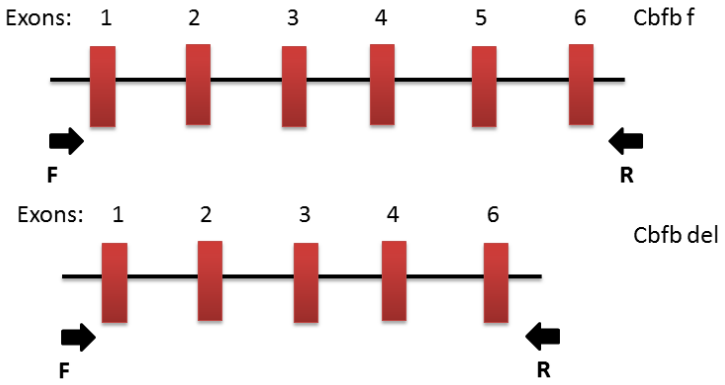


Figure 2-3 The location of Cbfb primers used for cloning.F: forward, R: reverse.

## 2.4 Virus production

One day before transfection, $4x10^6$ GP2-293 cells (Clonetech) were seeded into a 10-cm plate with 8 ml of pre-warmed of (D10): Dulbecco's Modified Eagle Medium (DMEM, Gibco) supplemented with 10% fetal bovine serum (FBS, SIGMA), 100 IU/ml of penicillin and streptomycin (SIGMA). The transfection was carried out by adding a mixture contained (414 µl of $H_2O$, 15 µg of 1µg/µl of DNA construct, 9µg of 1.0 µg/µl Vesicular Stomatitis Virus Glycoprotein Epitope (pVSV-G), 1µg of 1µg/µl Green Fluorescent protein (GFP), 61µl of 2M $Cacl_2$ and 500µl of 2X HBS onto the seeded GP2-293 cells. The transfected cells were incubated overnight at $37^oC$, 5%$CO_2$ and their efficiency were determined based on the percentage of GFP expression under the fluorescence microscope. Twenty-four hours after transfection, the old medium was replaced with 10ml pre-warmed D10 and the 48-h virus were collected by aspirating the supernatant with 10ml syringe and filtered through a 0.45 µm filter. The virus was concentrated by using the Optima$^{TM}$ L-100 XP Ultracentrifuge (Beckman) at 25000 rpm, $4^oC$ for 3 hours. The supernatant of the concentrated virus (3ml) was resuspended and stored in 500µl aliquots at $-80^oC$ until required.

## 2.5 Isolation of c-kit+ (CD117) cells from mouse bone marrow

The femurs and tibias of the experimental mice were isolated and 10ml of suspension medium (SM, PBS with 0.2% FBS and 100 IU/ml of penicillin and streptomycin) were used to flush the bone morrow into 15ml test tube using 10ml syringe attached with 25G needle (Terumo®, Belgium). The bone morrow cells were

centrifuged at 1300 rpm for 5 minutes at room temperature (Allegra® X-15R centrifuge, Bechman coulter). The cell pellet was resuspended in 1ml of red cell lysis buffer (10mM $KHCO_3$, 150mM $NH_4Cl$, and 0.1mM EDTA) and incubated for 10 minutes at room temperature. This reaction was terminated by adding 10ml of SM and the cells were filtrated using 40µM cell strainer (BD Falcon™). Then, the cell pellet was resuspended in 500µl of SM and incubated with 15µl of c-kit beeds(MACS, MiltenyiBiotec) for 30 minutes at 4°C. At the end of the incubation, 500µl and 30ml of SM were used to equilibrate the MS column and to wash the incubated cells, respectively. The cell pellet was resuspended with 500µl of SM and the mixture was applied to the equilibrated MS column which was attached onto a magnetic stand. Cells were washed twice with 500µL of SM and the MS column was transferred into 1.5ml microcentrifuge tube in which 1ml of SM was used to flush c-kit+ cells using a plunger. 200µl of R10 supplemented with IL3, IL6 (10ng/ml) and SCF (20ng/ml) cytokines were used to plate the required number of c-kit+ cells in a 96-well plate. Cells were incubated overnight at 37°C with 5% $CO_2$ (Zeisig and So 2009).

## 2.6 Isolation of fetal liver cells

Timed mating between Cbfb breeding pairs was set up in the late afternoon and the vaginal plug of the female was checked in the early morning of the next day to separate the male and also to start counting the days of conception. The embryos were aged E0.5 at noon of the day on which the vaginal plug was seen and we usually harvest the fetal live cells around E11.5-E15.5. The pregnant female was culled using $CO_2$ chamber and under sterile conditions all the embryos were

collected into 50-ml tube contained PBS. Livers from foetuses were surgically removed into 15 ml tubes with 5 ml SM and passed several times through a syringe with an 18G and then 25G needles. The mixture was filtered using a 40µm cell strainer. Cells were centrifuged at 1300 rpm for 5 minutes at room temperature and the pellet was resuspended in 3ml of red cell lysis buffer for 5 minutes on ice. Cells were washed using 10ml of SM and cultured at 1-2x$10^6$/ml of RPMI medium supplemented with 10ng/ml IL3, IL6, 20ng/ml SCF, and 15% FBS. Fetal liver cells were incubated overnight at 37$^o$C with 5% $CO_2$.

## 2.7 Sorting and analysing of haematopoietic stem/progenitors cells

### 2.7.1 Sorting

A protocol from Yeung and So (Yeung and So 2009) was adapted and slightly modified to sort haematopoietic stem/progenitor cells. MNCs were isolated from five WT mice or KO mice and stained with primary lineage unconjugated rat IgG (Ter 119, Mac 1, Gr 1, CD3e, CD4, CD8 and B220, Biolegend ) at a dilution of 1:40. The stained cells were incubated at 4$^0$C for 30 minutes and then washed with SM. Cells were incubated with washed Dynabeads (sheep anti-rat IgG, Dynal, Invitrogen, 120.21D) for 30 minutes at 4$^o$C. At the end of the incubation, the magnet was applied to the mixture for 3 minutes and the unbound lineage depleted cells were transferred to a fresh 10 ml test tube. Then, cells were stained with goat anti-rat-PECy5.5 at a dilution of 1:50 to exclude cells that escaped the depletion process, and then washed with SM. Cells were blocked with rat IgG (Sigma) for 30 minutes at 4$^o$C. After that, cells were washed with SM and stained with secondary antibodies as indicated in table2.2. Stained Cells were washed and resuspended in SM with

1µg/ml of propidium iodine (PI), and then subjected to sort LSK (Lin $^{-/low}$ Sca1 $^{+}$ c-Kit$^{+}$), CMP (Lin $^{-/low}$ Sca1 $^{-}$ c-Kit $^{+}$ CD34 $^{+}$ CD16/32 $^{low}$), GMP (Lin $^{-/low}$ Sca1 $^{-}$ c-Kit $^{+}$ CD34 $^{+}$ CD16/32 $^{hi}$) and MEP (Lin $^{-/low}$ Sca1 $^{-}$ c-Kit $^{+}$ CD34$^{-}$ CD16/32 $^{low}$) using ARIA cell sorter (BD Bioscience). Sorted cells were seeded in sterile 96-well plate contained R10 supplemented with cytokines (20ng/ml SCF, 10ng/ml of IL3 and IL6) and incubated overnight at 37$^{o}$C with 5% CO2.

The purity of the sorted stem/progenitor cells was assessed using Colony-Forming Unit (CFU) assay in which 1000 cells from LSK, CMP, GMP and MEP were plated into a methylcellulose (STEMCELL$^{TM}$) supplemented with 20 ng/ml SCF, 10 ng/ml of IL3, IL6, GM-CSF, 100 IU/ml penicillin, 100 µg/ml streptomycin and 5 units of Erythropoietin. The cells were incubated at 37$^{o}$C with 5% CO2 for 7-14 days and burst-forming unit-erythroid (BFU-E), colony-forming unit-granulocyte, macrophage (CFU-GM), Colony-forming unit-granulocyte (CFU-G), colony-forming unit-macrophage (CFU-M), colony-forming unit-granulocyte, erythroid, macrophage, megakaryocyte (CFU-GEMM) colonies were scored.

Table 2-2 Secondary antibodies and their dilutions that used to stain haematopoietic stem/progenitor cells for sorting.

| Antibody | Source/Clone | Dilution |
|---|---|---|
| **c-Kit-PE** | Biolegend/2B8 | 1:100 |
| **Sca1-PE-Cy7** | eBioscience/D7 | 1:50 |
| **CD34-FITC** | eBioscience/RAM34 | 1:25 |
| **CD16/32-APC** | Biolegend/93 | 1:75 |

### 2.7.2 Analysis

Haematopoietic stem/progenitor cells analysis was carried out similarly to the sorting protocol with slight modification. 3-4x$10^6$ MNCs from each mouse were used to conduct the analysis and the incubation with Dynabeads was skipped in this protocol. Cells were stained with secondary antibodies as illustrated in table 2.3. The stained cells were subjected to LSK, LT-HSC (LSK CD150+CD48-), ST-HSC (LSK CD150- CD48-) (Cai, Gaudet et al. 2011), LMPP (LSK CD150- CD48+), CLP (Lin $^{-/low}$ IL-7R α + Sca1 lo c-Kit $l^{ow}$), CMP, GMP and MEP analysis using ARIA (BD Bioscience) and FlowJo software.

Table 2-3 Secondary antibodies and their dilutions that used to stain haematopoietic stem/progenitor cells for analysis

| Antibody | Source/Clone | Dilution |
|---|---|---|
| **c-Kit-PE** | Biolegend/2B8 | 1:100 |
| **Sca1-PECy7** | eBioscience/D7 | 1:50 |
| **CD34-FITC** | eBioscience/RAM34 | 1:25 |
| **CD16/32-APC** | Biolegend/93 | 1:75 |
| **CD150-BV421** | Biolegend/TC15-12F12.2 | 1:25 |
| **CD48-Alexa flour 700®** | Biolegend/HM48-1 | 1:50 |
| **Biotin anti mouse IL-7** | Biolegend/A7R34 | 1:100 |
| **Streptavidin APC/cy7** | Biolegend | 1:50 |
| **CD45.2-BV 650** | Biolegend/104 | 1:50 |

## 2.8 Spinoculation and methylcellulose replating assay

The spinoculation and methylcellulose replating protocol was adopted from Zeisig and So (Zeisig and So 2009). LSK, CMP, GMP, MEP or c-Kit seeded cells in 96-well plate contained R10 supplemented with cytokines (20ng/ml SCF, 10ng/ml of IL3, IL6 and 10mg/ml of polybrene) were subjected to spinoculation with viruses carrying different leukaemia associated transcription factors. Spinoculation was carried out by centrifugation for 2 hours at 800g, $32^0$C and then cells were incubated overnight at $37^o$C with 5% $CO_2$. The transduced cells were transferred into 0.9 ml of pre-warmed methylcellulose (STEMCELL$^{TM}$) supplemented with 20 ng/ml SCF, 10 ng/ml of IL3, IL6, GM-CSF, 100 IU/ml penicillin, 100 µg/ml streptomycin and 1mg/ml geneticin or 1.3µg/ml puromycin. Cells were mixed well and transferred into one well of 24-well culture plate and incubated for 5-to 7 days at $37^o$C with 5% $CO_2$ and then colonies of the $1^{st}$ round were scored. After that, colonies were harvested using 8 ml of SM and transferred into a 15 ml test tube and were centrifuged for 5 minutes at 1300 rpm, $20^o$C. Cells were counted and 1-2x$10^4$ cells were re-plated into 0.9 ml methylcellulose supplemented with cytokines. This re-plating was carried out for $2^{nd}$, $3^{rd}$ and subsequent rounds and after each round few cells were kept for genotyping, WB and RNA isolation.

## 2.9 Co-immunoprecipition (Co-IP)

To test the interaction between Flagged AE and HA tagged Cbfb (WT and its spliced isoform), 293 GP2 cells were co-transfected with the appropriate constructs. Two days later, the medium was aspirated and the cells were washed twice using cold PBS. The cell pellets were lysed in a buffer containing Tris-HCl PH 8.0 (50mM),

Nacl (150mM), NP40 1% and Roche Protease inhibitor (1:25) for 60 minutes at 4oC with rotation. Cells were centrifuged (1400g) for 15 minutes at 4oC and the supernatant was collected in a new Eppendorf tube. The lysate was incubated overnight with ANTI-FLAG® M2 Affinity Gel (Sigma) at 4$^{o}$C with rotation. Then, the cells were washed three times using 0.5ml of TPBS for 5 minutes with rotation. The Flagged AEs were eluted from the affinity gel using SDS-PAGE sample buffer and loaded into gels for Western blotting.

## 2.10 Western blotting

1-2x10$^{6}$ cells were lysed using 2x SDS-PAGE sample buffer (0.5M Tris-HCl, Glycerol, 10% SDS and 0.5% bromophenol blue) and incubated for 5 minutes at 95$^{o}$C. 10µl of protein ladder (PageRuler $^{TM}$ plus Prestained protein ladder, Fermentas) and 20µl of each samples were loaded into 12% gradient SDS polyacrylamide gel (NEXT GEL $^{TM}$, Amresco) and separated at 140 V for 90 minutes, and then blotted onto a nitrocellulose membrane (Amersham $^{TM}$ Hybond $^{TM}$ ECL) for 1 hour at 100 V. After that, the transferred membrane was blocked using 2.5 g of milk dissolved in 50 ml of PBS-T with 0.1% Tween 20 (Promega) for 2 hours at room temperature. Then, the membrane was probed with anti-Cbfβ antibody (ab33516, 1:500), anti-flag M2 antibody (Sigma, 1:7000) or anti-HA antibody (Covance, 1:4000) for overnight at 4$^{o}$C. The membrane was washed with PBS-T (3 times, 10 minutes) and incubated with secondary antibody conjugated with HRP for 1 hour at room temperature. The membrane was washed and the signal was detected using ECL detection system (Amersham $^{TM,}$ GE Healthcare) and developed on X-ray film (Amersham$^{TM}$, Hyperfilm ECL) using photon imaging system.

## 2.11 Reverse transcriptase (RT) and Quantitative Reverse Transcriptase Polymerase Chain Reaction (qRT-PCR)

Total RNA were extracted using either Macherey-Nagel (MN) or mirVana™ miRNA Isolation Kits according to the manufacturer's instructions and the RNA concentration was measured using NanoDrop 8000 (Thermo Fisher Scientific). The cDNA synthesis was carried out using SuperScript III kit (Invitrgen). Briefly, for 20µl reaction volume: 1 µl of oligo dT (50µM), 1µl of 10 mM dNTP mix, 10pg –3µg total RNA and sterile water was added to get 13µl volume. Then, the mixture was incubated at 65$^0$C for 5 minutes followed by 1 minute incubation on ice. After that, 7 µl of a master mix of (4 µl of 5X First-Strand Buffer, 1 µl of 1 µl 0.1 M DTT, 1 µl RNaseOUT™(40U/ µl), 1 µl of SuperScript™ III RT (200 units/µl) were added to each sample and subjected to PCR reaction using Veriti® Thermal Cycler machine programmed with the following conditions: 25$^o$C for 5 minutes, 50$^o$C for 60 minutes, 70 $^o$C for 15 minutes and hold at 4$^o$C. To confirm the presence of AE or AE9a in the transformed or leukaemic cells, 1µl of cDNA template was amplified using the following PCR conditions together with the primers listed in table 2.4: denaturation for 45 seconds at 94$^o$C, annealing for 45 seconds at 58 $^o$C, and extension for 90 seconds at 72 $^o$C (Yan, Kanbe et al. 2006). To quantify the expression level of our genes of interest, real time PCR was carried out either by TaqMan® Fast Universal Master Mix (table 2.5) or Fast SYBR® Green Master Mix (table 2.6) using StepOnePlus™ Real-Time PCR System (Applied Biosystems®).

Table 2-4 Primers pairs for RT-PCR

| | | |
|---|---|---|
| **AE** | **5’-GAGGGAAAAGCTTCACTCTG -3’** | **Forward** |
| | **5’-TCGGGTGAAATGTCATTGCC-3’** | **Reverse** |
| **mGAPDH** | **5’- ACCACAGTCCATGCCATCAC -3’** | **Forward** |
| | **5’- CACCACCCTGTTGCTGTAGCC -3’** | **Reverse** |

Table 2-5 Primers pairs and probes for qRT-PCR using TaqMan

| | | |
|---|---|---|
| **Cbfb major** | **5'-CAGGAAGATGCATTAGCACAA-3'** | **Forward** |
| | **5'- FAM-CCTTTGAAGAGGCTCGAAGAAGAACTCGA -TAMRA -3'** | **Probe** |
| | **5-'CATTTCCTCCCGGTGAGAC-3'** | **Reverse** |
| **Cbfb minor** | **5'-GGGTTGCCTGGAGTTTGATC-3'** | **Forward** |
| | **5'-FAM-CCCAGGCAAGAAGACAGCAAGACCC-TAMRA-'3** | **Probe** |
| | **5'-ACCGCCACCTAAGTTAGAACCA-3'** | **Reverse** |

Table 2-6 Primers pairs for qRT-PCR using SYBR green

| | | |
|---|---|---|
| **Mouse Mpl** | **5’- TCACCTTGGTGACTGCTCTG-3’** | **Forward** |
| | **5’-CCACAAAGCATGCCTCAGTC-3’** | **Reverse** |
| **Mouse Cebpα** | **5’-GCAAAGCCAAGAAGTCGGTG-3’** | **Forward** |
| | **5’-CACCTTCTGTTGCGTCTCCA-3’** | **Reverse** |
| **Mouse Gapdh** | **5’-GTATGACTCCACTCACGGCAAA-3’** | **Forward** |
| | **5’-TTCCCATTCTCGGCCTTG-3’** | **Reverse** |

## 2.12 RNA Sequencing

Briefly, mirVana™ miRNA Isolation Kit (life technology) was used to extract RNA from 1-3 x$10^6$ cells according to the manufacturer's instructions and the quality of the extracted RNA was assessed using the Agilent 2100 bioanalyzer (Agilent Technologies). cDNA libraries were prepared using TruSeq Stranded Total RNA LT Sample Prep Kit (Illumina® ) and the sequencing was carried out at department of haematological medicine, (KCL) using HiSeq™ 2000 Sequencing System, Illumina®. Our RNA sequencing data was analysed by Dr. Magdalena Zarowiecki who is the bioinformatics head in our research group. Dr. Zarowiecki performed the following analysis:

The FASTQ files were de-tagged, and the quality of the FASTQ files inspected using FastQC v.0.11.2. Remaining adapters were trimmed using TRIMGalore v.0.3.7. Reads were mapped to the Ensembl mouse genome using TopHat2 v2.0.13, reads filtered for quality and counted using samtools v.0.1.18 and bedtools v2.23.0-10-g447cb97. Differential expression was determined either using DESeq2 Negative Binomial GLM fitting and Wald statistics. Functional enrichment analysis was conducted using the GSEA software, using the Molecular Signature Database c2 set (MSigDB), and a custom made gene sets. For the GSEA analysis, human-mouse gene orthologues were identified using MGI list of orthologous genes, and Ensembl bioMart used to transfer MGI IDs to Ensembl gene IDs. The visualization of reads mapping to Cbfb was done using the software Artemis.

## 2.13 FACS analysis of Transformed cells

### 2.13.1 General Stain

5-10 X$10^4$ cells were stained in FACS tubes with master mix of antibodies (PE-c-Kit, PE/Cy7-Mac-1, PerCP/cy5.5-Gr-1(Biolegend), Pacific Blue-B220, Alex Flour®700-CD4, APC-eFlour®780-CD8 (eBioscience), FITC-CD45.1 and APC-CD45.2 (Biolegend) in 1:200 dilutions for 30 minutes in a dark place at 4$^o$C. The stained cells were washed with SM and resuspended in 300 µL of SM with 1µg/ml of PI. Cells were analysed using LSRII flow cytometer (BD Bioscience).

### 2.13.2 Cell Cycle Analysis using Propidium Iodide (PI)

0.1-1x$10^6$ cells were washed twice with cold PBS in FACS tubes and centrifuged for 5 minutes at 300 g. The supernatant was aspirated and cells were resuspended in 200 ul of PBS and fixed by 70% cold ethanol for at least 1 hour at 4$^o$C. The fixed cells washed twice with cold PBS and stained with 200 ul of PI stain (PBS: 0.2X FBS, 40ug/ml RNase (Sigma), 40ug/ml PI (Sigma) for 30 minutes at 4$^o$C in a dark place. The stained cells were analysed using LSRII flow cytometer (BD Bioscience).

## 2.14 Transplantation

A mixture of 1 x$10^6$ of MNCs or cell lines with 2x$10^5$ rescue cells were resuspended into 150µl of PBS and injected (tail vein) into irradiated (1100 or 1350 rad, 2 doses) mice. CD45.1 and CD45.2 (Biolegend) markers were used to distinguish donor from recipient cells. For generating a leukaemia mouse model, fetal liver cells or BM c-kit+ cells were harvested and plated into 6-well plates as

described earlier. The cultured cells were transfected with 2 ml of MigR1 AE9a viral suspension and subjected to the first spinoculation. 24 hours later, the media were aspirated leaving only 1 ml and the second spnioculation was carried out using 2 ml of the MigR1 AE9a viral suspension and at the end of this step 2 ml of fresh media were added. The cells were expanded for 48 hours and their phenotypes were analysed using FACS machine and then transplanted as described earlier. For *in vivo* Cre-recombinase, mice were injected with 2-5 consecutive intraperitoneal (IP) injections (120µL of 10mg/ml in corn oil) of tamoxifen (Sigma). The sick animals routinely subjected to a comprehensive analysis as illustrated in figure 2.4.

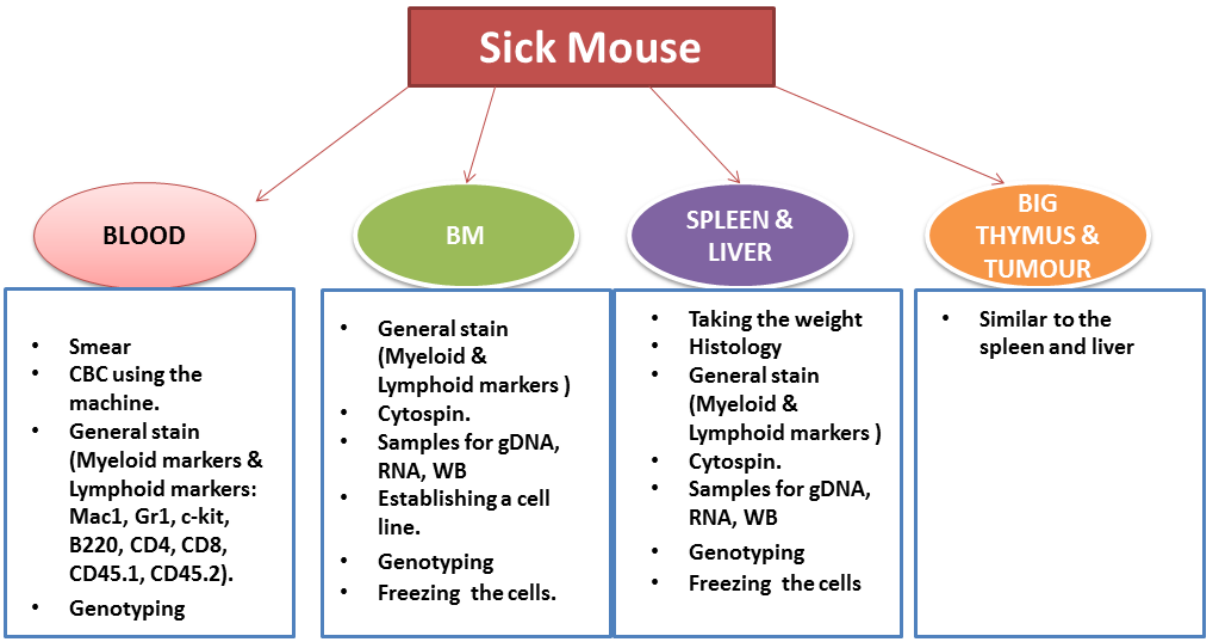


Figure 2-4 Analysis of sick mouse.

The figure illustrates the method that I used to analysis a sick mouse.

## 2.15 Tail Vein Bleeding (TVB)

TVB was performed by a qualified person who got the animal license after passing a training course. In this procedure, a small cut was made at the end to the tail and then few drops of blood were squeezed into an Eppendorf tubes pre-coated with 0.01 M Ethylenediaminetetraacetic acid (EDTA) (Sigma). The blood parameters (WBC, RBC, Platelets etc.) were measured using Mythic 18 Vet coulter machine (Woodley Company).

## 2.16 Giemsa stain

A peripheral blood smear was prepared by spreading a small drop of tail vein or heart puncture blood on a microscopic slide and left to dry for few minutes. BM, spleen and liver cytospins were prepared in a Cytospin™ 4 Cytocentrifuge (Thermo Scientific™) and span for 5 minutes at 300 rpm. The slides were firstly stain with May-Grünwald stain (Sigma) for 3 minutes and then washed with water. After that, the washed slides were stained with diluted Giemsa stain (1:20, Sigma) for 20 minutes and then washed with water. Finally, the slides were left to dry for several minutes and examined under a microscope equipped with a camera.

## 2.17 Histology

Spleen and liver samples were fixed in 10% formalin buffer and sent to histopathology department at king's college hospital. The samples were processed and stained with Hematoxylin and eosin (HE) stains.

## 2.18 Statistical analysis

All the statistical analyses were performed by GraphPad software using a two-tailed unpaired student t-test. Kaplan-Meier survival curves were also generated by this software and statistically analysed using a Log-rank (Mantel-Cox) test.

## 2.19 Ethical approval

All the animal works in this thesis were approved by the UK Home Office (Project license number 70/7867 & personal license number 70/19320). In addition, all the animal handling and procedures that carried out in our lab were reviewed and approved by the Biological Services Unit (BSU) at King's College London.

# 3 Effect of Cbfb in Leukaemogenesis

## 3.1 A Brief Introduction

As mentioned earlier, AML1 and CBFB genes are among the most frequent targets for chromosomal translocations in acute leukaemia generating AML1-ETO (AE) fusion and CBFβ-SMMHC fusion, respectively. Based on mutagenesis studies, our group previously created Cbfb-interaction defective AE mutants and demonstrated that the *in vitro* transformation activities of these AE mutants were Cbfb independent. In addition, AE transformation activity remained largely unchanged when the endogenous expression of CBFβ was knocked down by around 95% using a shRNA approach (Kwok, Zeisig et al. 2009). However, a study by another group using Cbfb-interaction defective AE mutants in different experimental settings have yielded conflicting results, in which Cbfb-interaction defective AE mutants failed to transform (Roudaia, Cheney et al. 2009). Thus the exact functional role of Cbfb in AE mediated transformation was unknown at the start of my PhD project.

Definition of Cbfb requirement is important for understanding the biology of the disease and also for designing better cancer therapeutics, in particular when inhibitors targeting Cbfb/AML1 interaction are being developed for this purpose (Gorczynski, Grembecka et al. 2007; Cunningham, Finckbeiner et al. 2012). It is well recognized that it is almost impossible to generate mutations, which affect only a single property of a protein leaving other features untouched. Therefore the use of a Cbfb conditional KO mouse model in combined with wild type AE is considered as

a complementary approach to the mutant studies to draw a more definitive conclusion. To this end, I decided to investigate the role of Cbfb in AE leukaemogenesis by employing different experimental strategies (*in vitro* and *in vivo*) and examining different potential origins of LSC (BM and fetal liver).

## 3.2 Results

### 3.2.1 The impact of Cbfb deletion on the *in vitro* self-renewal of primary haematopoietic cells transformed with AEs.

#### *3.2.1.1 Cbfbf/f RosaYFP/WT mouse*

To investigate the effect of Cbfb in AEs transformation activity, I firstly used the Cbfbf/f RosaYFP/WT mouse model, which carried floxed alleles flanking exon 5 of Cbfb and a Rosa-stop-YFP marker but lacking a transgenic Cre-recombinase. Instead of disrupting the whole Cbfb function, the advantage of this KO model is its generation of exon 5-deleted Cbfb splicing variant that fails to interact with AML1. This mouse model was in a mixed background and has already been present at the start of my PhD study. c-Kit + haematopoietic stem and progenitor cells were isolated from bone marrow of these mice and subjected to RTTA in the absence or presence of Hit and Run Cre (HR-cre)(Silver and Livingston 2001; Yeung, Esposito et al. 2010) as shown in figure 3.1 A. RTTA is an *in vitro* serial replating assay, in which only transformed cells form colonies in each round of plating whereas non-transformed cells will exhaust their proliferative capacity after the first or second round of plating. As a result and similar to MAF9 controls, AE transformed cells yielded comparable number of $3^{rd}$ and $4^{th}$ round colonies in the absence or presence of HR Cre, suggesting that Cbfb may not be required for *in vitro* transformation mediated by AE (figure 3.1 B). However, PCR genotyping of cells from $3^{rd}$ round colonies showed incomplete Cbfb deletion in this experimental approach (figure 3.1 C) as a floxed band could still be detected in the HR-Cre co-transduced sample. To overcome this issue, YFP marker as a proxy for active Cre-recombination was used to purify Cbfb deleted cells (figure 3.2 A, B). As a result,

AE9a transduced cells subjected to YFP sort either after the first or second round of replating showed a similar transformation potential as their YFP negative counterparts but with slightly reduced number of colonies (figure 3.2 C, D). Crucially, the YFP positive AE9a transformed cells show a complete deletion of Cbfb in multiple round of replating (figure 3.2E), suggesting that Cbfb may be dispensable for AE9a transformation of bone marrow cells.

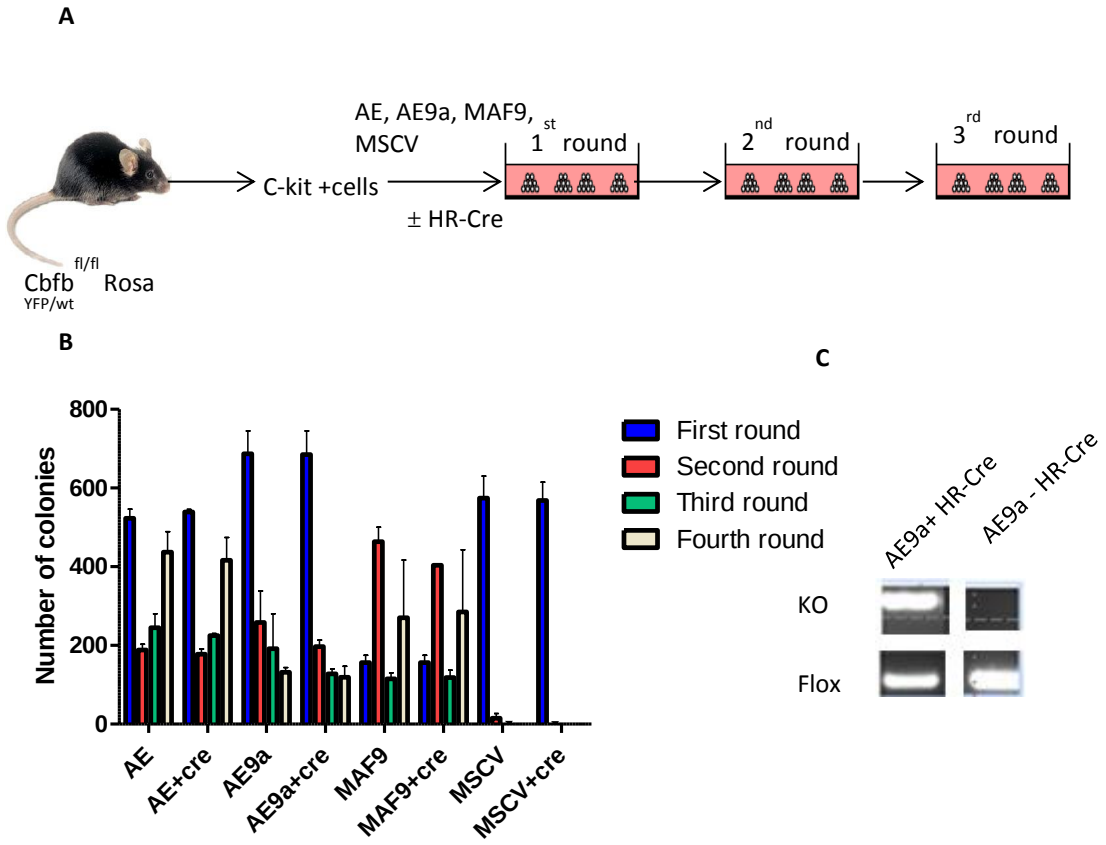


Figure 3-1 Complete deletion of Cbfb was not achievable using HR-Cre without sorting.

(A) A diagram shows the strategy for investigating the role of Cbfb in AE activity using c-Kit isolated from Cbfbf/f RosaYFP/WT mouse. (B) A bar chart illustrates numbers of first-, second-, third- and fourth-round colonies of AE, AE9a, MAF9 and MSCV transduced cells in the presence and absence of HR-Cre. Error bars indicate mean ± SD of three independent experiments. (C) A representative samples show genotyping of the third round colonies of AE9a transformed cells.

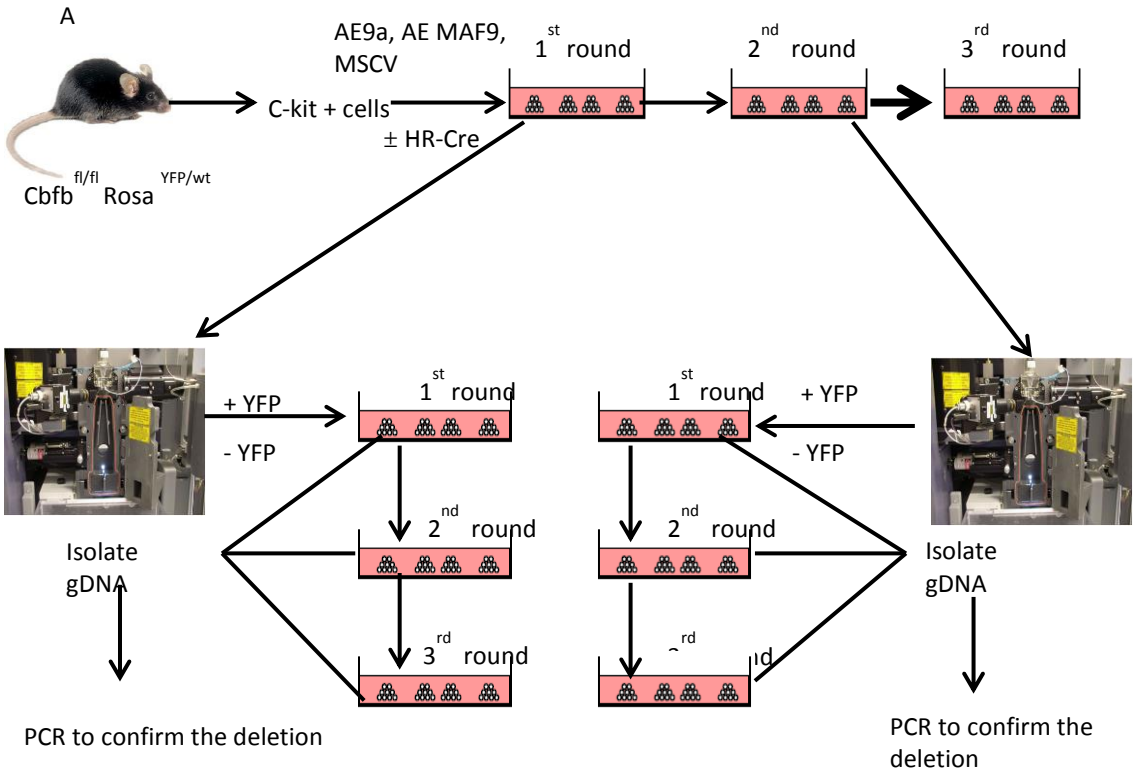
A
AE9a, AE MAF9, MSCV
1st round
2nd round
3rd round
C-kit + cells
± HR-Cre
Cbfb fl/fl Rosa YFP/wt
+ YFP
- YFP
Isolate gDNA
PCR to confirm the deletion
PCR to confirm the deletion

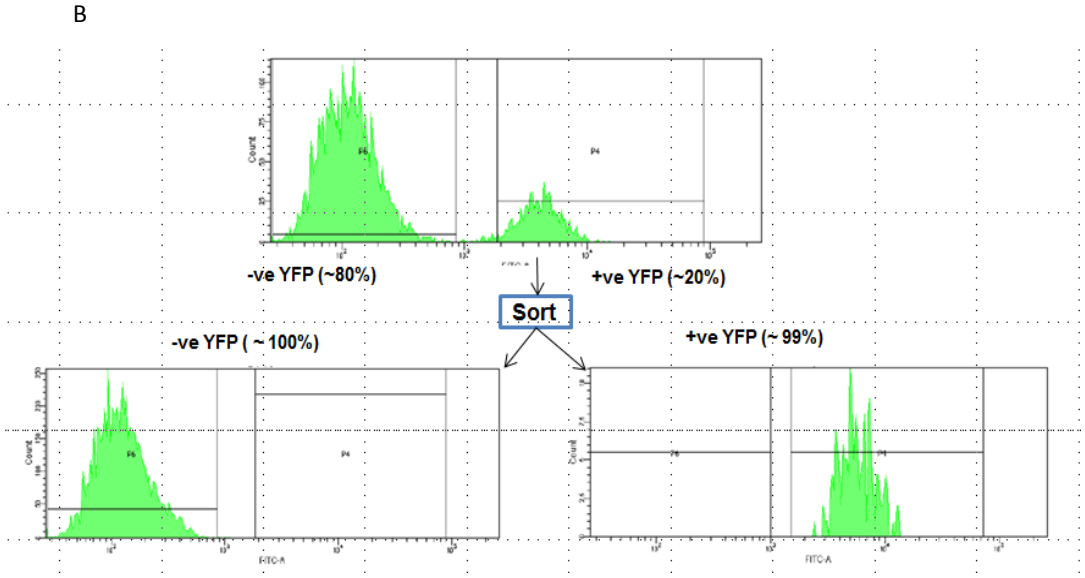
B
-ve YFP (~80%)
+ve YFP (~20%)
Sort
-ve YFP ( ~ 100%)
+ve YFP (~ 99%)

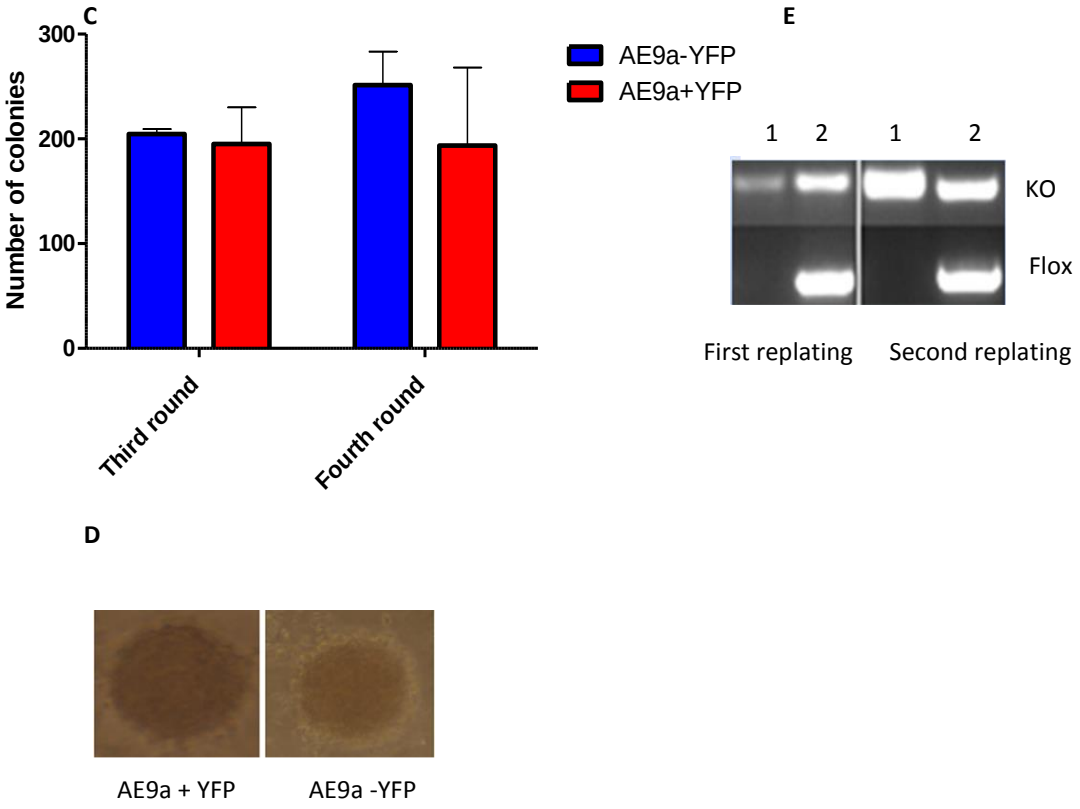


Figure 3-2 Sorting strategy to achieve a complete deletion of Cbfb.

(A and B) Diagrams show the sorting strategy to achieve a complete deletion of Cbfb and also to enrich the deleted cells (C) A bar chart illustrates numbers of third- and fourth - round colonies of sorted AE9a transduced cells. Error bars indicate mean ± SD of two independent experiments. (D) Photos show colony morphology of sorted AE9a - and + YFP transduced cells. (E) A representative samples show genotyping of the sorted AE9a transduced cells 1: AE9a + YFP, 2: AE9a –YFP.

### *3.2.1.2 Cbfbfl/fl Rosa 26 Cre ER mouse*

In order to reduce toxicity associated with viral Cre expression and to exert better control of the Cre recombinase, an improved Cbfbfl/fl Rosa26 CreER mouse model has been generated by crossing the existing Cbfbfl/fl mouse with a Rosa26 Cre ER mouse. This new mouse model has been also backcrossed for 6 generations with C57BL/6 mice to obtain a pure C57BL/6background for future transplantation studies. In contrast to the previous mouse model, the activity of Cre in the Cbfbfl/fl Rosa26 CreER mouse can be controlled by addition of tamoxifen both *in vivo* and *in vitro*. To further characterize this mouse model, qPCR primers and probes were designed to detect the expression level of both Cbfb major and minor transcripts. As illustrated in figure 3.3 A, exon 4-5 and exon 4-6 were considered to design primers and probe that specifically detect the expression level of the major and minor transcripts, respectively. *In vitro* incubation of AE9a transformed Cbfbfl/fl Rosa26 Cre ER bone marrow cells with tamoxifen (25nM 4-OHT, Sigma) for 3 days resulted in a complete deletion of the major transcript of Cbfb as determined by qPCR (figure 3.3 B). Although, the deleted cells still expressed the minor transcript mRNA (figure 3.3 B), its expression level was lower than the major one (figure 3.3 C). A higher concentration of 4-OHT (50nM) was required to achieve a complete deletion of cbfb in the MTA assay as determined by genotyping PCR on genomic DNA (figure 3.4 A). Also, similar results were observed at the protein level as demonstrated by WB (figure 3.4 B) confirming that deletion of Cbfb in this mouse model, and likely in the previous mouse model, as it utilized the same Cbfb targeting strategy, resulted in a spliced isoform lacking exon 5. To investigate the

properties of the spliced isoform, in particular its potential to interact with AE, both WT Cbfb as well as the spliced form were tagged with HA tag and co-expressed with Flag-tagged AEs. As expected, the WT Cbfb was able to bind both forms of AE (AE, AE9a) and failed to interact with mutant AE M106V carrying a point mutation that disrupts Cbfb binding (Kwok, Zeisig et al. 2009), whereas the Cbfb spliced form was not able to bind AEs (figure 3.4 C).

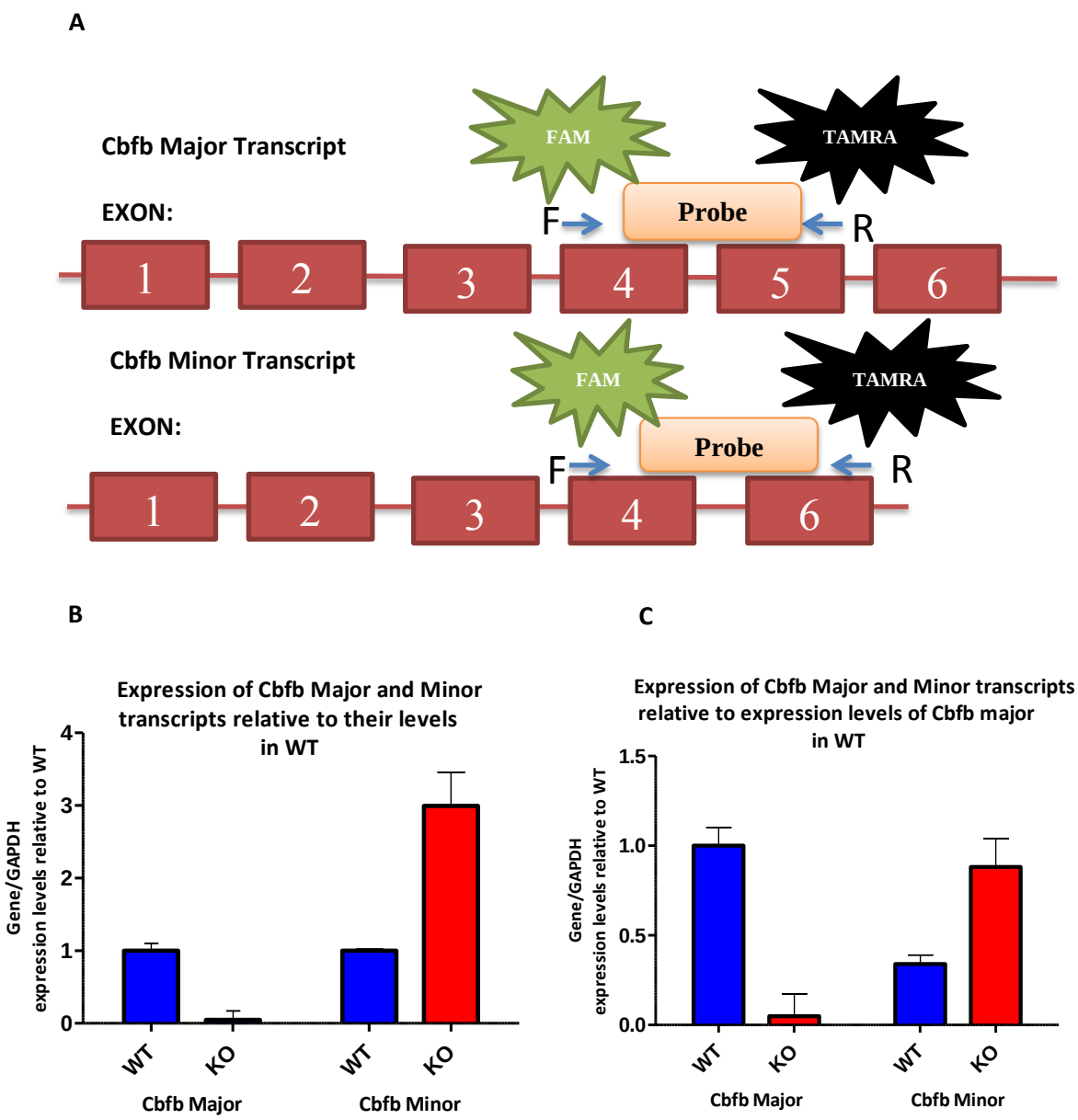


Figure 3-3 Quantifying the expression level of the major and minor transcripts of Cbfb.

(A) A diagram illustrates locations of the primers and probes that used for qPCR to detect the expression levels of Cbfb transcripts. (B) Expression of cbfb major and minor transcript in WT and KO samples relative to their levels in WT assessed by RT-qPCR. (C) Expression of cbfb major and minor transcript in WT and KO samples relative to the expression level of Cbfb major transcript in WT assessed by RT-qPCR. Error bars represent mean ± SD of three independent experiments.

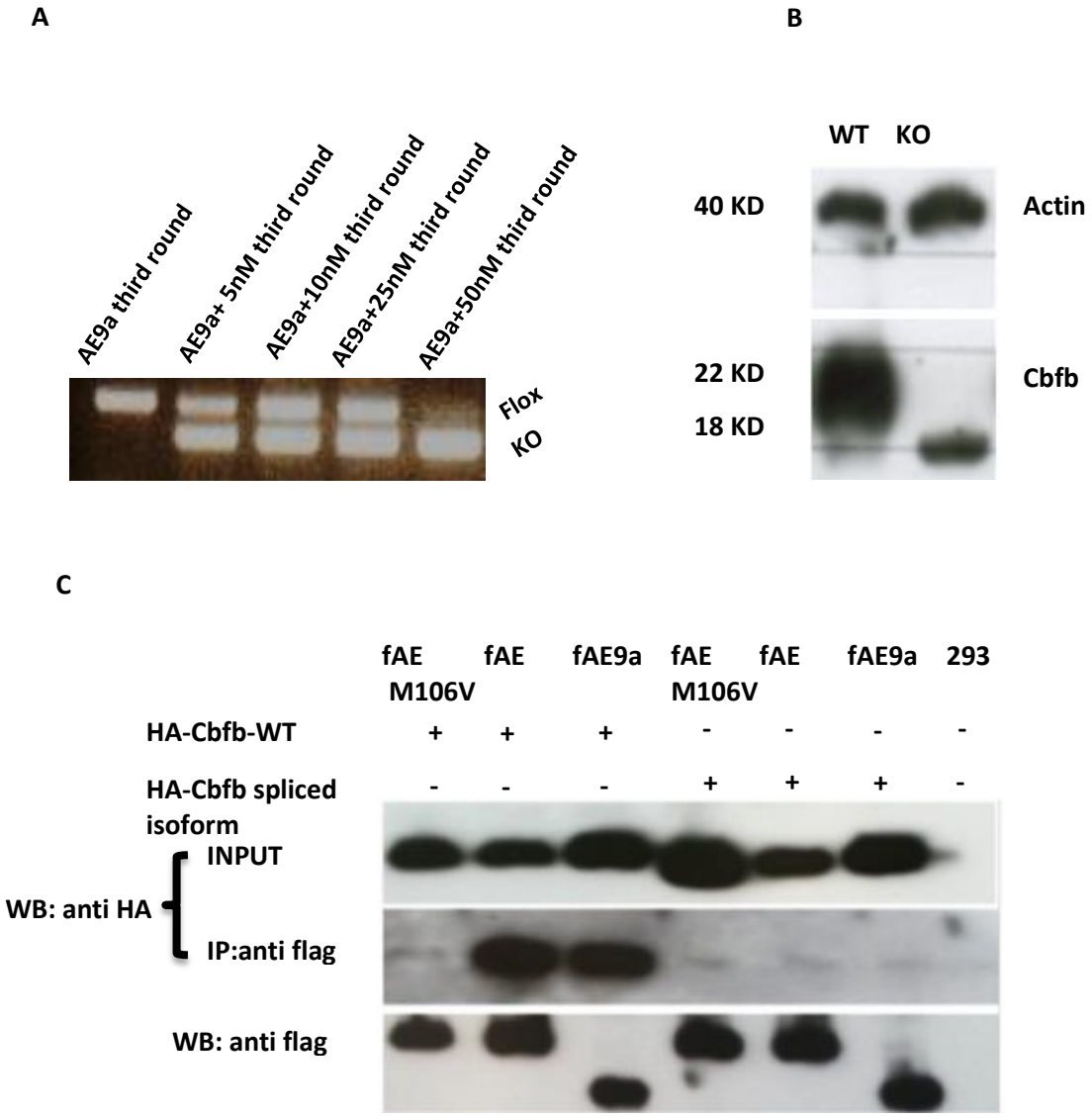


Figure 3-4 Clarifying the interaction between AEs and Cbfb.

(A) Genotyping of c-kit+ cells isolated from Cbfbfl/fl Rosa26 CreER mouse and subjected to RTTA using different concentration of 4-OHT (5, 10, 25, 50nM). (B) Western blot (WB) of transformed primary bone morrow cells with or without 4-OHT treatment using anti Cbfb or anti actin antibodies (loading control). (C)Co-immunoprecipitation assay between flag-tagged AEs and HA-tagged Cbfb constructs. Anti-flag Antibodies used for immunoprecipitation (IP) and anti-HA antibodies used for WB.

To gain better insight into the role of Cbfb in AE *in vitro* transformation, c-kit positive haematopoietic stem/progenitor cells were isolated from Cbfbfl/fl Rosa26 CreER mice, transduced with AE, AE9a and MN1 and subjected to RTTA as described earlier in the absence or presence of tamoxifen (50 nM 4-OHT, Sigma). Cells were serially replated following either tamoxifen or the vehicle (ethanol) treatment after the first round of plating. Although a reduction in the numbers of colonies of the tamoxifen treated AE and AE9a transduced cells was observed particularly during the third round of plating along with modest changes on the morphology, AE transformation was impaired but not completely abolished as these cells were able to form third and fourth-round colonies (figure 3.5 A, E). PCR genotyping confirming a complete deletion of Cbfb in tamoxifen treated samples (figure 3.5 B) demonstrating the robustness of the new mouse model. In addition, the transformed cells do express AE as it was confirmed using RT-PCR (figure 3.5 D). In contrast, colony numbers of MN1 transformed cells were similar with or without tamoxifen treatment, suggesting that MN1 *in vitro* mediated transformation is Cbfb totally independent (figure 3.5 A). To investigate the impact of Cbfb deletion on maintenance of AE or MN1 transformation, transformed cells were harvested after the third round and subjected to 4-OHT treatment and plated for further rounds. The maintenance of AE transformed cells was significantly compromised upon Cbfb deletion as it resulted in a significant reduction of colonies compared to the control and loss of Cbfb had no effect on the maintenance of MN1 transformation (figure 3.5 C).

To investigate the role of Cbfb in MN1 leukaemogenesis, pre-LSC MN1 cell lines (early transformed primary cells) for both Cbfb WT and KO were established after the third round of replating and then injected into sub lethal irradiated SJL mice. Both Pre-LSC cell lines could effectively induce leukaemia in primary recipients (figure 3.5 F). Interestingly, mice injected with Pre-LSC MN1-del Cbfb developed leukaemia faster than the non-deleted cells (figure 3.5 F). Similar results were also obtained when Cbfb was deleted *in vivo* after the transplantation (figure 3.5 F). PCR genotyping showed that a complete Cbfb deletion was achieved in MN1 leukaemic cells (figure 3.5 G). These data strongly suggest that MN1 leuakemogenesis is independent of Cbfb and its deletion may even promote MN1-mediated leukaemogenesis.

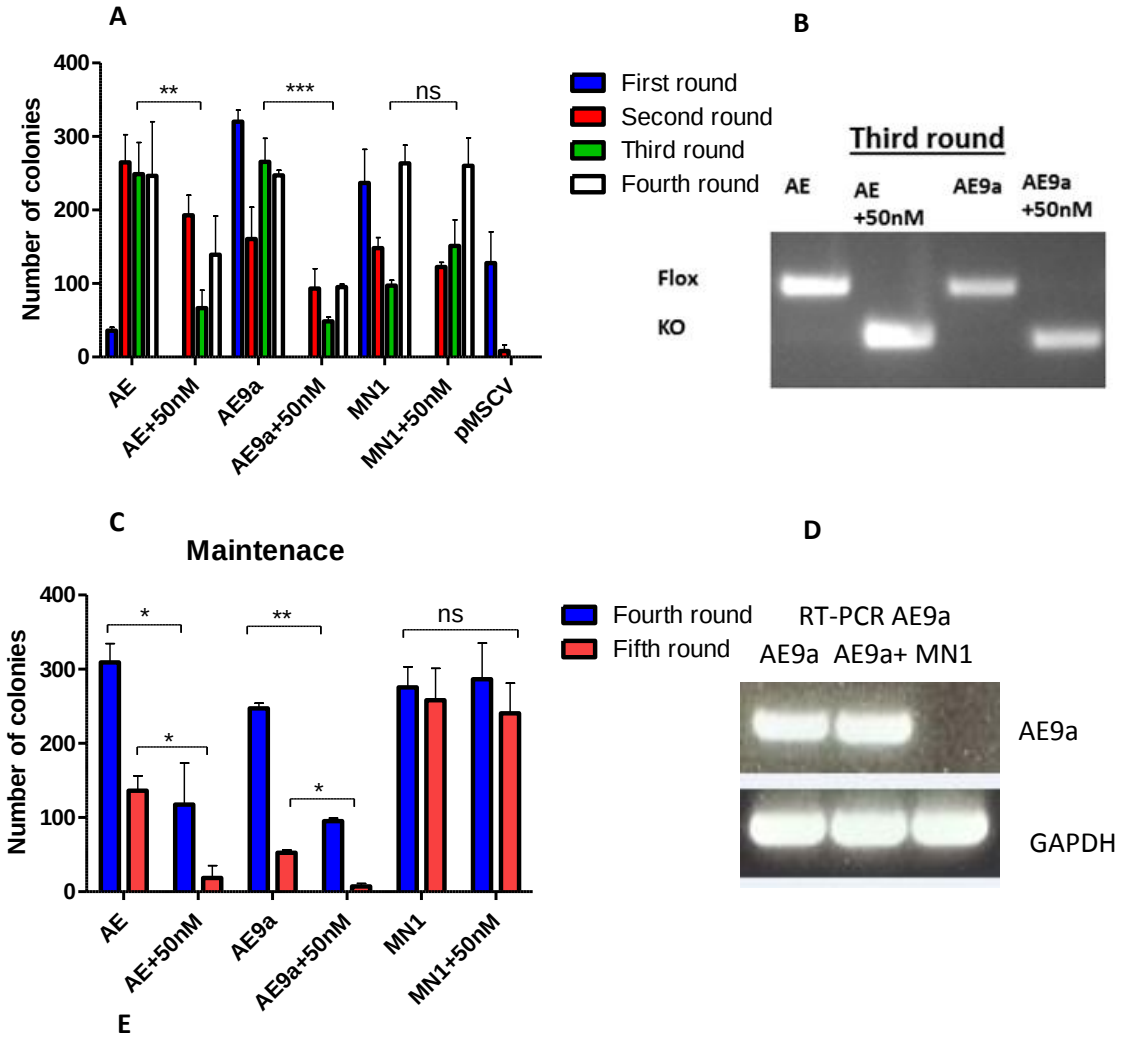
A
Number of colonies
400
300
200
100
0
**
***
ns
AE
AE+50nM
AE9a
AE9a+50nM
MN1
MN1+50nM
pMSCV
B
First round
Second round
Third round
Fourth round
Third round
AE
AE +50nM
AE9a
AE9a +50nM
Flox
KO
C
Maintenace
Number of colonies
400
300
200
100
0
*
*
**
*
ns
AE
AE+50nM
AE9a
AE9a+50nM
MN1
MN1+50nM
D
Fourth round
Fifth round
RT-PCR AE9a
AE9a
AE9a+ MN1
AE9a
GAPDH
E
pMSCV AE
pMSCV AE +50nM
pMSCV AE9a
pMSCV AE9a +50nM
4X
10X
20X

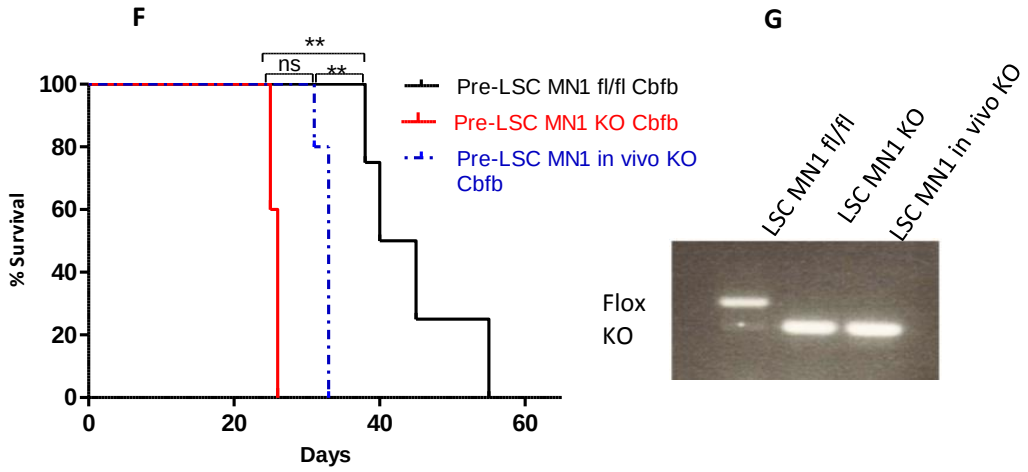


Figure 3-5 AE in vitro activity was affected upon cbfb deletion but does not completely abolished.

(A) A bar chart illustrates numbers of first-, second-, third- and fourth-round colonies of AE, AE9a, MN1 and MSCV transduced cells in the presence and absence of 4-OHT. Error bars indicate mean ± SD of four independent experiments. (B) Representative samples for genotyping of the AE transformed cells showing the deleted as well as the floxed bands of Cbfb. (C) A bar chart illustrates numbers of fourth- and fifth-round colonies of AE, AE9a, MN1 transformed cells with or without 4-OHT treatment. Error bars indicate mean ± SD of two independent experiments. (D) Representative samples for RT-PCR confirming the expression of AE9a. (E) Colony morphology of AEs transformed primary bone marrow cells in the 3rd round of plating with and without 4-OHT treatment using different magnifications. (F) Kaplan-Meier survival curve of MN1 transplanted mice with and without tamoxifen treatment (WT cbfb n=4, KO cbfb n=5, in vivo KO n=5). (G) Representative samples show genotyping of LSC MN1 cells.

### 3.2.2 The impact of Cbfb deletion on the *in vitro* self-renewal of LSK, CMP and GMP cells transformed with AEs.

In addition to investigate the role of Cbfb in AE transformation of bone marrow c-kit+ haematopoietic stem/progenitor cells, another aim of my study was to identify the identity of haematopoietic cells susceptible to AE transformation, i.e. the cell of origin and determine the Cbfb dependency in AE mediated transformation in these populations. In addition to the use of primary bone marrow cells carrying Cbfb floxed alleles, a complementary approach using AE mutants with specific mutations affecting Cbfb interaction was also employed. For the latter, haematopoietic stem/progenitor cells were sorted from WT mice and subjected to RTTA with AE full length, AE9a short form, empty vector and the AEY113A/T161A mutant, which carries 2 point mutations disrupting its Cbfb interaction (Roudaia, Cheney et al. 2009; Kwok, Zeisig et al. 2010). Briefly, mononuclear cells were isolated from 5 WT mice, pooled together and then subjected to lineage (lin) depletion. Lin- cells were collected and stained with Sca1, c-kit, CD34 and CD16/32. Progenitors and LSK were gated using Sca1 and c-kit markers and then CD34 together with CD16/32 were used to differentiate between GMP and CMP within the progenitors' population (figure 3.6 A)(Yeung and So 2009). To confirm the purity of the sorted cells, a post-sort analysis for LSK, CMP and GMP was conducted which showed a good purity (>91%)(figure 3.6 B). In addition to phenotypic purity analysis, functional CFU assay was performed using the sorted cells and it showed that, as expected, LSK formed mainly GM colonies and the percentage of G and M colonies was higher with GMP comparing to CMP (figure 3.6 C).

Moreover, at the molecular level, we used known markers to further validate the purity of the sorted cells such Mpl and Cebpa that were shown to be highly expressed in LSK and GMP, respectively (Zhang, Iwasaki-Arai et al. 2004; Chou and Mulloy 2011) (figure 3.6 D, E). Interestingly, our data also demonstrated that expression of Cbfb is high in HSCs and then decreases through haematopoietic differentiation (figure 3.6 F).

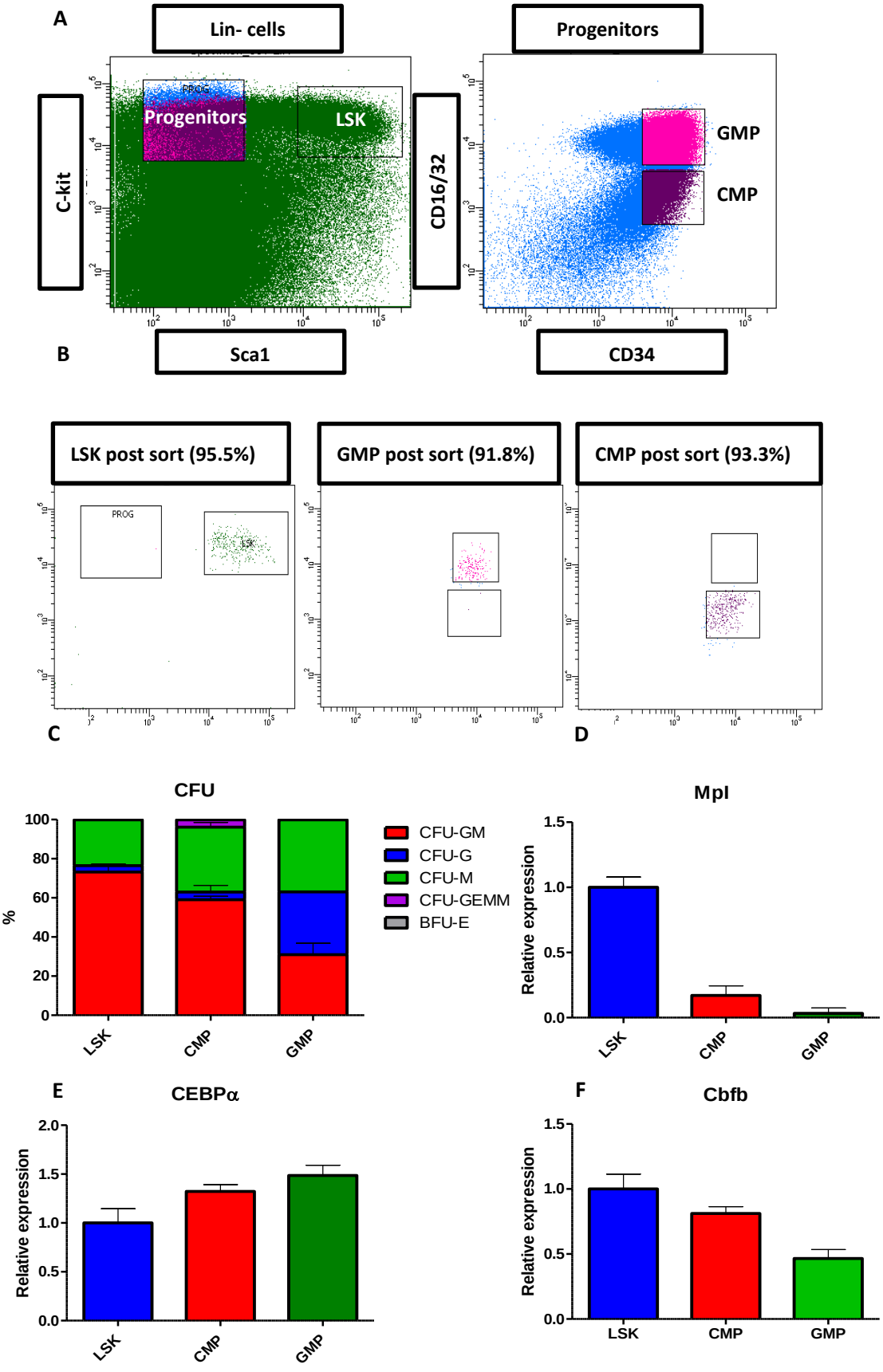
A
Lin- cells
Progenitors
LSK
C-kit
Sca1
B
Progenitors
CD16/32
CD34
GMP
CMP
LSK post sort (95.5%)
GMP post sort (91.8%)
CMP post sort (93.3%)
PROG
LSK
C
D
CFU
%
CFU-GM
CFU-G
CFU-M
CFU-GEMM
BFU-E
LSK
CMP
GMP
MpI
Relative expression
E
CEBPα
F
Cbfb

Figure 3-6 Sorting of murine haematopoietic stem/progenitor cells.

(A) Our gating strategy for LSK and progenitors in which lin- cells were gated using Sca1 and c-kit markers, GMP and CMP were gated from the progenitors using CD34 and CD16/32 markers. (B) Post sort analysis for LSK, GMP and CMP showing the percentage of their purity. (C) A bar chart illustrates CFU assay of LSK, GMP and CMP cells and the percentage of GM-G-M-GEMM-BFU-E colonies that were able to form. (D-F) A bar chart shows expression of Mpl, Cebpa and Cbfb in LSK, CMP, and GMP isolated from WT mice. Error bars indicate mean ± SD of two independent experiments.

Results from the RTTA demonstrated that AE, AE9a as well as the Cbfb-interaction defective AE mutant Y113A/T161A albeit with reduced numbers of colonies compared to the controls were all able to transform all tested sorted haematopoietic cell populations isolated either from WT (figure 3.7 A) or Cbfbfl/fl Rosa26 CreER mice (figure 3.7 B-D). Collectively, these data suggest that the two forms of AE are able to transform multiple distinct haematopoietic stem/progenitor cell populations and that disrupting the binding between AE and Cbfb either by using a mutant AE (Y113A/T161A) or by deleting Cbfb using 4-OHT (figure 3.7 E) does compromise but not completely impair the *in vitro* AE-mediated transformation suggesting that Cbfb might have a moderate effect on AE-mediated transformation of stem/progenitor cells.

An AE9a transformed cell line from Cbfbfl/fl Rosa26 CreER LSK was established after the RTTA and transplanted into mice to test if a novel AE leukaemia model could be created. This cell line expressed Mac1, Gr1 and was CD45.2 positive (figure 3.7 F) and was injected into two groups of irradiated mice; one of them was treated with tamoxifen a week later to delete Cbfb, the other served as control. Although mice were followed up for almost one year, neither AE9a Cbfb f/f nor Cbfb KO was able to induce leukaemia (figure 3.7 G) .

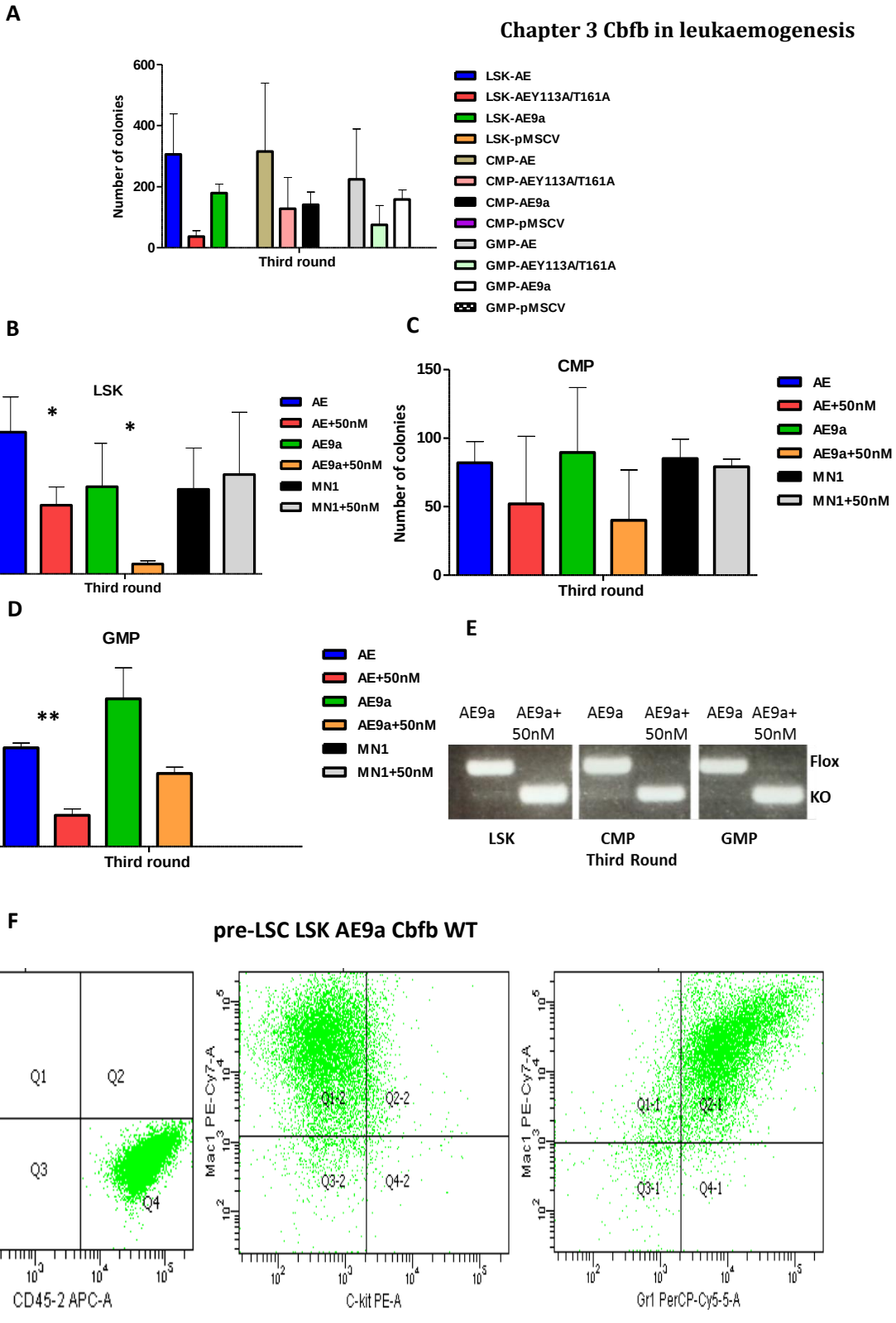
A
Number of colonies
Third round
LSK-AE
LSK-AEY113A/T161A
LSK-AE9a
LSK-pMSCV
CMP-AE
CMP-AEY113A/T161A
CMP-AE9a
CMP-pMSCV
GMP-AE
GMP-AEY113A/T161A
GMP-AE9a
GMP-pMSCV
B
LSK
AE
AE+50nM
AE9a
AE9a+50nM
MN1
MN1+50nM
C
CMP
D
GMP
E
AE9a
AE9a+ 50nM
Flox
KO
LSK
CMP
GMP
Third Round
F
pre-LSC LSK AE9a Cbfb WT
CD45-1 FITC-A
CD45-2 APC-A
Mac1 PE-Cy7-A
C-kit PE-A
Gr1 PerCP-Cy5-5-A

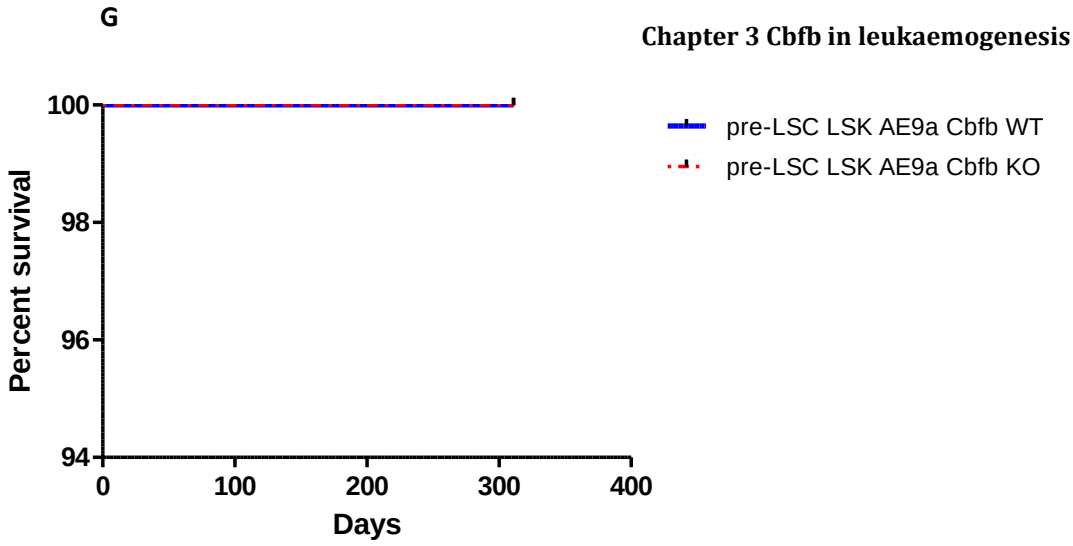


Figure 3-7 Deletion of Cbfb resulted in a reduced numbers of third -round colonies of AE transformed LSK, CMP and GMP.

(A) Numbers of third-round colonies of sorted distinct haematopoietic cell populations (LSK, CMP, and GMP) isolated from WT and transduced by AE, AE9a and AEY113A/T161A mutant. (B-D) Numbers of third-round colonies of sorted distinct haematopoietic cell populations (LSK, CMP, and GMP) isolated from Cbfbfl/fl Rosa26 CreER mice and transduced by AE, AE9a and MN1 with and without 4-OHT treatment. Error bars indicate mean ± SD of two independent experiments. (E) Representative samples for genotyping of the third round of the AE9a transformed LSK, CMP and GMP showing the deleted as well as the floxed bands of Cbfb. (F) Flow cytometric analysis showing the phenotype of pre-LSC LSK AE9a Cbfb WT. (G) Kaplan-Meier survival curves of mice transplanted with pre-LSC LSK AE9a Cbfb WT cells with and without tamoxifen treatment (WT cbfb n=5, KO cbfb n=5).

### 3.2.3 Establishing an *in vivo* model to further clarify the role of Cbfb in AE leukemogenesis.

It is well known that the full length AE alone is not able to induce leukaemia in murine models and other mutations in e.g. KIT or RAS cooperating with AE are needed to establish AE leukaemia in murine models (Wang, Zhao et al. 2011; Zhao, Zhang et al. 2014). On the hand, the short form of AE (AE9a) which was detected in AML patients can efficiently induce leukaemia in murine models only when fetal liver cells are used (Yan, Kanbe et al. 2006). Therefore, we used the fetal liver approach together with AE9a to establish our AE leukaemia model with conditional Cbfb floxed alleles. To first characterize their self-renewal property *in vitro*, fetal liver cells (E11-E15.5) were isolated from Cbfbfl/fl Rosa26 CreER embryos and subjected to RTTA assay with or without 4-OHT treatments using MigR1AE9a construct, which carries a GFP marker. As a result, enhanced self-renewal of fetal liver cells transformed with AE9a was observed as the transformed cells harbouring Cbfb floxed alleles were able to form colonies for multiple rounds of replating (figure 3.8 A). In contrast, deletion of cbfb resulted in a significant reduction in AE9a mediated transformation ability as the deleted cells started to lose their ability to form colonies comparing to the Cbfb floxed controls (figure 3.8 A). Moreover, a cell line was created after the third round of plating and subjected to an *in vitro* 4-OHT treatment (20nM) for 72 hours which was sufficient to achieve a complete deletion of Cbfb (figure 3.8 B). The Cbfb-deleted cells lost their ability to proliferate, started to attach to the flask and the cytospin preparations showed that most of them differentiated in mature myeloid cells such as macrophages (figure 3.8 C).

To test the *in vivo* leukaemia properties, the established cell line was injected into irradiated mice and the transplanted animals were divided into two groups; one group received tamoxifen treatment to induce the deletion of Cbfb one week after transplantation, the other served as control. Unfortunately, neither the control group nor the treated one develop leukaemia and this experiment was terminated after around a year (figure 3.8 D).

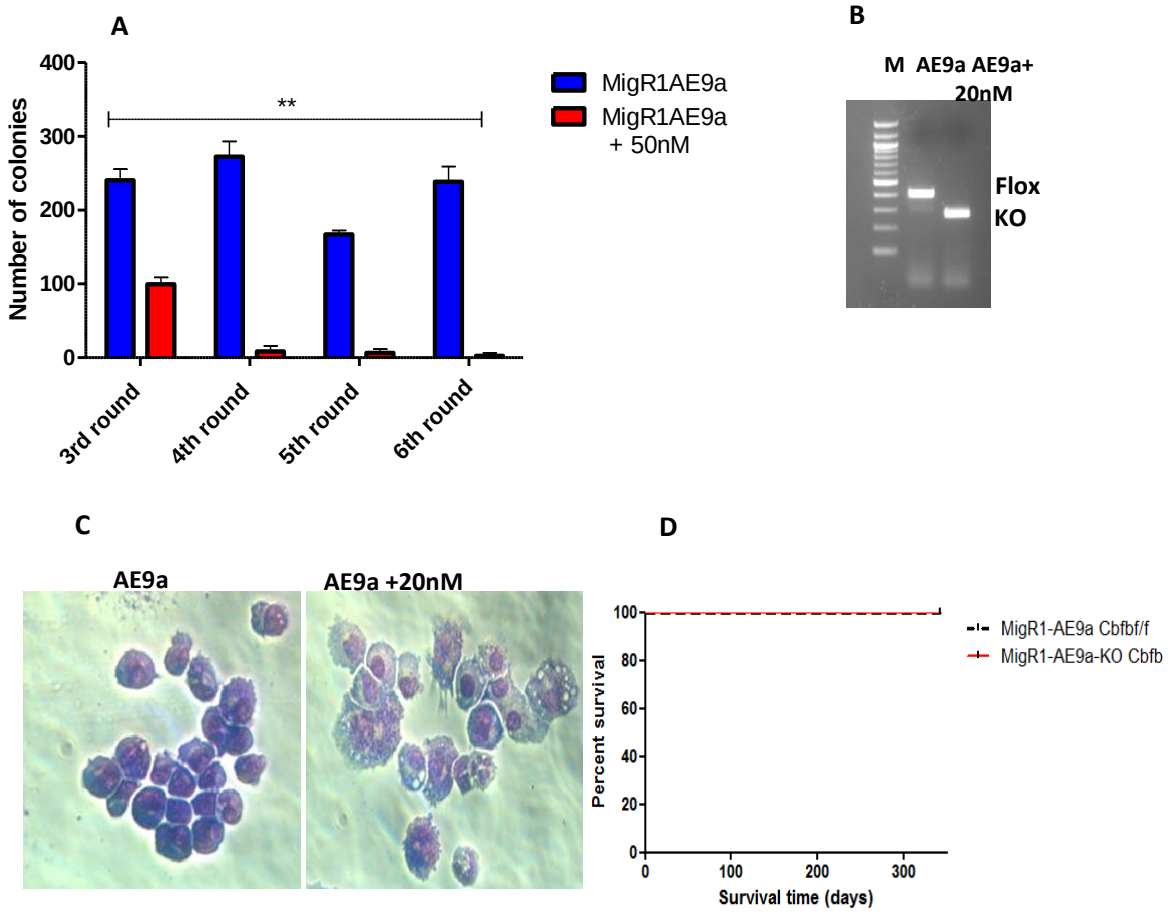


Figure 3-8 Self-renewal of fetal liver cells transformed with AE9a was severely compromised upon Cbfb deletion.

(A) A bar chart illustrates numbers of third-, fourth-, fifth- and sixth-round colonies of AE9a with or without 4-OHT treatment. Error bars indicate mean ± SD of two independent experiments. (B) Representative samples for genotyping of the AE9a transformed cells showing the deleted as well as the floxed bands of Cbfb. (C) Cytospin stains for AE9a transformed cells with and without 4-OHT treatment. (D) Kaplan-Meier survival curves of mice transplanted with AE9a cell line with and without tamoxifen treatment (WT cbfb n=5, KO cbfb n=5).

In parallel, another approach was used in which fetal liver cells (E15.5) were isolated from Cbfbfl/fl Rosa26 CreER embryos and transduced with MigR1 AE9a and transplanted into mice 2 days after retroviral transdcution. The phonotypes of the transduced cells were analysed before transplantation into irradiated mice. One week after transplantation mice were split in to two groups with one group receiving tamoxifen treatment and the other serving as control (figure 3.9 A). Before transplantation, around 10-12% of live cells expressed GFP, are expressing MigR1 AE9a and around 33 % of cells expressed c-Kit (figure 3.9 B).

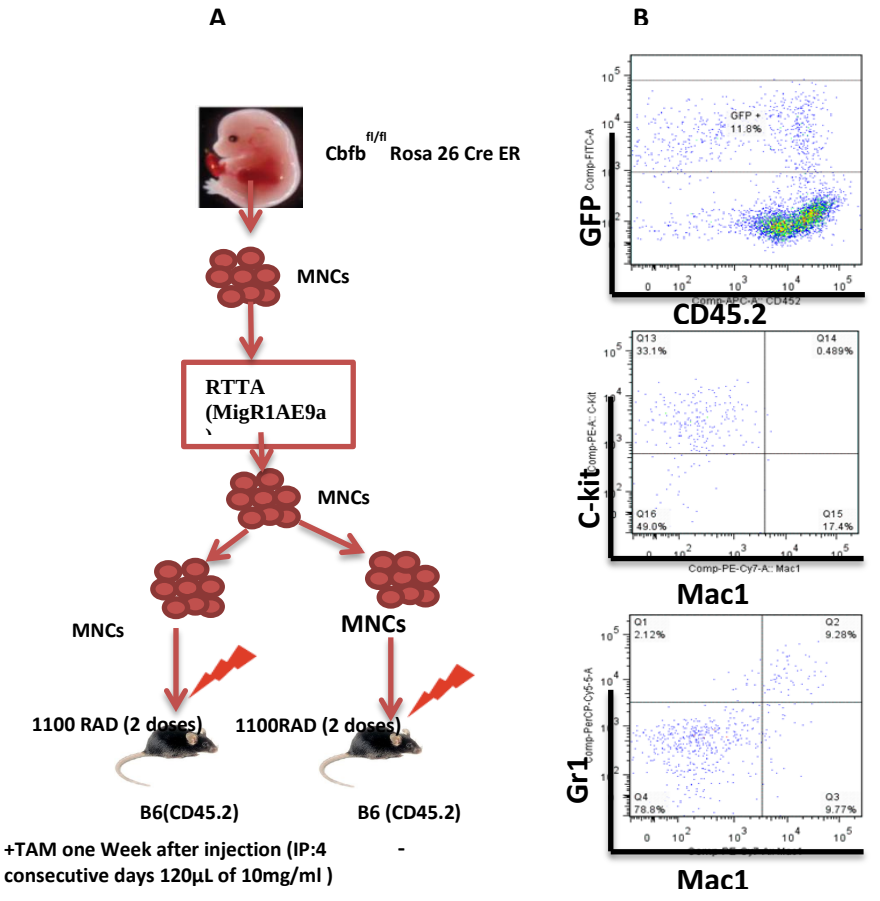


Figure 3-9 Our in vivo approach to establish the leukaemia model.

(A) Schematic diagram illustrating the *in vivo* leukaemogenic experiment. (B) Flow cytometric analysis showing phenotype of the transplanted cells.

### *3.2.3.1 AE9a leukemogenesis is dependent of Cbfb*

The MigR1 AE9a transplanted mice (figure 3.9 A) were monitored for signs of sickness such as loss of weight, weakness and difficulty of breathing. Interestingly, MigR1 AE9a cbfbf/f mice got sick whereas the KO group remains healthy (figure 3.10 A). The sick mice were anaemic, showed high white blood cell (WBC) and had pale femurs, enlarged spleens as well as enlarged livers (table 3.1, figure 3.10 B). Flow cytometric analysis of cells harvested from BM, spleen and liver of the sick mice showed high percentage of $GFP^+$ cells which were c-$Kit^+$ with no expression of lineage markers such as CD11b and Gr-1 (figure 3.10 C). Consistent with previous report showing that CD45 is a downstream target repressed by AE (Lo and Peterson 2013), GFP+ cells didn't express CD45.2. Moreover, the expression of AE9a in GFP+ cells isolated from bone marrow, spleen and liver expressed AE9a was confirmed by RT-PCR (figure 3.10D). In addition, histological hematoxylin/eosin (HE) staining showed infiltration of the blast cells in the spleens and livers comparing to the WT (figure 3.10 E). Moreover, high numbers of blast cells were observed in the peripheral blood (PB), BM, spleen and liver (figure 3.10 F). Together these data not only show that I successfully generated a murine *in vivo* AE9a leukaemia model with Cbfb floxed alleles, but that Cbfb is absolutely required for AE9a mediated leukaemia in this experimental system.

Table 3-1 Features of sick mice injected with MigR1 AE9a fetal liver transformed cells.

| | **WT** | **MigR1 AE9a** |
|---|---|---|
| **WBC ($10^9$/L)*** | 9.1 ± 3.9 | 45.2 ± 30.6 |
| **RBC ($10^{12}$/L)*** | 8.5 ± 0.77 | 2.3 ± 0.9 |
| **HGB (g/dL)*** | 11.1 ± 0.82 | 4.05 ± 1.5 |
| **PLT ($10^9$/L)*** | 687.4 ± 306.5 | 132.4 ± 123.7 |
| **Spleen weight (g)*** | 0.086 ± 0.014 | 0.64 ± 0.12 |
| **Liver weight (g)*** | 1.2 ± 0.28 | 2.5 ± 0.69 |

* Values presented as mean ±SD

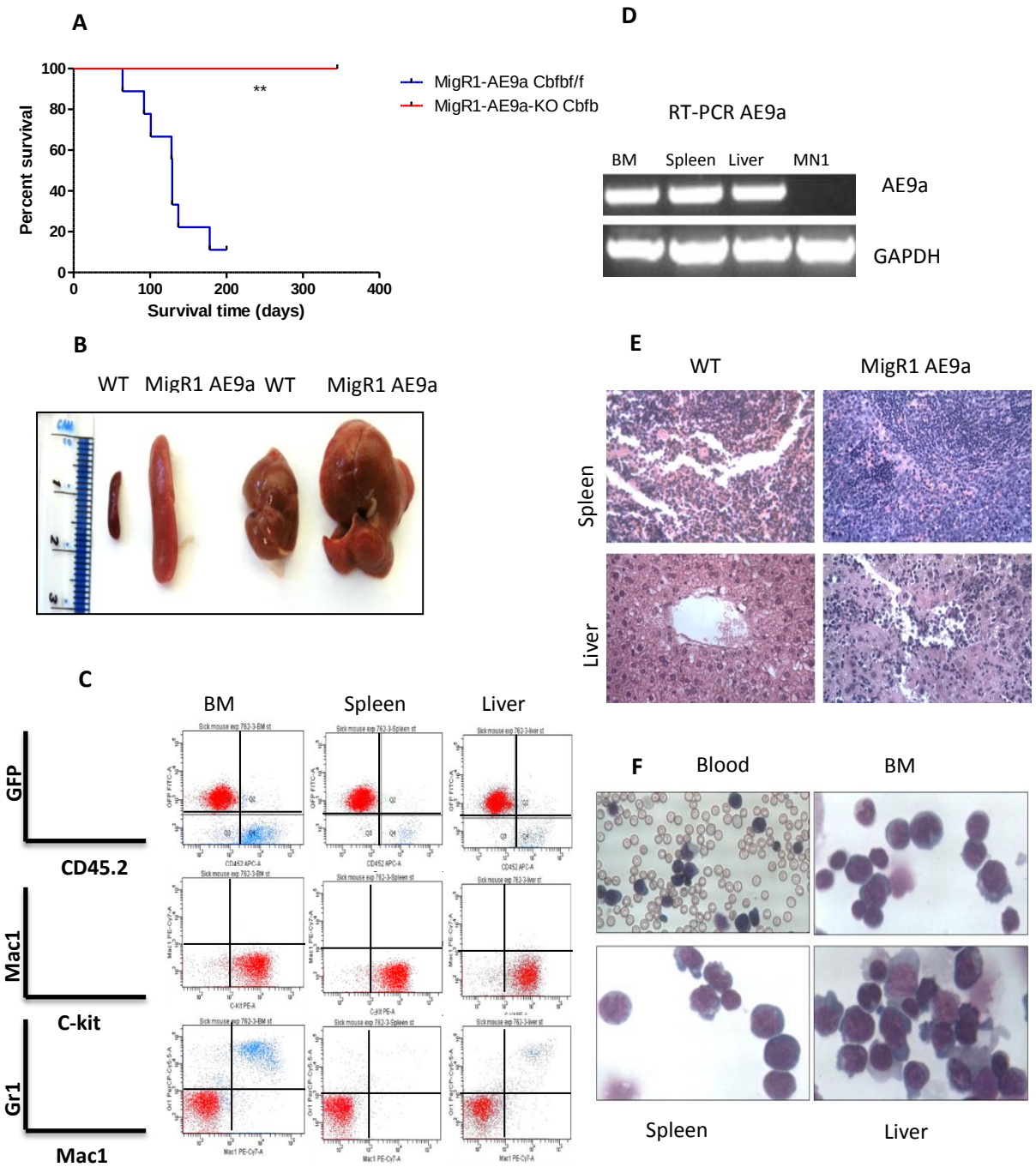


Figure 3-10 AE9a leukemogenesis is dependent of Cbfb.

(A) Kaplan-Meier survival curve of AE9a transplanted with and without tamoxifen treatment (WT cbfb n=12, KO cbfb n=12) (B) Representative photos show the sizes of spleen and liver of healthy WT mice comparing to MigR1 AE9a sick mice. (C) Representative flow cytometry profiles of cells harvested from the BM, spleen and liver of the sick mice. (D) Representative RT-PCR test showing the expression of AE9a. (E) Representative photos show the HE stain of spleen and liver of healthy WT mice comparing to MigR1 AE9a sick mice. (F) Representative photos show the Giemsa stain of cells harvested from PB, BM, spleen and liver of the MigR1 AE9a sick mice.

Next, the impact of Cbfb deletion on maintaining AE9a leukaemia was investigated. To this end, leukaemia cells from primary leukemic mice were harvested and transplanted into two groups of irradiated mice. One group was injected with tamoxifen one week after transplantation to delete Cbfb *in vivo*, the other group served as control. In contrast to mice transplanted with AE9a Cbfb floxed allele leukaemic cells which got sick rapidly with a median survival of 23 days, the Cbfb KO cells were significantly compromised to induce leukaemia in the transplanted mice (figure 3.11 A). Sick mice were anaemic with massive spleens and livers suggesting the infiltration of blasts cells in these organs which was confirmed by HE and Giemsa stains (figure 3.11 B, E, and F). Moreover, these cells expressed AE9a and their phenotypes were identical to the transplanted one as they only expressed c-Kit but not CD45.2, Gr-1 and Mac-1 (figure 3.11 C and D).

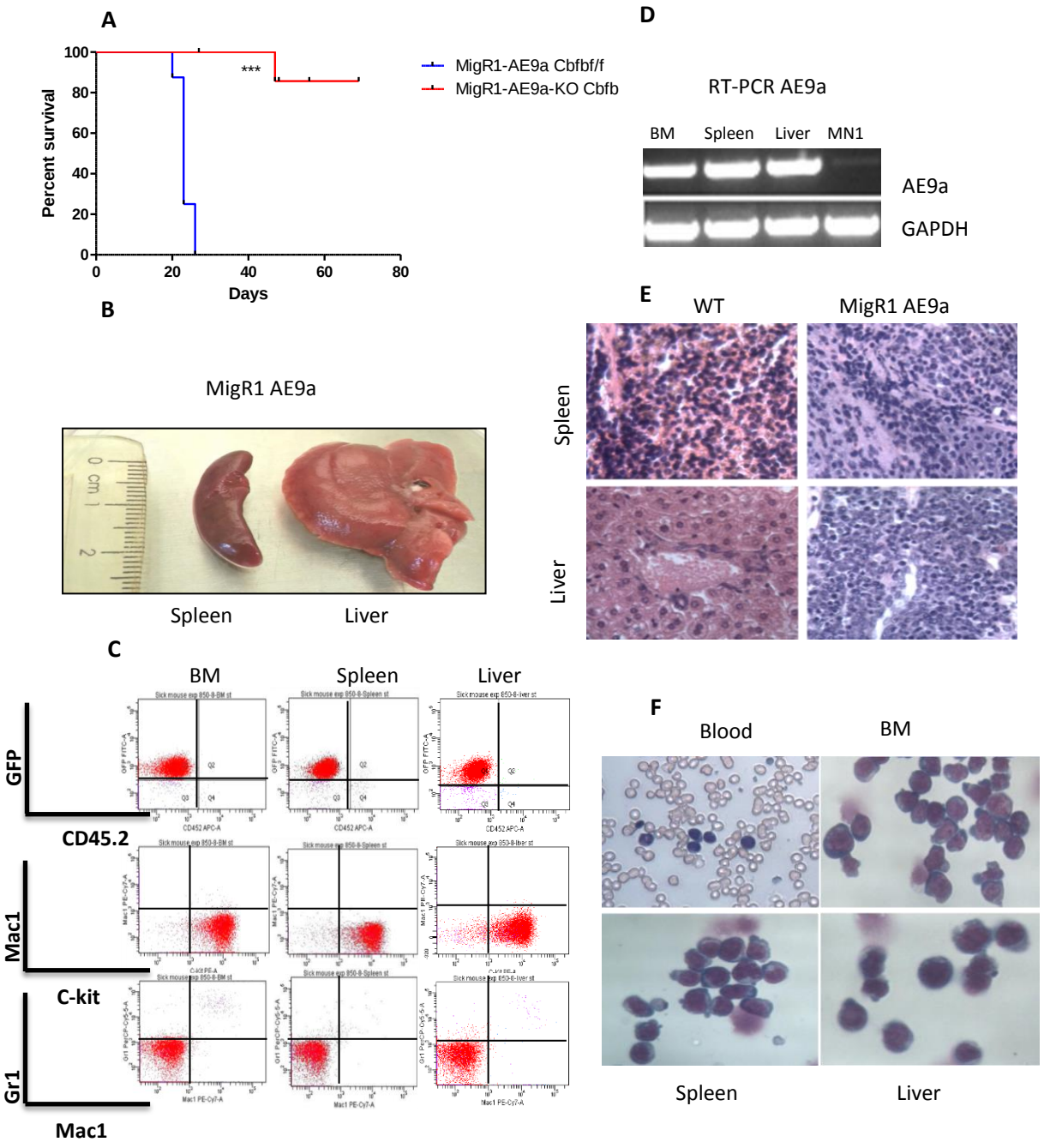


Figure 3-11 The maintenance of AE9a leukemogenesis is dependent of Cbfb.

(A) Kaplan-Meier survival curve of LSCs AE9a transplanted with and without tamoxifen treatment (WT cbfb n=8, KO cbfb n=8) (B) Representative photos show the sizes of spleen and liver of AE9a sick mice. (C) Representative flow cytometry profiles of cells harvested from the BM, spleen and liver of the sick mice. (D) RT-PCR test showing the expression of AE9a. (E) Representative photos show the HE stain of spleen and liver of healthy WT mice comparing to AE9a sick mice. (F) Representative photos show the Giemsa stain of cells harvested from PB, BM, spleen and liver of the AE9a sick mice.

### *3.2.3.2 Expanding of AE9a leukaemic cells*

Given that fetal liver AE9a Cbfb KO cells were severely compromised in their *in vitro* growth and failed to induce leukaemia, I tried to further characterize the fetal liver AE9a Cbfb floxed allele leukaemic cells in the absence or presence of TAM treatment. Several attempts to expand these cells *in vitro* using RPMI medium supplemented with 10ng/ml IL3, 10ng/ml IL6, 20ng/ml SCF, 15% FBS and 1% Pen/Strep failed. To overcome this issue, we transplanted leukaemic cells isolated from our primary leukaemia mouse into two groups of irradiated mice (figure 3.12). A week later, some animals were sacrificed to examine the homing property while the remaining animals were subjected to *in vivo* TAM treatment (3 consecutive injections).

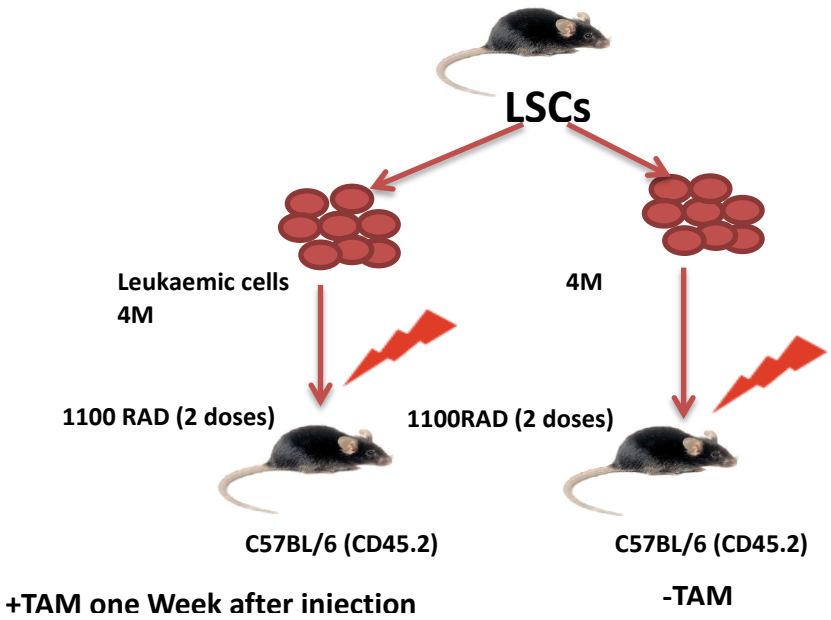


Figure 3-12 Our in vivo approach for expanding LSCs MigR1 AE9a.

Our data showed that the percentage of the leukemic cells that were able to home inside the BM after one week was around 10 % (figure 3.13 A) . 24 h after the third tam injections, the transplanted cells were harvested from the BM of both treated and control groups. They were then subjected to GFP sort for further studies such as genotyping, FACS and cell cycle analysis. The GFP percentage of the leukemic cells from the Cbfb KO group was significantly reduced comparing to the Cbfb floxed control (figure 3.13 B and C). In addition, the percentage of cells expressing c-kit$^{high}$ dropped dramatically after Cbfb KO suggesting a change in the phenotype of these cells (figure 3.13 D and E). Cell cycle analysis revealed that the KO cells were arrested at G0/G1 stage and failed to enter S or G2/M stages compared to the control cells (figure 3.13 F). Consistently, the KO cells were unable to induce leukaemia into secondary recipient whereas the Cbfb floxed controls group succumbed to leukaemia within 21 days (figure 3.13 G).

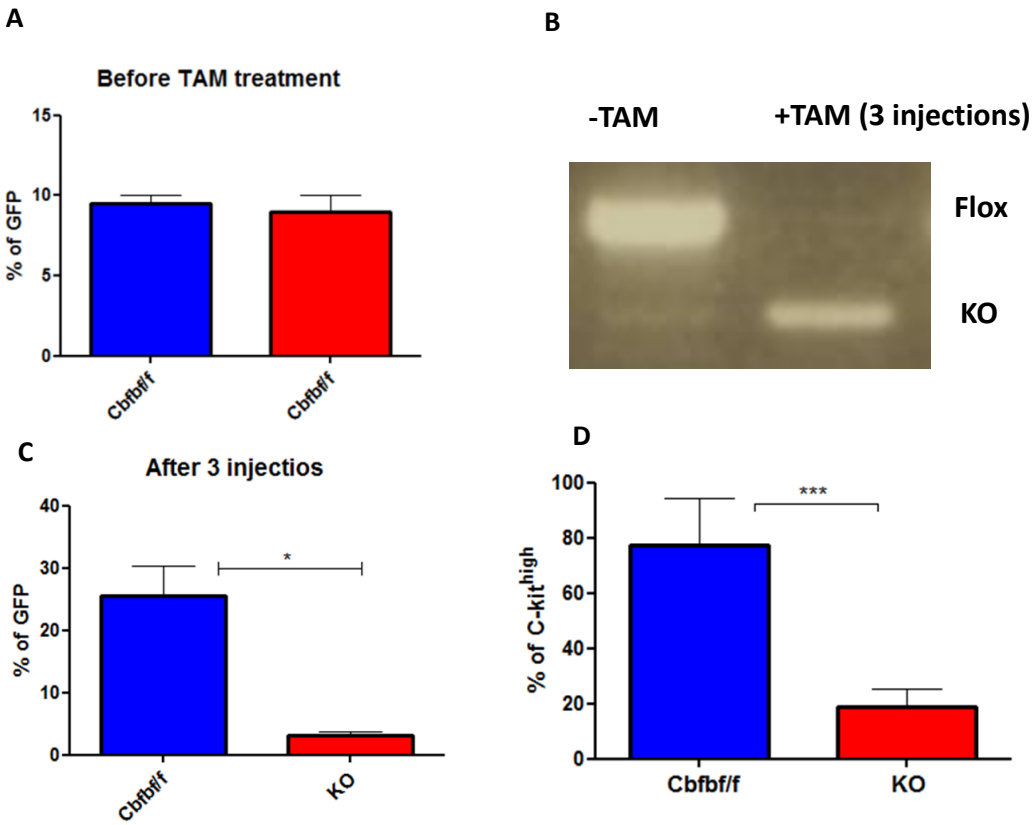

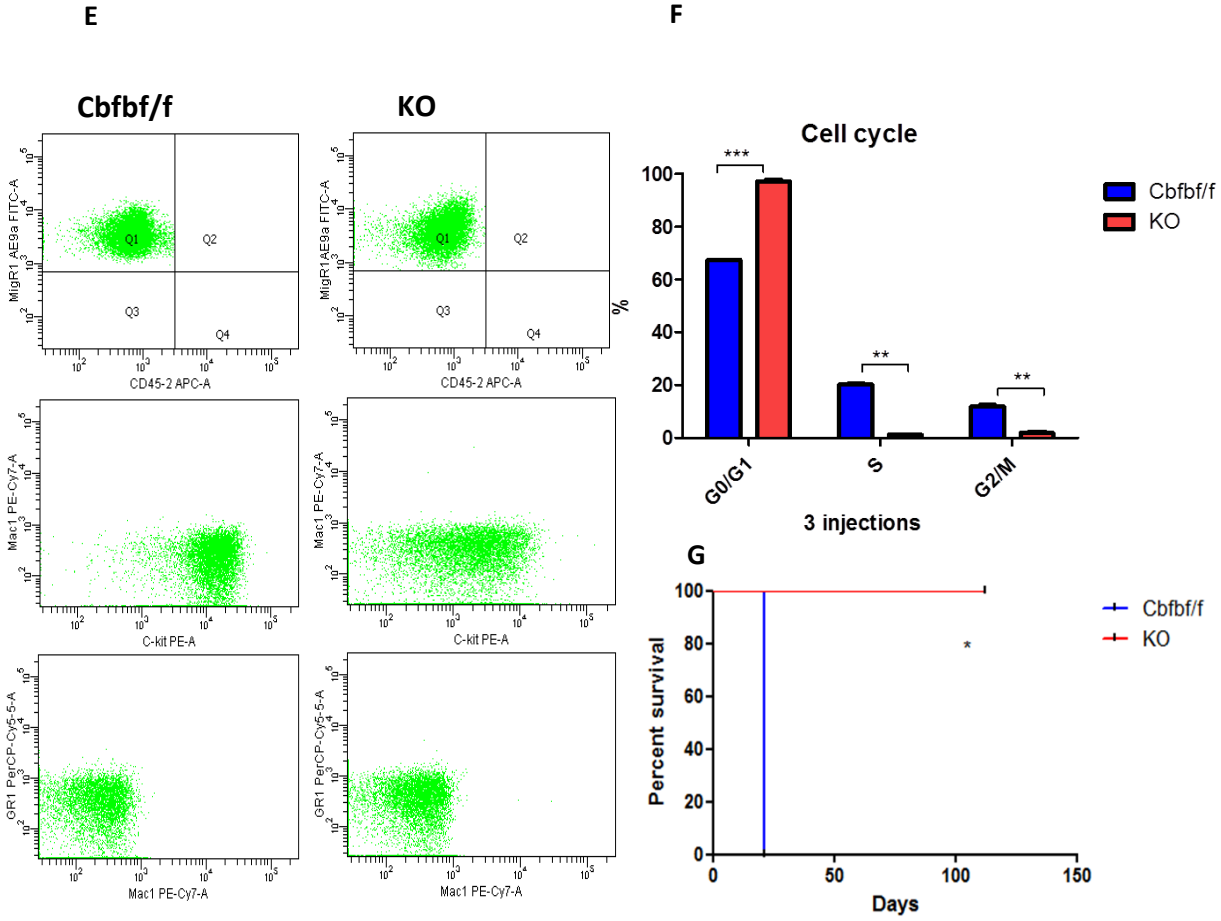


Figure 3-13 Deletion of Cbfb reduced the expansion of AE9a leukaemic cells.

(A) A bar chart illustrates the percentage of leukaemic cells ($GFP^+$) that were able to home in the BM of secondary recipients and harvested one week post transplantation before tamoxifen treatment. (B) Representative samples for genotyping of the AE9a leukemic cells with and without TAM treatment. (C) A bar chart shows the percentage of AE9a leukaemic cells ($GFP^+$) isolated from the Cbfbf/f and KO groups after 3 injections of tamoxifen. (D) A bar chart shows the percentage of AE9a leukaemic cells (sorted $GFP^+$) that expressed c-$kit^{high}$ isolated from the Cbfbf/f and KO. (E) Flow cytometry profiles shows the phenotypes of AE9a leukaemic cells (sorted $GFP^+$) isolated from the Cbfbf/f and KO groups. (F) A bar chart shows the cell cycle profiles of AE9a leukaemic cells ($GFP^+$) cells Cbfbf/f and KO cells. (G) Kaplan-Meier survival curves of AE9a leukaemic cells ($GFP^+$) transplanted mice with and without tamoxifen treatment (Cbfbf/f n=4, KO n=4). AE9a leukaemic cells ($GFP^+$) harvested from primary leukemic mice (MigR1 AE9a Cbfbf/fRosa 26 Cre ER) in this figure are labelled as Cbfb f/f, whereas the tamoxifen treated one are labelled as KO. Error bars indicate data presented as mean ± SD.

### *3.2.3.3 Frequency of AE9a leukaemia initiating cells*

Limiting dilution assays (LDAs) were performed to assess the impact of Cbfb deletion on the frequency of AE9a leukaemia initiating cells. Serially increasing numbers of the leukemic cells (1000 (n=3), 5000 (n=3), 10000 (n=4), 50000 (n=4)) were injected into irradiated mice without TAM treatment. To quantify the LSCs in the Cbfb KO group, 2 cell doses ($0.5x10^6$ (n=4) and $4x10^6$(n=4) were transplanted and subjected to TAM treatment in a week later (4 injections). As a result, all mice injected with 50000 LSCs-AE9a Cbfb floxed allele came down whereas 2 out of 4 from the 10000 cell group got sick. Up-to-now neither 1000 nor 5000 LSCs were able to induce leukaemia (figure 3.14 A and C). Although higher dose of cells ($0.5x10^6$ and $4x10^6$) were used for the KO group, neither of them were able to induce leukaemia (figure 3.14 B and D). Therefore, the estimated frequency of leukaemia initiating cells was calculated using ELDA (Extreme Limiting Dilution Analysis) (Hu and Smyth 2009) and for the WT group it was found as 1/17468 and for the KO one it was below 1/6008548.

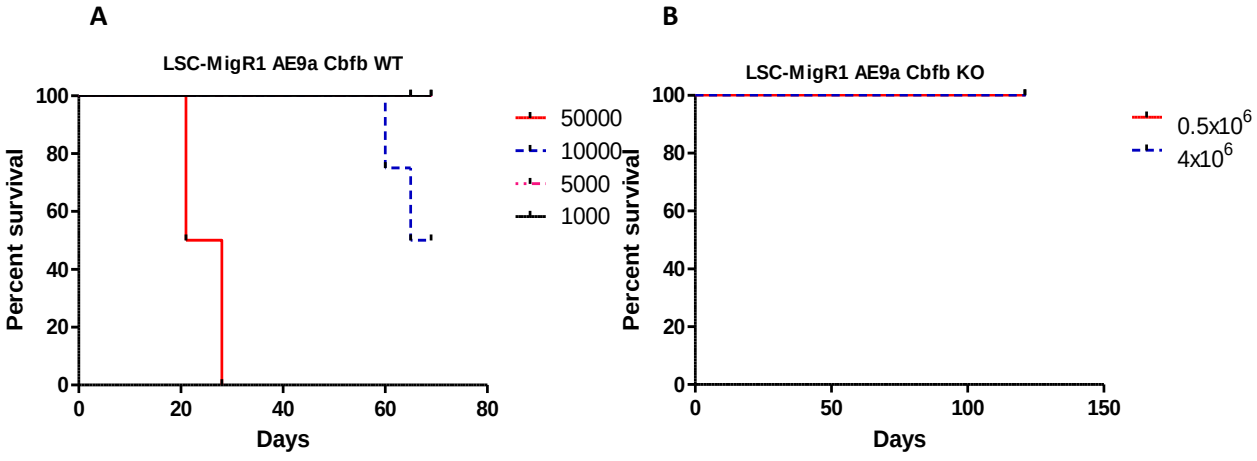

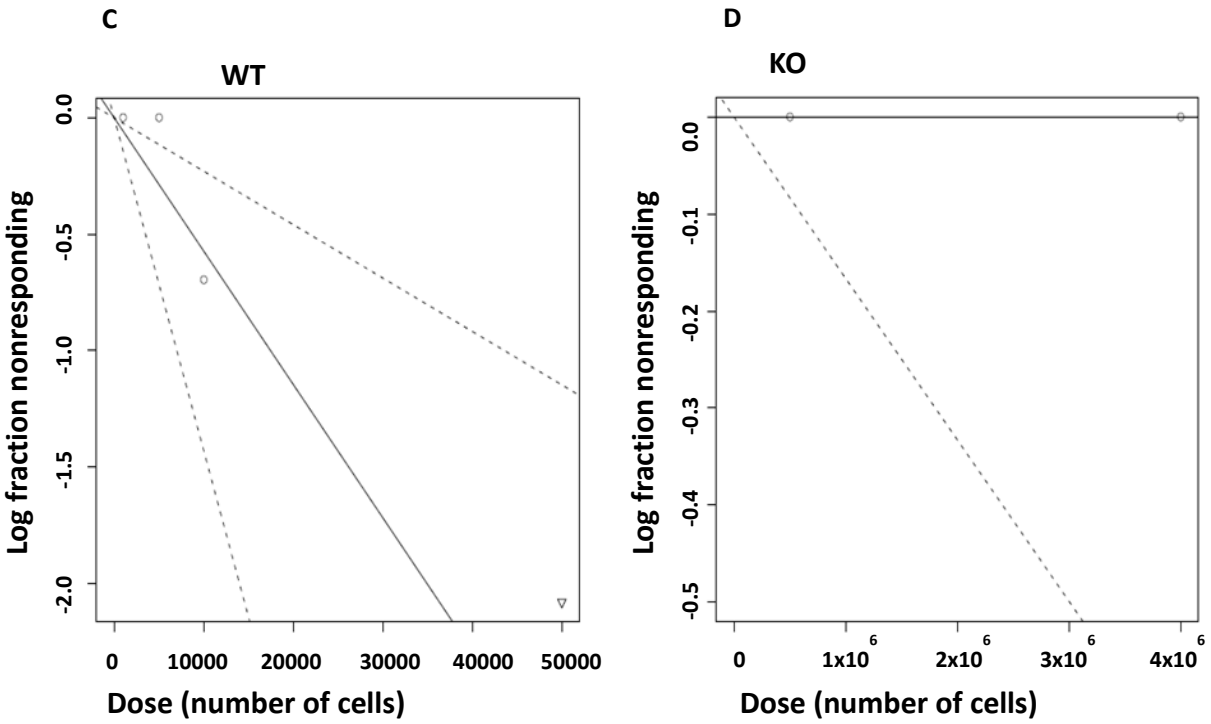


Figure 3-14 Deletion of Cbfb affected the frequency of the AE9a leukaemia initiating cells.

(A and B) Kaplan-Meier survival curves of mice transplanted with different numbers of LSCs (A: WT group: 1000 (n=3), 5000 (n=3), 10000 (n=4), 50000 (n=4), B: KO group: (0.5x106 (n=4) and 4x106(n=4). (C and D) LDAs showed the frequencies of leukaemia initiating cells of the WT (C) and KO (D) cells. Dotted lines indicate 95% confidence intervals.

### *3.2.3.4 Establishing AE9a leukaemia model using c-Kit + BM cells.*

Toward the end of my PhD, I decided to test the ability of AE9a fusion to generate a leukaemia model using BM cells. To this end, c-kit+ cells were isolated from the BM of Cbfbf/f Rosa 26 Cre ER mice were transduced with MigR1 AE9a and then subjected to a direct injection into two groups of irradiated mice without any *in vitro* replating assay. A week later, one group was treated with tamoxifen to induce the deletion of Cbfb (figure 3.15).

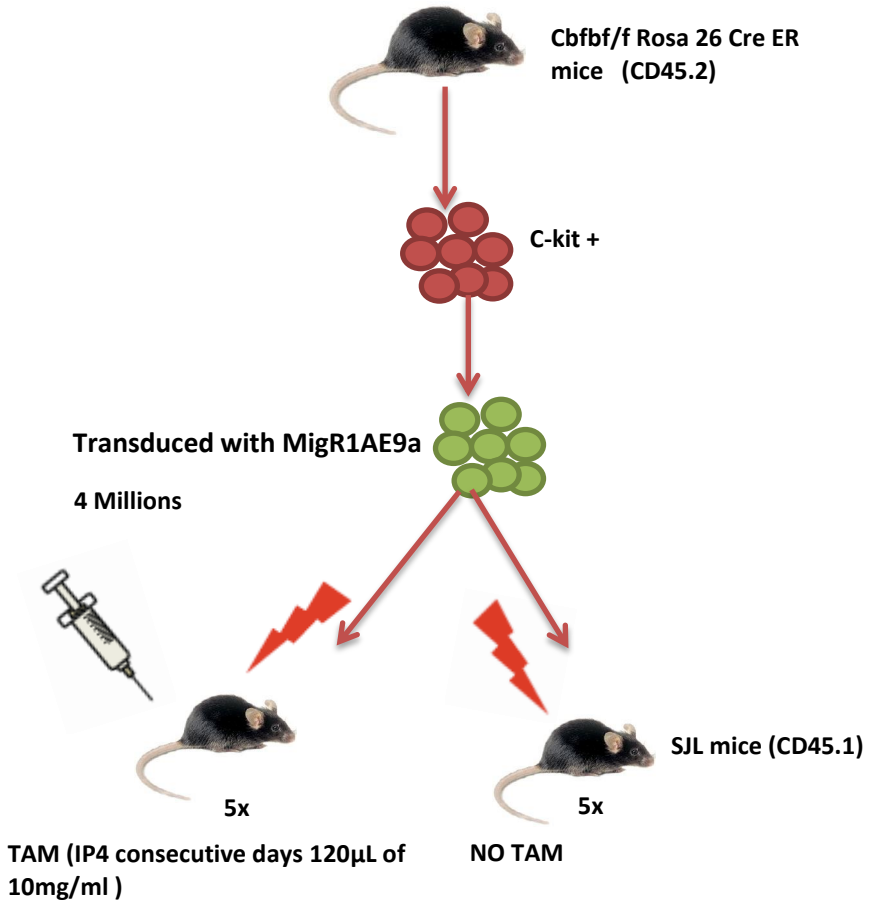


Figure 3-15 Our in vivo approach for establishing a leukaemia model using BM c-Kit + cells.

As a result, two out of five mice from the control group got sick whereas the KO group remains healthy (figure 3.16 A). Interestingly, the disease latency was longer than AE9a transformed cells derived from fetal liver. To further define the role of Cbfb in disease maintenance, spleen cells were harvested from the sick mouse and subjected to secondary transplant into two groups of irradiated animals. One of them was then treated with TAM a week after transplantation. All the control mice from the untreated group came down within a median survival of 28 days, whereas the Cbfb KO group remained healthy even after 2 months (figure 3.16 B). The phenotypes of the leukaemic cells from the primary or the secondary transplants were identical to the fetal liver cells, which expressed c-Kit but not Mac-1 or Gr-1 (figure 3.16 C and D).

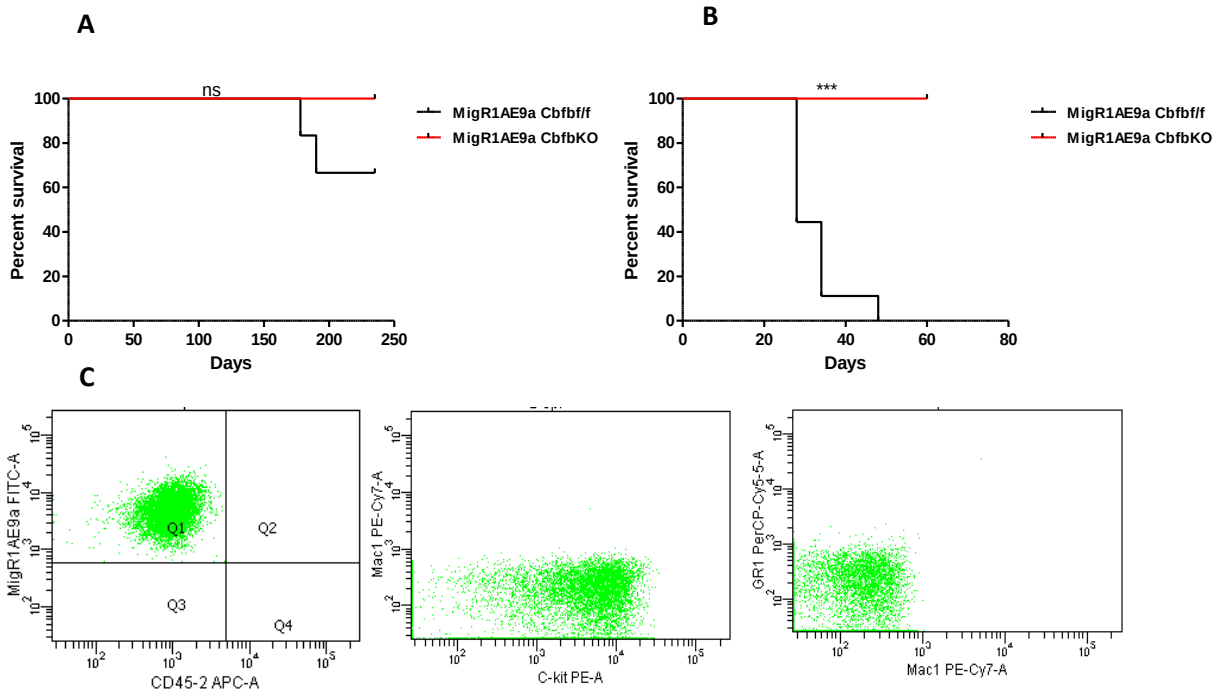

**D**

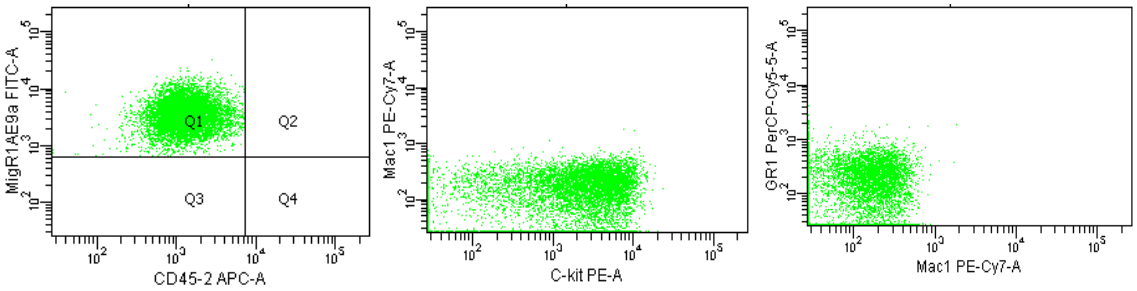


Figure 3-16 BM AE9a leukemogenesis is dependent of Cbfb.

(A) Kaplan-Meier survival curve of AE9a primary transplanted mice with and without tamoxifen treatment (WT cbfb n=5, KO cbfb n=5) (B) Kaplan-Meier survival curve of AE9a secondary transplanted mice with and without tamoxifen treatment (WT cbfb n=9, KO cbfb n=9) (C and D) Representative flow cytometry profiles of leukaemic cells harvested from primary (C) and secondary (D) transplanted mice.

### 3.2.4 Preliminary RNA sequencing data showed that some of AE9a target genes were dysregulated upon Cbfb deletion.

To gain insights into the underlying mechanisms and identify key downstream targets of Cbfb responsible for the phenotypes, RNA sequencing was carried out using AE9a *in vitro* transformed c-kit+ BM cells. As shown in table 3.2, two biological replicates of AE9a transformed cells (3rd round of replating from figure 3.5 A) carrying Cbfb f/f alleles were treated with TAM during the 2nd round of replating to induce Cbfb deletion. RNA from these cells with or without TAM treatment were prepared for RNA sequencing. The successful deletion of Cbfb was confirmed by both qPCR (figure 3.17 A) and the RNA sequencing showing their specific depletion of exon 5 (figure 3.17 B). The PCA plot of the data demonstrated that 55% of the variance segregated with the KO (PC1), whereas 36% of the variance segregated according to the experiment (PC2) (figure 3.18 A). As shown by the MA plot and the heatmap, number of genes were significantly dysregulated (P-value <0.05) as a result of Cbfb deletion (figure 3.18 B and C), in which 455 genes were down-regulated (list 1) and 340 genes were upregulated (list 2) (appendix table A1 and A2).

Table 3-2 Summary for the samples which were submitted for RNA sequencing.

| Sample | Description |
|---|---|
| 1 | AE9a in Cbfb flox background (Exp36-4 3rd round) |
| 2 | AE9a in Cbfb KO background (Exp36-4+ 3rd round ) |
| 3 | AE9a in Cbfb flox background (Exp37-6 3rd round ) |
| 4 | AE9a in Cbfb KO background (Exp37-6+ 3rd round) |

**+ indicates 4-OHT treatment (50nM only during the second round)**

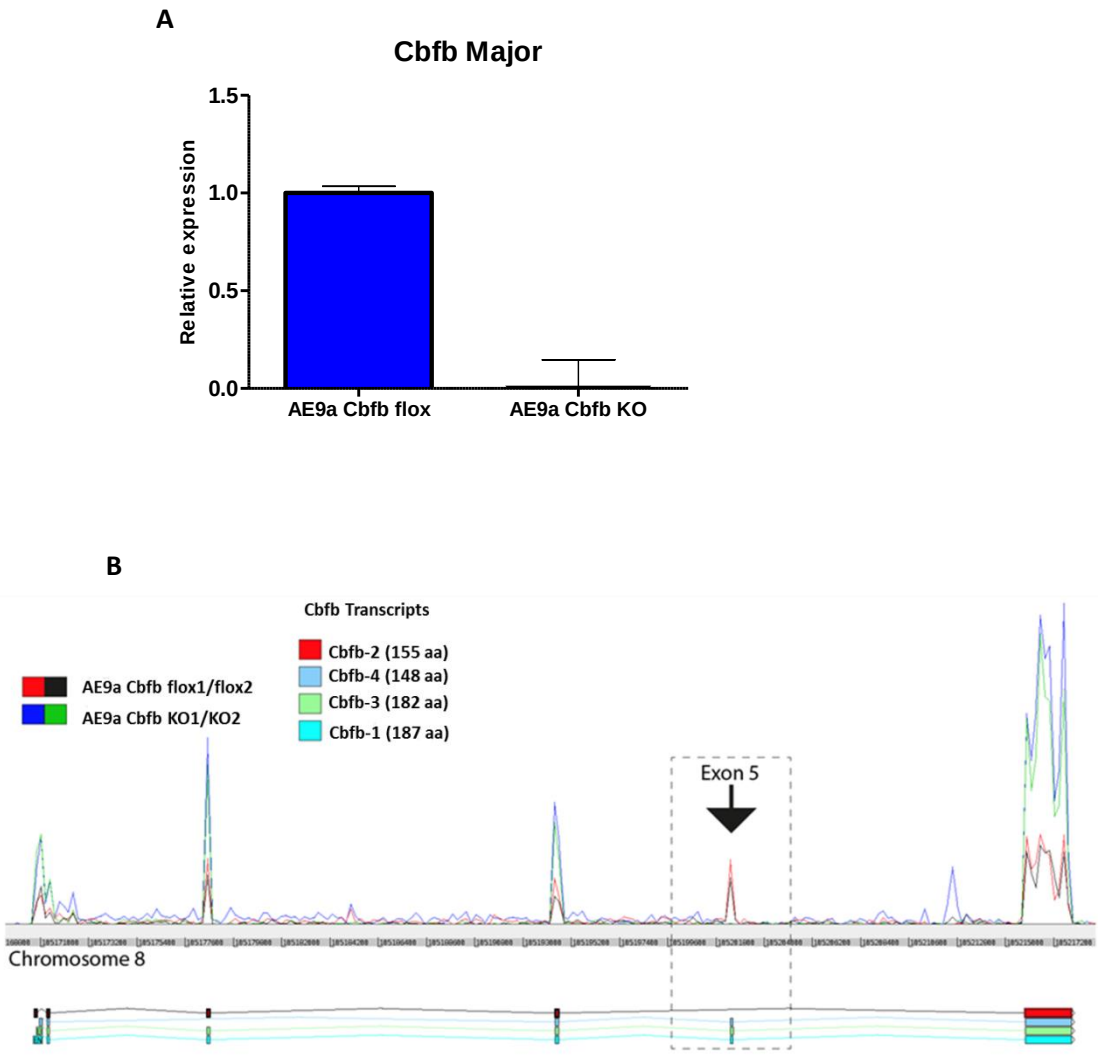


Figure 3-17 The KO samples lost the expression of Cbfb major transcript.

(A) Expression of cbfb major transcript of AE9a Cbfb flox and AE9a Cbfb KO samples. (B) A diagram illustrates the deletion of exon 5 in the KO samples (blue and green colours) comparing to the flox one (red and black colours).

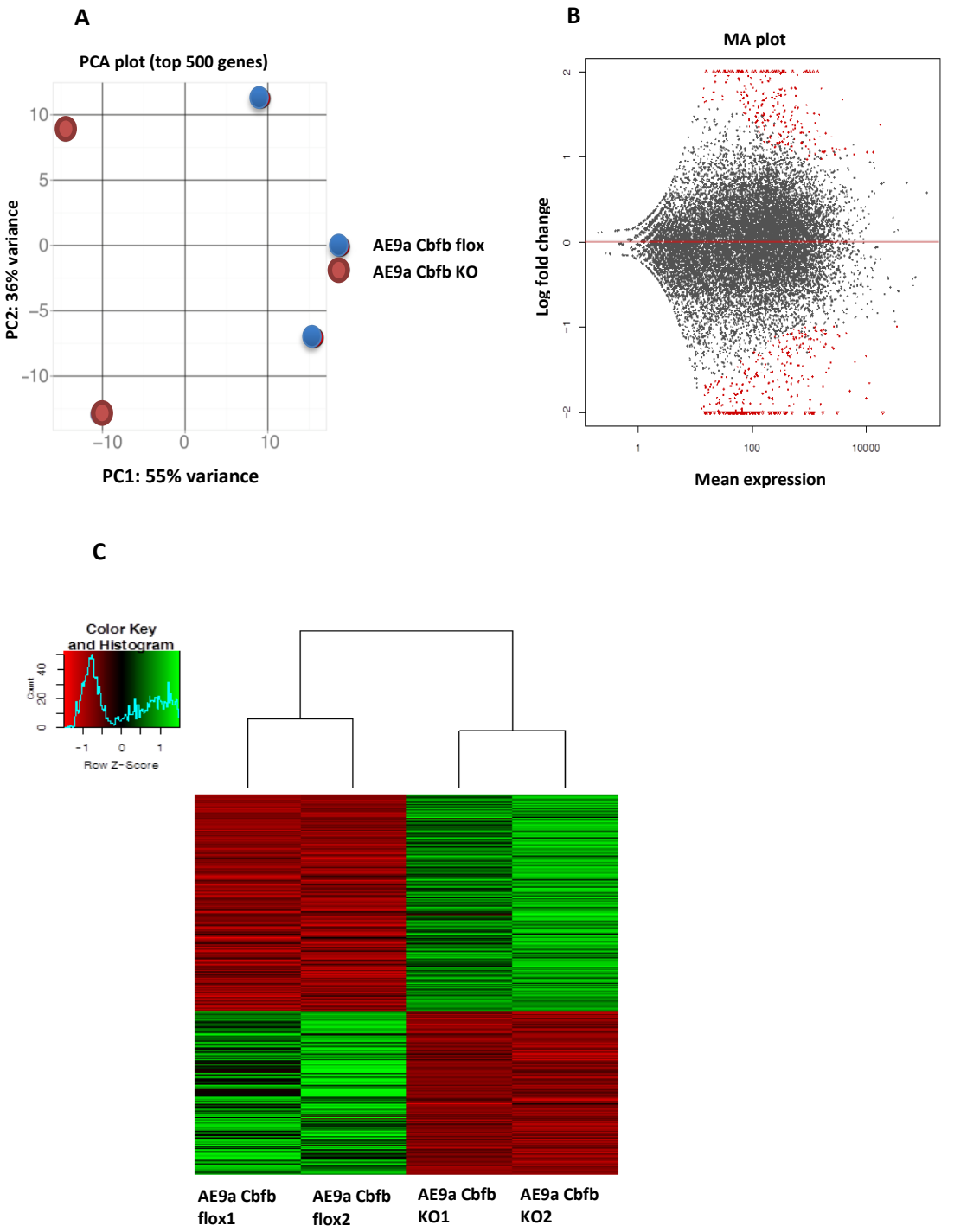


Figure 3-18 Deletion of Cbfb resulted in dysregulation of some genes in AE9a transformed cells.

(A) PCA plot in which PC1 explains 55% of variance and segregates with Cbfb KO, whereas PC2 explains 36% of variance and segregates according to experiment. (B) MA plot showing significantly differentially expressed genes (red) and all other genes (black). (C) Heatmap the significantly differentially expressed genes.

Recently, murine AE9a leukaemia microarray analysis showed that around 1050 genes were dysregulated by AE9a (Lo and Peterson 2013). This will give us an opportunity to identify common downstream targets between AE9a and Cbfb. Therefore, these genes were compared with our Cbfb regulated gene lists (list 1 and list 2). As a result, we identified 79 commonly regulated genes including 44 down- and 35 up-regulated genes, respectively (figure 3.19 and appendix table A3 labelled as List 3 and 4).

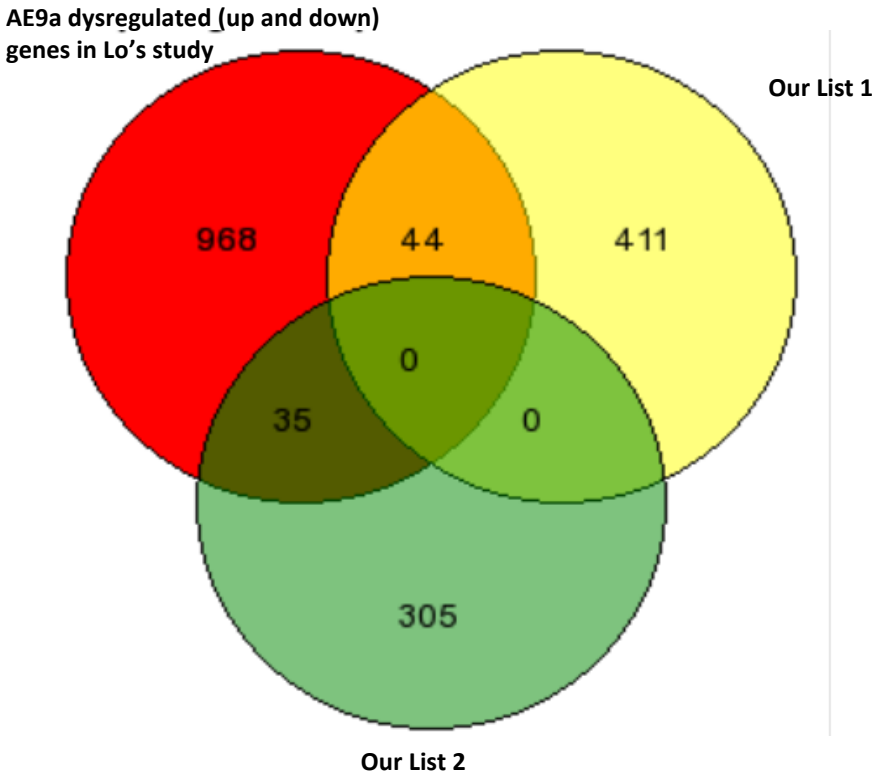


Figure 3-19 Venn diagram illustrates the overlap between AE9a dysregulated genes in Lo's study with our List 1 and List 2.

In addition, Lo and colleges performed cross compression between the gene expression and ChIP-Chip data where they were able to identify some potential AE9a direct downstream targets (Lo and Peterson 2013). Interestingly, comparing list3 with these targets showed overlap of 12 genes (figure 3.20 and table 3.3 List 5), in which 7 of them were contra regulated. For instance, Alox5, Erol1 and Ets1 were upregulated by AE9a but their expressions were downregulated by Cbfb deletion. Similar comparison was carried out for list 4 and 5 genes were overlapped and 3 of them were contra regulated after Cbfb ablation (figure 3.20 and table 3.3 List 6). However, future validation experiments are required to investigate if these genes represent potential targets or not. In addition, the current data will be compared with another set of AE9a data which were generated in our lab using similar experimental strategies.

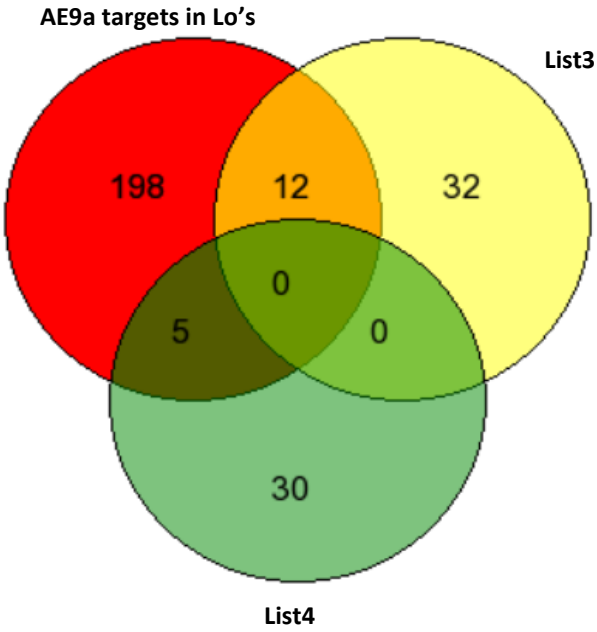


Figure 3-20 Venn diagram illustrates the overlap between AE9a targets in Lo's study with List 3 and List 4.

Table 3-3 Name of overlapped genes between AE9a targets, list 3 and list 4.

| Name of genes in List 5 | Name of genes in List 6 |
|---|---|
| Alox5* | Atp10a* |
| Csrnp2* | Dlg3* |
| Ero1l* | Phb |
| Ets1* | Plekha8* |
| Gatsl3* | Pmp22 |
| Gpc1 | |
| Ndrg2* | |
| Ptprs | |
| Rnf144a | |
| Rras* | |
| Serpine2 | |
| Sorl1 | |

* indicates contra regulated genes.

## 3.3 Discussion

In my initial experiments, I used c-Kit+ cells from the Cbfbf/fRosa26YFP/WT mouse (mixed background) and subjecting them to RTTA with AE in the presence or absence of HR-Cre. Although a complete deletion in the bulk population was not achieved in this model, it was clear that the Cbfb deleted AE transduced cells proliferated and contributed to the observed transformation phenotypes. To overcome the issue of mixed populations (Cbfb deleted and non-deleted cells), I took the advantage of having a YFP marker as a proxy for Cre-recombination to sort the AE transduced YFP+ and YFP– cells. Consistent with my previous results as well as published results from our group (Kwok, Zeisig et al. 2009), I was able to show that AE still transformed c-Kit+ cells in vitro after deletion of Cbfb. At the same time, I started to generate an improved mouse line, Cbfbfl/fl Rosa 26 Cre ER mouse, which possess a tamoxifen inducible Cre (Cre ER), which requires only addition of tamoxifen for Cre activation.

As expected, I showed that the Cbfb spliced isoform without exon 5 was unable to bind neither to the full length AE nor the short form AE9a. The results attest the usefulness of our model to specifically investigate the role of Cbfb interaction in AE mediated transformation. After optimizing the tamoxifen treatment conditions, I used *in vitro* transformation assay (RTTA) with c-Kit+ BM cells and showed that Cbfb deleted AE transformed cells formed reduced number of 3$^{rd}$ round colonies than untreated controls. However, these cells were still able to continue forming colonies for subsequent rounds of replating, suggesting that loss of Cbfb does not abolish AE mediated *in vitro* transformation of adult c-kit+ BM

cells. These findings are also highly concordant with our groups previous study which reported a slight reduction of the 3rd round colonies of AE (Y113A/T161A) mutant transformed cells, without a significant overall negative impacts on their *in vitro* transformation (Kwok, Zeisig et al. 2010).

To gain further insight into the role of Cbfb in AE-mediated transformation different haematopoietic populations such as LSKs, GMPs and CMPs, I was able to show that AE, AE9a and AE (Y113A/T161A) mutant were able to transform LSKs, GMPs and CMPs. Similarly, deletion of Cbfb resulted in a reduced number of colonies but did not completely abolish AE activity, suggesting that loss of Cbfb might only have a moderate impact on AE *in vitro* replating ability. Moreover, I also identified multiple haematopoietic populations such as LSK, CMP and CMP as potential cell of origins for AE mediated transformation. Although AE could competently transform all these populations *in vitro*, further *in vivo* studies are needed to confirm the cell of origin for AE mediated leukaemia. However, AE *in vivo* leukaemia models so far can only be achieved with an addition of secondary mutations such as RAS, TEL-PDGFR and KIT (Grisolano, O'Neal et al. 2003; Wang, Zhao et al. 2011; Zhao, Zhang et al. 2014). If AE models with secondary mutations are employed, the impact of the second mutation must be carefully assessed to allow definitive conclusion about the cell of origin as well as the impact of Cbfb in AE mediated *in vivo* leukaemia.

In contrast to my data obtained using adult BM cells, AE9a-mediated *in vitro* self-renewal of fetal liver cells was severely compromised upon Cbfb deletion and these cells started to differentiate comparing to the floxed controls, strongly

suggesting an important role of Cbfb in maintaining the self-renewal and growth of these cells. In contrast to models using adult BM cells, AE9a alone is sufficient to transform fetal liver cells and induce AML *in vivo* (Yan, Kanbe et al. 2006; Lo and Peterson 2013). Therefore I adopted this approach to establish an AE9a leukaemia model, which allows conditional deletion of Cbfb. My data clearly demonstrated that Cbfb is essential for initiation of AE9a leukaemia *in vivo* as the KO cells failed to induce the disease. Moreover, the maintenance of AE leukaemia was also Cbfb dependent, further highlighting the importance of Cbfb in AE9a leukaemogenesis from fetal liver cells. The findings in the fetal liver are also in stark contrast to the *in vitro* results obtained in adult BM cells, where loss of Cbfb has minimal impact on AE mediated transformation. While this highlights the critical impact the choice of experimental system might have, it is not clear which experimental system actually is more relevant to the human disease as cell-of-origin for human AE leukaemia has not been identified. In general, the most stringent experimental settings to study leukemogenesis are *in vivo* models that induce leukaemia whereas *in vitro* assays may only act as surrogates. The development of alternative *in vivo* leukaemia models in which adult BM cells are transformed by AE alone may represent new opportunities and allow comparison to existing fetal liver model, which may help to define their relevance with respect to the human disease.

The phenotypes of the leukaemic cells of the fetal liver model in this study were identical to the ones reported in previous studies as they expressed only c-kit but not Mac1/Gr-1 and CD45 was downregulated in these cells (Lo and Peterson 2013). It has been shown that all haematopoietic cells express high level of CD45

which plays a fundamental role in B and T cells antigen receptor signalling (Penninger, Irie-Sasaki et al. 2001). In addition, CD45 has been found to be negatively regulating JAK/STAT signalling pathway (Irie-Sasaki, Sasaki et al. 2001) and this pathway was activated in AE9a leukaemic cells (Lo and Peterson 2013). Consistently, CD45 is down-regulated also by AE full length in patient samples as t(8;21) patients had more than 90 % reduction in their CD45 mRNA (Lo and Peterson 2013). Moreover, coexpression of AE9a with CD45.1 resulted in attenuated JAK/STAT pathway and also delayed the onset of the disease (Lo and Peterson 2013). These data clearly revealed the importance of CD45 downregulation in AE9a leukaemogenesis. Our *in vitro* data showed that CD45 downregulation was not achieved neither in the AE9a BM cell line nor the fetal liver one. Also, these cell lines lacked the expression of c-kit and this might explain why these cells failed to induce leukaemia as it seems external signals from the microenvironment might be irreversibly missing in the *in vitro* culture. Further experiments are definitely required to gain more insight into the role of CD45, c-Kit Jak-Stat5 and the microenvironment in AE mediated *in vivo* leukaemogenesis.

To develop the alternative *in vivo* AE leukaemia model using adult BM and AE9a alone, I employed a direct injection instead of *in vitro* repalting strategy. Interestingly, 2 out of 5 mice developed leukaemia with a similar phenotype compared to that obtained using the fetal liver model, i.e. lack of CD45 expression and high c-Kit expression, although the latency was longer and the penetrance reduced. This mouse model was immediately used to investigate the role of Cbfb in AE9a leuakemogenesis in BM. Similar to the fetal liver model, the BM AE9a

leuakemogenesis was Cbfb dependent and the phenotypes of these cells were identical to the fetal liver cells, strongly suggesting that Cbfb is absolutely required for AE9a mediated leukemogenesis also in BM leukaemia model. For the first time we have shown that 2 different AE9a *in vivo* models using different starting cell populations without secondary mutations are dependent on Cbfb. This result is also consistent with the findings of Roudaia using AE with secondary mutation in adult BM cells (Roudaia, Cheney et al. 2009). I conclude that AE transformation *in vitro* is less stringent than AE transformation *in vivo,* which may explain the different requirement of Cbfb in adult BM *in vitro* and *in vivo*. Surprisingly, AE9a fetal liver cells show consistent results with respect to their Cbfb dependence but the reasons are currently unclear. Together, my results demonstrate that AE9a *in vivo* mediated transformation is critically dependent on Cbfb in different model systems.

In stark contrast, *in vitro* transformation activity of MN1 and its *in vivo* leukaemogenesis is completely Cbfb independent. Interestingly, deletion of Cbfb might indeed accelerate MN1-mediated leukaemogensis. It has been shown that leukaemogenesis of CBFB-SMMHC was accelerated after disrupting its binding with RUNX1 through deletion of the high affinity binding domain (HABD) (Kamikubo, Zhao et al. 2010). Intriguingly, MN1 was also upregulated in these leukaemic cells, and have been shown to collaborate with CBFB-SMMHC for leukaemia induction (Kamikubo, Zhao et al. 2010). It is tempting to speculate that selective disruption of Cbfb-Runx1 interaction may indeed promote leukaemogenesis in certain

circumstances, although further experiments are clearly required to test this hypothesis.

By analysing RNA sequencing data generated using AE9a *in vitro* transformed cells, we identified only few hundred genes dysregulated by Cbfb ablation. There might be several factors responsible for this. For instance, PCA plot showed that 36% of variance was due to some differences between the two experiments which were carried out to produce biological replicates. However, I decided to compare these data with some known AE9a targets (Lo and Peterson 2013). It is also worth to mention this comparison is not a perfect one due to the differences in the experimental settings and the source of cells. I found some genes that were contra regulated between the two studies - Alox5 is one of them. Alox5 was upregulated by AE9a but ablation of Cbfb downregulates its expression. It has been demonstrated that the induction of chronic myeloid leukaemia by BCR-ABL required Alox5 and its inhibition delayed the onset of the disease (Chen, Hu et al. 2009). Although *in vitro* activity of AE9a was reduced after Alox5 ablation, AE9a *in vivo* leukaemogeneis was not affected (DeKelver, Lewin et al. 2013), suggesting that the *in vivo* leukaemogenic activity might not be fully reflected by the *in vitro* transformation assays. Nevertheless, identification of Alox5 as Cbfb target in AE leukaemia attests the usefulness of our model for discovering key Cbfb targets. Future RNA-seq analysis in combined with Cbfb ChIP-seq study will provide important insights into the underlying mechanisms.

# 4 Effect of Cbfb in normal haematopoiesis

## 4.1 A Brief Introduction

As mentioned earlier, core binding factors play a pivotal role in haematopoiesis through regulating different haematopoietic genes such as GM-CSF, IL3 and T-cell antigen receptor (Shoemaker, Hromas et al. 1990; Redondo, Pfohl et al. 1992; Takahashi, Satake et al. 1995). Moreover, knock-out studies have shown that the two genes are essential for definitive haematopoiesis and mice lacking these genes died at E12.5 with very similar phenotypes, suggesting the importance and collaborative nature of these two genes for normal haematopoiesis. The impact of Cbfb deletion on the development of normal adult HSCs was poorly understood at the beginning of my PhD.

Recently, Ouguro *et al* have demonstrated that LSK population can be subdivided into four main fractions based on their expression of SLAM markers CD150 and CD48: HSCs are CD150+CD48-LSK; MPPs are CD150-CD48-LSK, HPC-1 CD150-CD48+LSK and HPC-2 CD150+CD48+LSK. In addition, using another two SLAM markers CD229 and CD244 they were able to subdivide HSCs into two fractions called HSC-1 (CD150+CD48-CD229-/lowCD244-LSK) ,HSC-2 (CD150+CD48-CD229+CD244-LSK) and MPPS into three fractions called MPP1 (CD150-CD48-/lowCD229-/lowCD244-LSK), MPP2 (CD150-CD48-/lowCD229+CD244-LSK) and MPP3 (CD150-CD48-/lowCD229+CD244+LSK) (Oguro, Ding et al. 2013). The cell cycle analysis of these population using Ki-67 and PI in Ouguro's study has demonstrated that higher that 90% of HSC-1, HSC-2, MPP-1 and MPP-2 were in G0,

but MPP-2 had fewer percentage comparing to them. Moreover, the most actively cycling cells in LSK were HPC-1 and HPC-2 which also incorporated more 5-bromo-deoxyuridine (Brdu) satin (Oguro, Ding et al. 2013). Furthermore, reconstitution experiments have suggested that HPC-1 cells are a heterogeneous population of restricted progenitors that contains early lymphoid progenitors and some cells that can give a transient reconstitution to myeloerythroid lineages. Whereas, most of the HPC-2 recipient mice were transiently reconstituted with very low level of erythrocytes and platelets and only few mice had myeloid and B cells suggesting that HPC-2 cells contain heterogeneous restricted progenitor with very limited reconstitution ability *in vivo (Oguro, Ding et al. 2013)*.

I decided to take the advantage of having our conditional knockout Cbfbfl/fl Rosa 26 Cre ER mouse model and using SLAM markers (CD150 and CD48) to shed light onto this issue. Three different experimental strategies were designed to address the cell autonomous versus non-cell autonomous role of Cbfb in normal haematopoietic development. Firstly, Cbfb was ablated in the whole animal simply by treating them with tamoxifen. Secondly, Cbfb was only ablated from the haematopoietic cells after their transplantation into WT mice. Finally, Cbfb was targeted in the microenvironment by transplantation of WT haematopoietic cells into Cbfb-deleted animals. Then the haematopoietic systems of these animals were analysed at different time points to report any abnormality.

## 4.2 Results

### 4.2.1 Conditionally deleted Cbfb mice show perturbations in haematopoietic stem/progenitor cells

Cbfb was firstly deleted in the whole animal using the new Cbfbfl/fl Rosa 26 Cre ER mouse model. Two groups of mice (Cbfbfl/fl Rosa 26 Cre ER and cbfbfl/fl) were treated with tamoxifen (100µl of 10mg/ml) for four consecutive days. They were then subjected to detailed haematopoietic analysis four, eight and twelve weeks after tamoxifen administration. The distribution of HSC and early progenitors in bone marrow were analysed using classical LSK and SLAM family markers (CD150 and CD48)(Yeung and So 2009; Oguro, Ding et al. 2013). After four weeks, Cbfb KO mice had a significant increase in the LSK ($Lin^-Sca1^+c\text{-}Kit^+$) population and further analysis of this population revealed severe reductions in $CD150^+CD48^-$ (HSC), $CD150^-CD48^-$ (MPP: Multipotent progenitor) but a significant increase in $CD150^-CD48^+$ (HPC-1: Haematopoietic progenitor cell-1) and $CD150^+CD48^+$ (HPC-2: Haematopoietic progenitor cell-2) populations. Moreover, CMP and GMP of these mice were also reduced whereas no significant difference in the CLP and MEP populations were observed comparing to the control floxed mice (figure 4.1 A). PCR genotyping confirmed a completed Cbfb deletion in different haematopoietic organs such bone marrow, spleen, liver and thymus of the treated group (figure 4. 1 B).

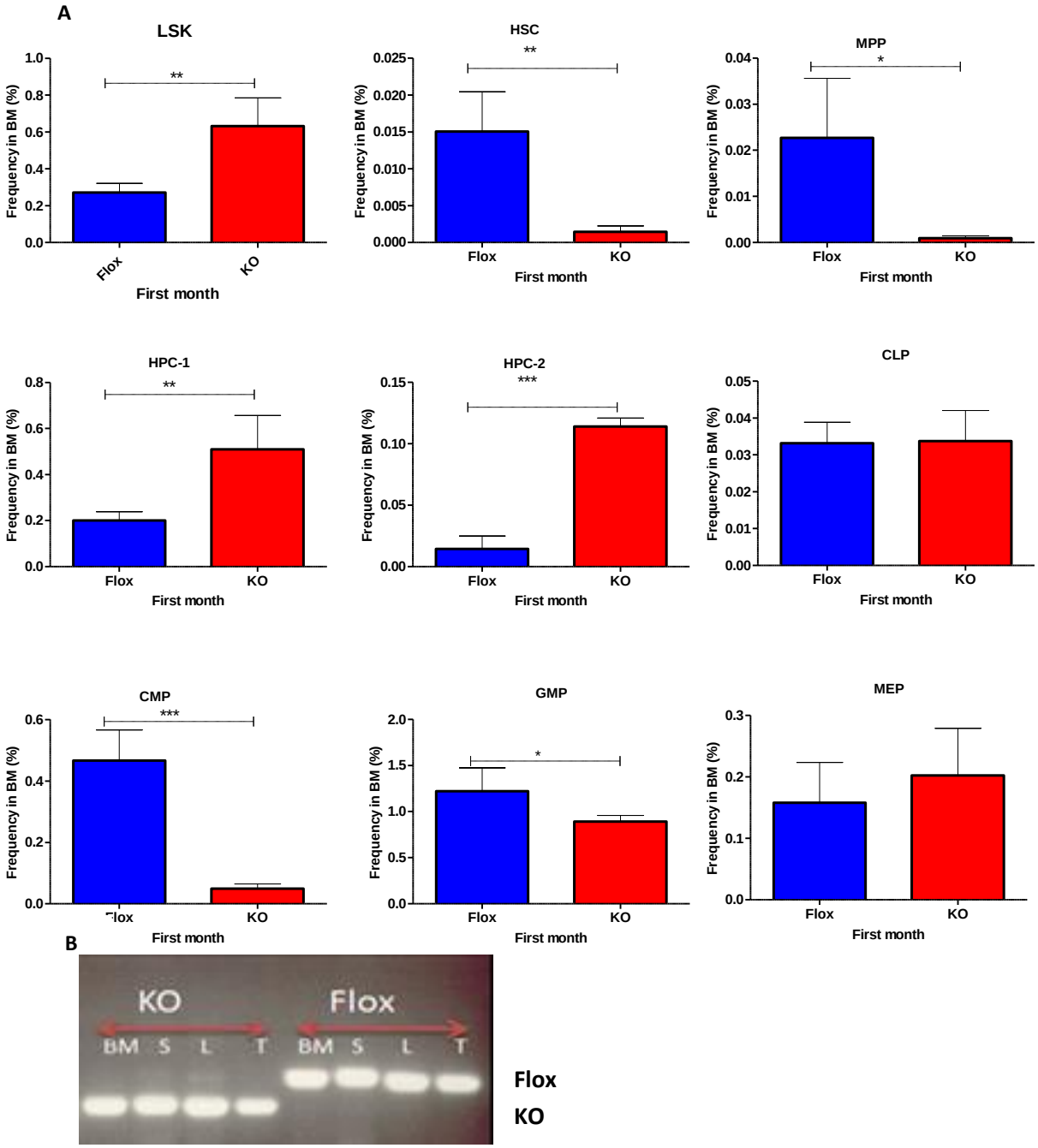


Figure 4-1 Deletion of Cbfb in the whole animal resulted in stem and progenitors defect.

(A) Percentage of LSK and progenitors of the analysed mice Flox: Cbfβfl/fl , KO: Knock out. Error bars indicate mean ± SD of two independent experiments (n=4). (B) Genotyping of the experimental mice (one representative sample is shown).

We also noted that the LSK gating of the Cbfb-deleted mice showed the presence of a new population (C-kit intermediate / Sca-1 high), which was absent or at a very low level in the Cbfb-floxed controls (figure 4.2 A). Gating of these cells revealed that the majority of them were CD150-CD48+, a phenotype reminiscent of HPC-1 (figure 4.2 B).

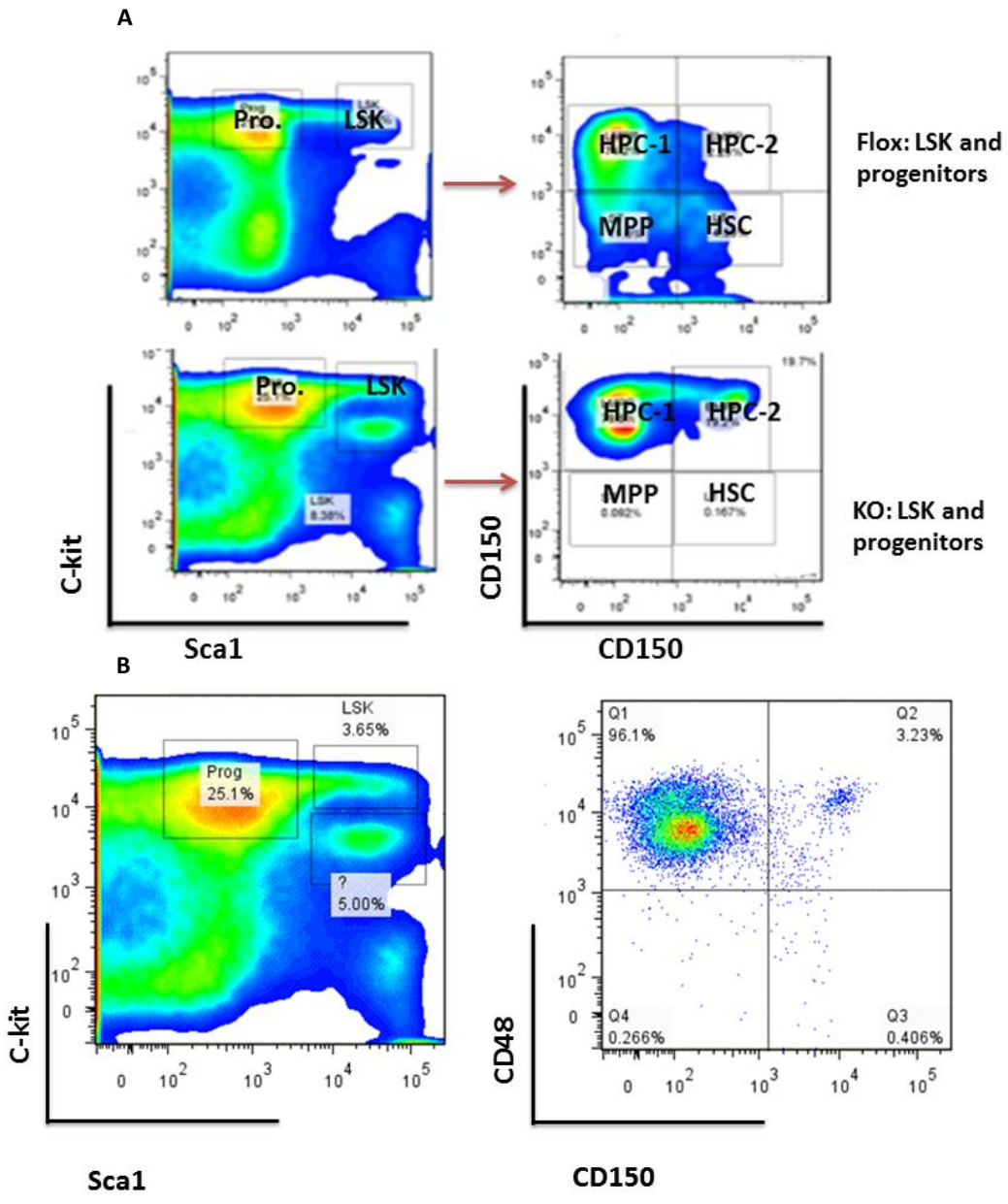


Figure 4-2 Cbfb deleted mice had more HPC-1.

(A) FACS profiles Show the LSK gating of the analysed mice, Floxed and KO. (B) FACS profile shows the KO new population (?).

However, analysis at 8-weeks post tamoxifen administration showed no significant differences between the stem/progenitor cells of the tamoxifen treated mice and the Cbfb flox control mice (figure 4.3 A). In contrast to PCR genotyping that confirmed a complete deletion 4 weeks after tamoxifen treatment, PCR genotyping 8 weeks post tamoxifen treatment revealed an incomplete Cbfb deletion (figure 4.3 B). The reappearance of the floxed band suggests a strong selection pressure against Cbfb deleted haematopoietic cells.

A

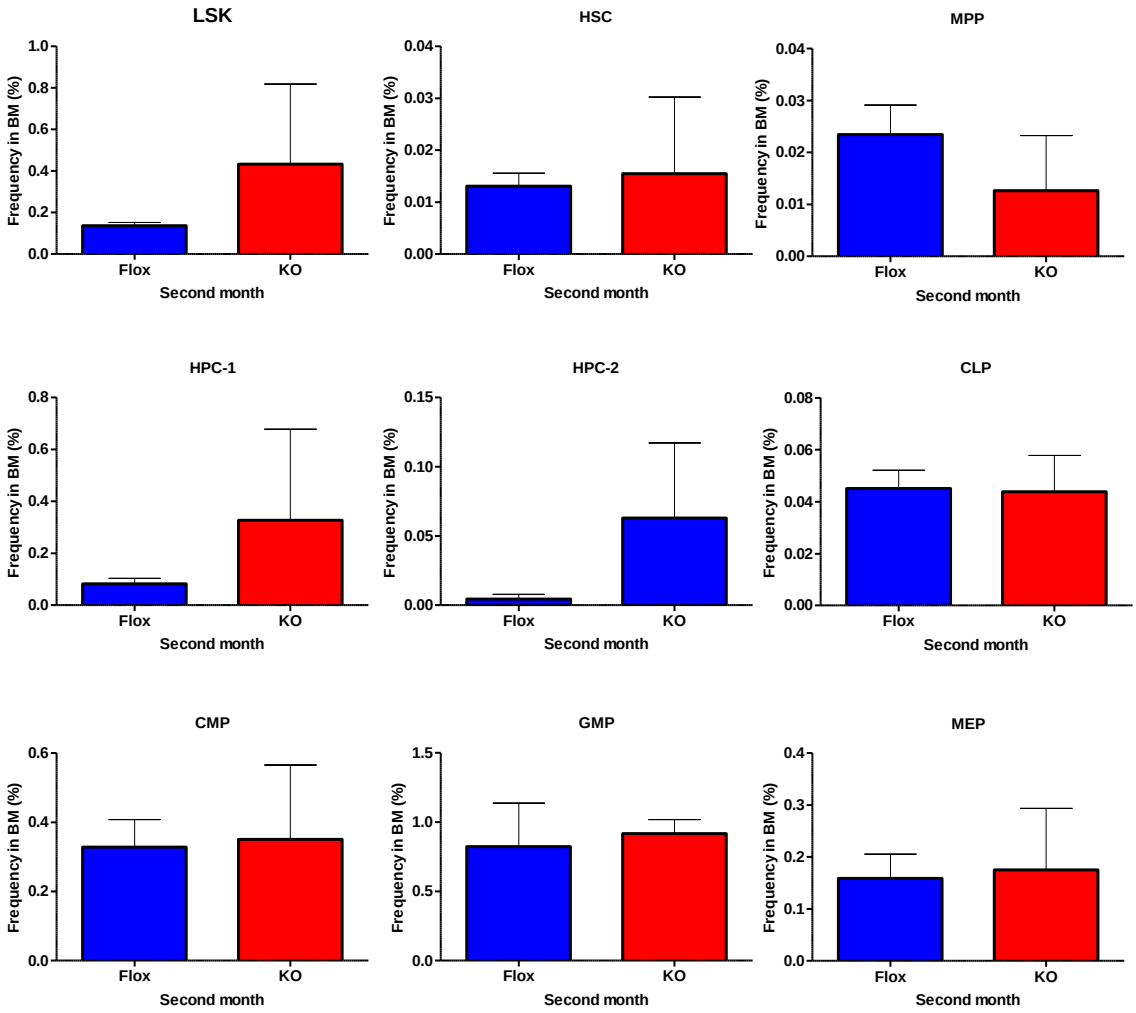

B

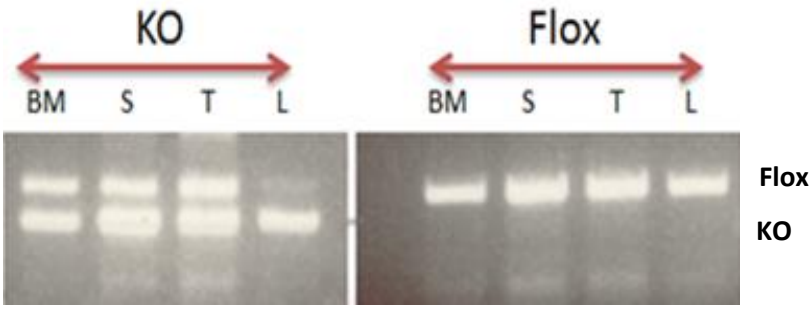


Figure 4-3 Four consecutive TAM injections were not enough to achieve a complete deletion of Cbfb.

(A) Percentage of LSK and progenitors of the analysed mice 8 weeks after TAM treatment. Error bars indicate mean ± SD of two independent experiments (n=4). (B) Genotyping of the experimental mice (one representative sample is shown).

To overcome this issue, we decided to repeat the experiments with a higher dose as well as the extended period of TAM treatment. The two groups of mice (Cbfbfl/fl Rosa 26 Cre ER and cbfbfl/fl) were treated with tamoxifen (120µl of 10mg/ml) for five consecutive days. Surprisingly, the KO mice got sick within two weeks and they were culled together with the floxed control group and subjected to haematopoietic analysis. Our data showed that the KO mice had a significant reduction in white blood cells (WBC), red blood cells (RBC), platelets (PLT), and haemoglobin (HGB) concentration (figure 4.4 A-D). Moreover, flow-cytometric analysis of the BM cells using myeloid and lymphoid markers demonstrated that the KO mice had an increased percentage of Mac1 but a significant reduction in Gr1, B220 and CD8 cells comparing to the floxed group (figure 4.4 E). PCR genotyping confirmed a complete deletion of Cbfb (figure 4.4 F).

HSCs analysis showed no significant difference in the term of the number of the LSK cells between the floxed and KO group. However, further analysis for this population showed significant reduction in HSC and MPP cells of the KO mice. In contrast, the KO mice had an increased percentage of HPC-2 comparing to the floxed one and a slight but not significant reduced percentage of the HPC-1 cells. With regards to the progenitors, the KO mice had a major reduction in CMP population but had relatively milder effect on the number of CLP, GMP and MEP (figure 4.4 G). Overall, these results generated at 2 weeks and 4 weeks after a complete deletion of Cbfb in the whole animal consistently indicate an important function of Cbfb in normal haematopoietic development. Next, we would like to examine if the effect was cell or non-cell autonomous.

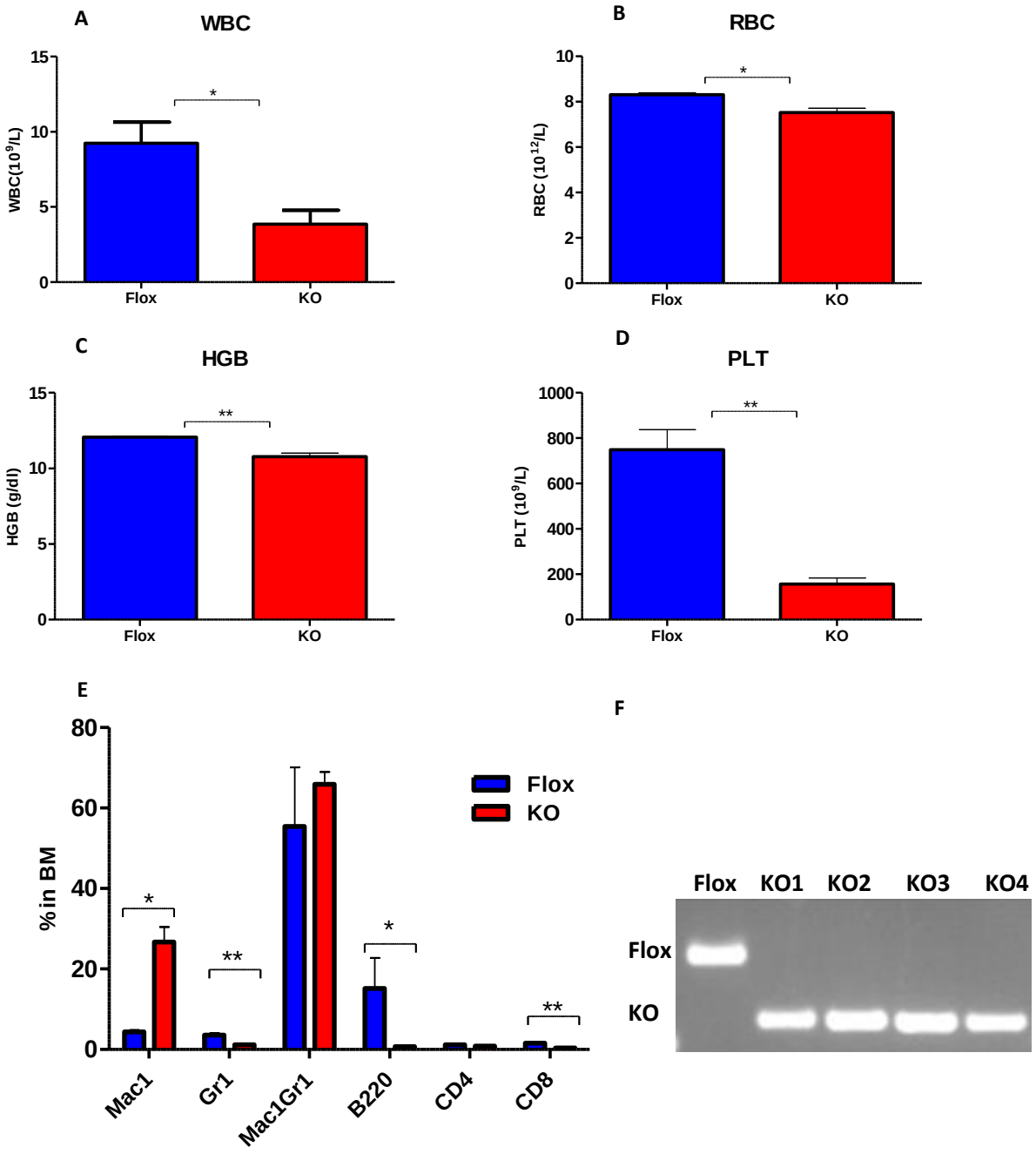
A
WBC
WBC(10^9/L)
15
10
5
0
*
Flox
KO
B
RBC
RBC (10^12/L)
10
8
6
4
2
0
*
Flox
KO
C
HGB
HGB (g/dl)
15
10
5
0
**
Flox
KO
D
PLT
PLT (10^9/L)
1000
800
600
400
200
0
**
Flox
KO
E
%in BM
80
60
40
20
0
Flox
KO
*
**
*
**
Mac1
Gr1
Mac1Gr1
B220
CD4
CD8
F
Flox
KO1
KO2
KO3
KO4
Flox
KO

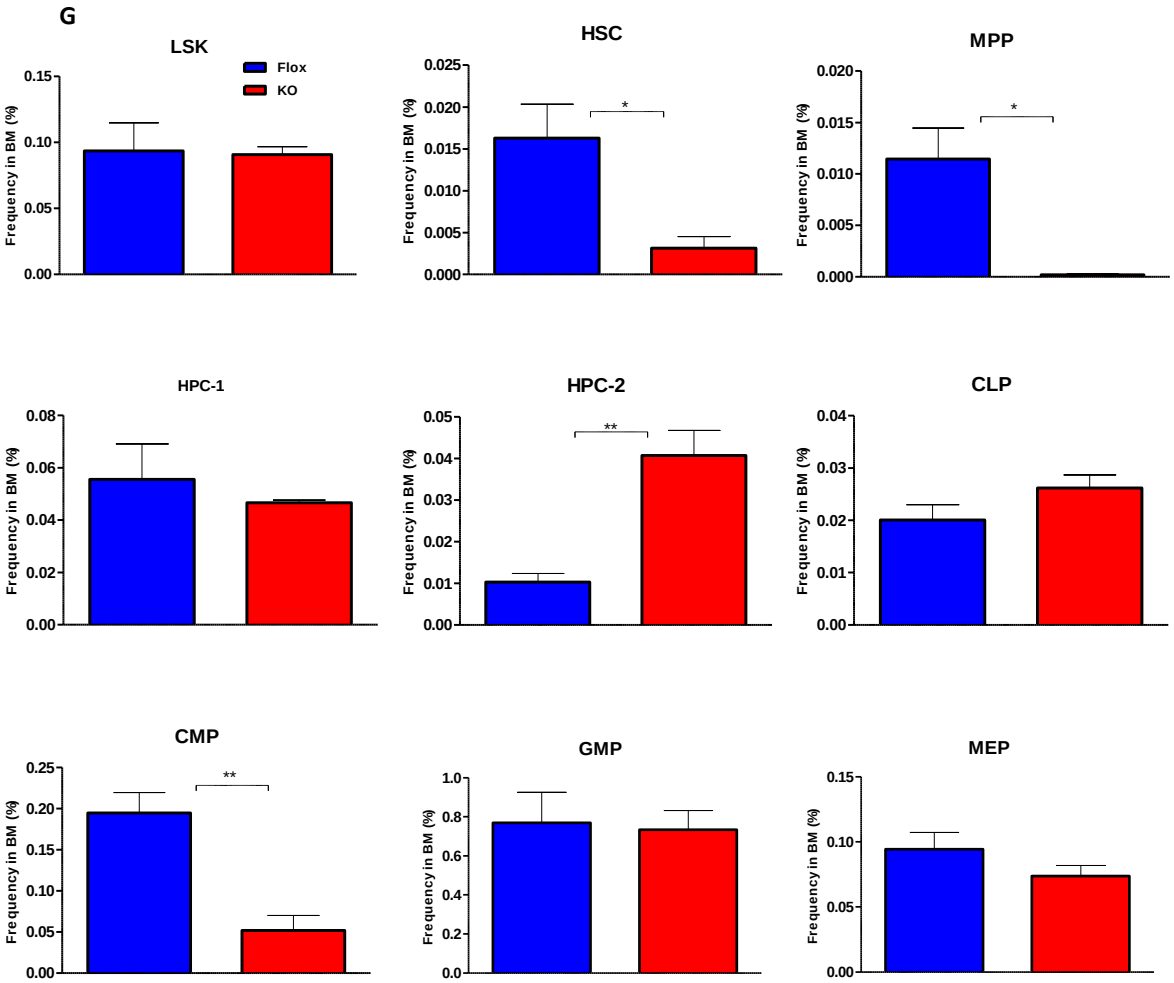


Figure 4-4 Deleted cbfb mice had a sever defect in HSC and CMP.

(A-D) Complete blood counts performed on flox and KO mice (n=4). (E) Percentage of myeloid and lymphoid cells in MB of flox and KO mice. (F) Genotyping of the analysed mice (representative samples). (G) Percentage of LSK and progenitors of the analysed mice. Error bars indicate mean ± SD of two independent experiments (n=5).

### 4.2.2 Targeting Cbfb only in the haematopoietic cells resulted in HSCs and progenitors defects

To complement the data obtained from Cbfb deletion in the whole animal, a transplantation assay was employed to delete Cbfb specifically in the haematopoietic cells of transplanted mice. To this end, mononuclear cells were isolated from two mouse models (Cbfbfl/fl Rosa 26 Cre ER and cbfbfl/fl). One million cells of each genotype were separately injected into irradiated SJL (CD45.1) mice together with $0.2x10^6$ rescue cells (figure 4.5). 4 weeks after transplantation, peripheral blood samples were taken and analysed for level of reconstitution, which would act as the basal line for subsequent comparisons. Mice were then subjected to tamoxifen treatment, in which Cbfb would only be deleted in the hematopoietic cells within the normal host environments. Then detailed HSC analyses were carried out at 4-, 8- and 12- weeks after tamoxifen treatment.

While good and comparable reconstitutions were achieved using both Cbfbfl/fl Rosa 26 Cre ER and cbfbfl/fl cells, the percentage of CD45.2 donor cells in Cbfb KO mice was dramatically decreased compared with the flox control upon TAM treatment (figure 4.6 A and B). The FACS analysis of the PB showed no differences between the floxed and KO group before TAM treatments (figure 4.6 C). However, four weeks later the KO mice had reduced Mac1, Gr1, and CD4 positive cells with slightly higher percentage of Mac1Gr1 cells (figure 4.6 D). The FACS analysis at 8- and 12-weeks showed the KO mice had reduction only in Gr1, CD4 and CD8 positive cells comparing to the control group (figure 4.6 E and F).

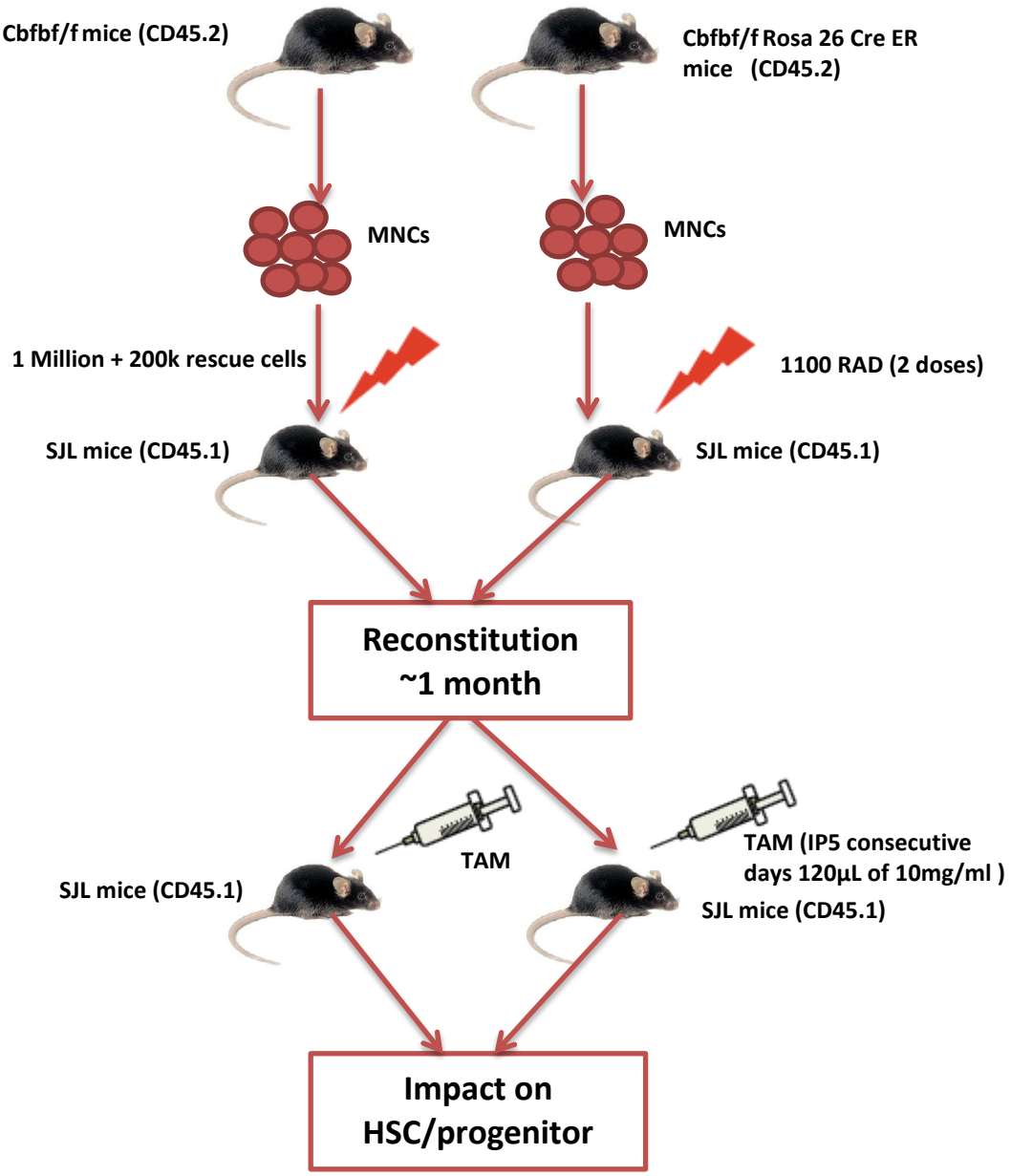


Figure 4-5 Our in vivo approach to target Cbfb only in the haematopoietic cells.

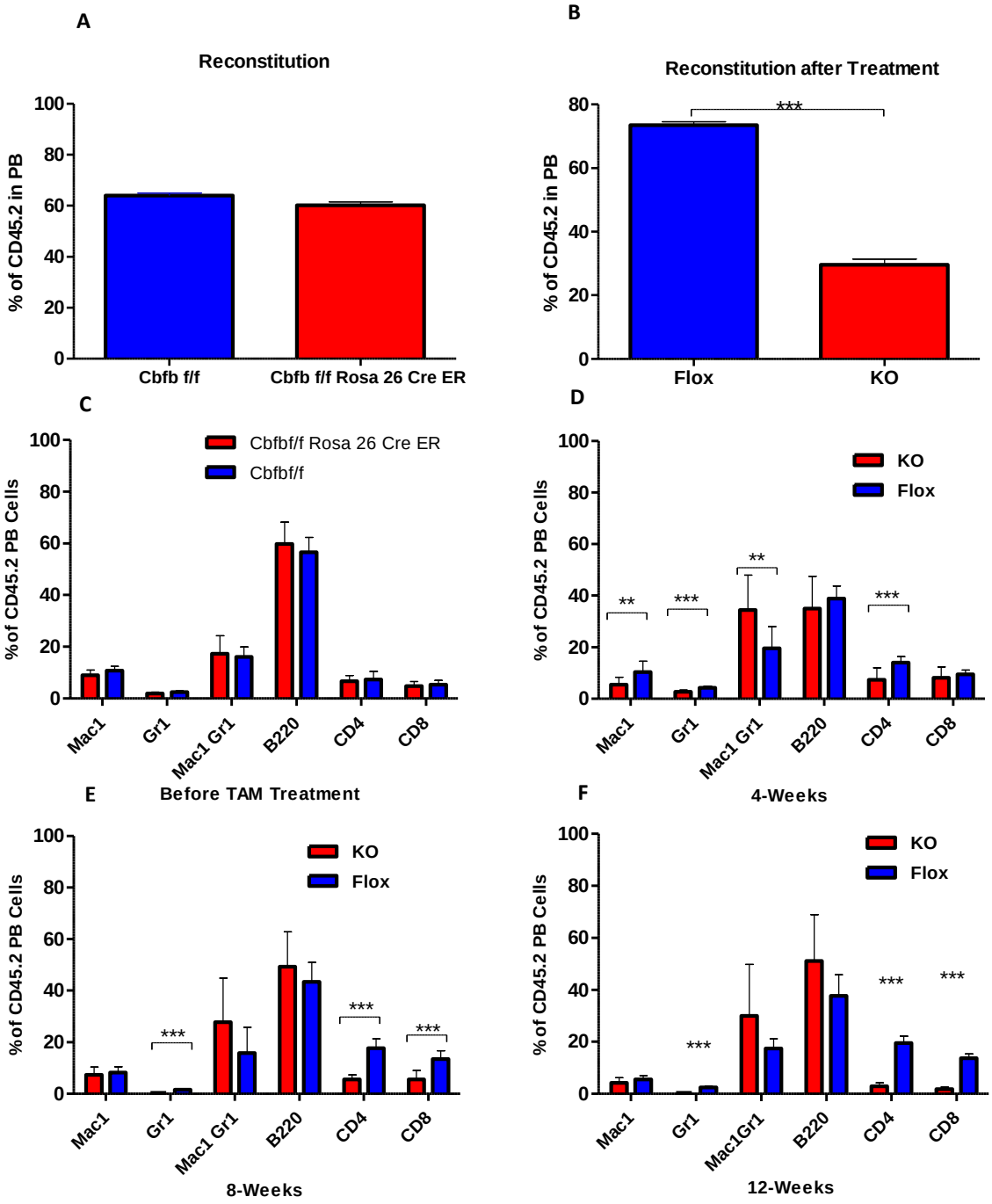


Figure 4-6 Deletion of cbfb in the haematopoietic cells affect the distribution of myeloid and lymphoid cells in the peripheral blood.

(A and B) Percentage of blood reconstitution (CD45.2 in PB) before (A) and after (B) TAM treatments. (C-F) FACs analysis of PB cells before TAM treatment (C) and post treatment at 4-, 8- and 12- weeks. Error bars indicate mean ± SD of two independent experiments (n=6 mice for each group at each time point)

During the HSCs analysis, we observed a significant reduction in the number of CD45.2 BM mononuclear cells (MNCs) of the KO mice at 4-, 8- and 12-weeks post TAM treatments comparing to the floxed one (figure 4.7 A). In addition, FACS analysis of the BM cells showed KO mice had more Mac1 positive cells but with reduction in B220 positive cells (figure 4.7 B-D). These data were similar to what previously observed when Cbfb was ablated in the whole animal. Furthermore, the Gr1 positive cells of the KO mice started to reduce at 8-weeks post TAM treatment (figure 4.7 C and D). Complete deletion of Cbfb was maintained throughout the analysis including the 12-Weeks as it was confirmed by PCR genotyping (figure 4.7 E).

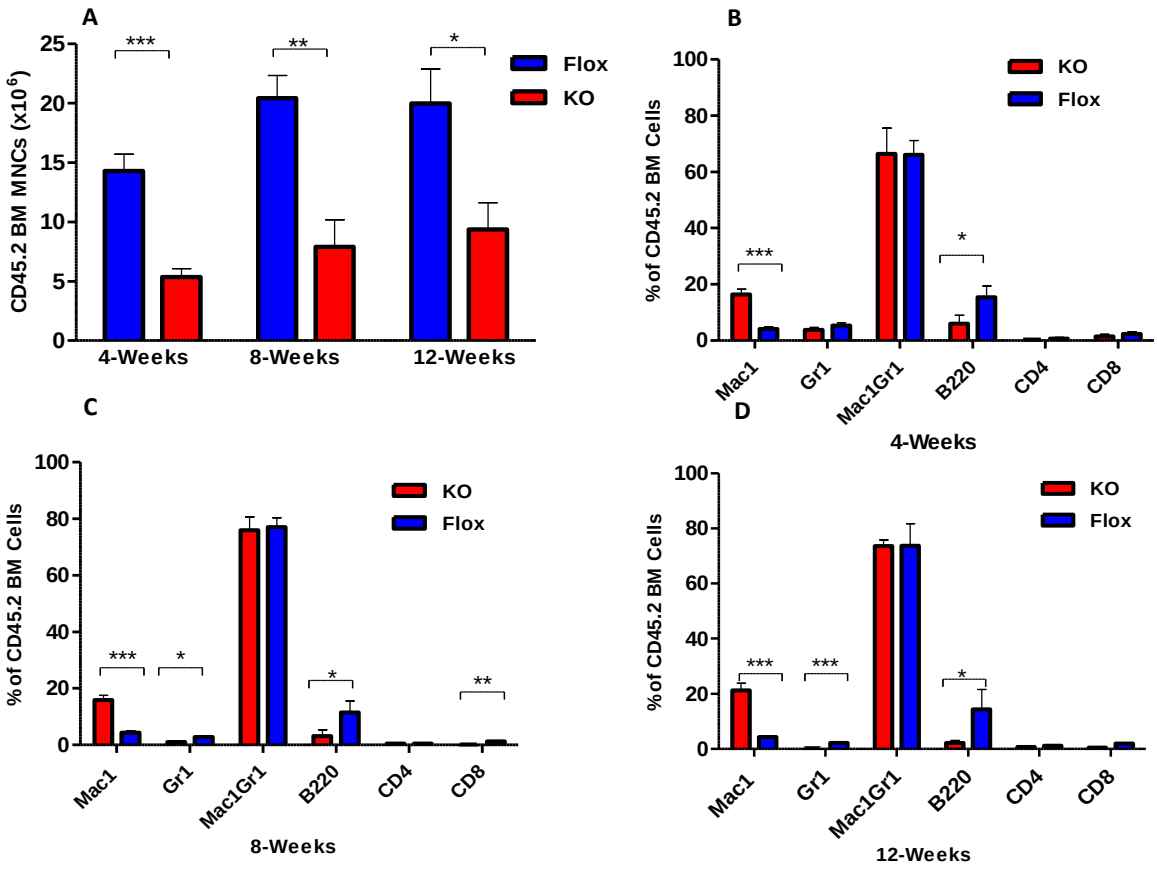

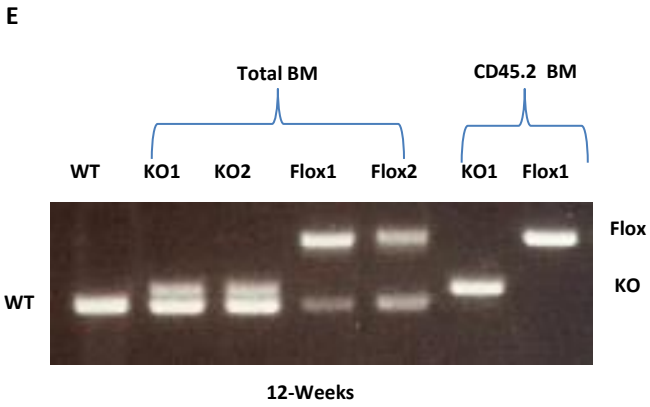


Figure 4-7 Deletion of cbfb in the haematopoietic cells affect the distribution of myeloid and lymphoid cells in the BM.

(A) CD45.2 BM MNCs cell count at 4-, 8- and 12-weeks post TAM treatment. (B-D) FACs analysis of BM cells at 4-, 8- and 12-weeks post TAM treatment. Error bars indicate mean ± SD of two independent experiments (n=6 mice for each group at each time point). (E) Genotyping of the analysed mice at 12-weeks (representative samples).

To evaluate the impact of Cbfb deletion on the phenotypically defined stem and progenitor cells, FACS analysis were carried out at each time point to assess the percentage of these cells. We observed that LSK populations of the KO mice were gradually increased throughout the analysis in spite of a significant reduction of HSC and MPP at 8 and 12 weeks. This was mainly due to the drastic expansion of HPC-2 (Figure 4.8 A). Consistent with the reduction of HSC and MPP, further analysis of the progenitor cells revealed significant reduction in CLP, CMP, GMP and MEP of the KO mice at 8-and 12-weeks comparing to the control group. To further examine the self-renewal property of Cbfb KO cells, they were transplanted into secondary recipients. As result, the KO cells were unable to reconstitute secondary recipient mice (figure 4.8 B).

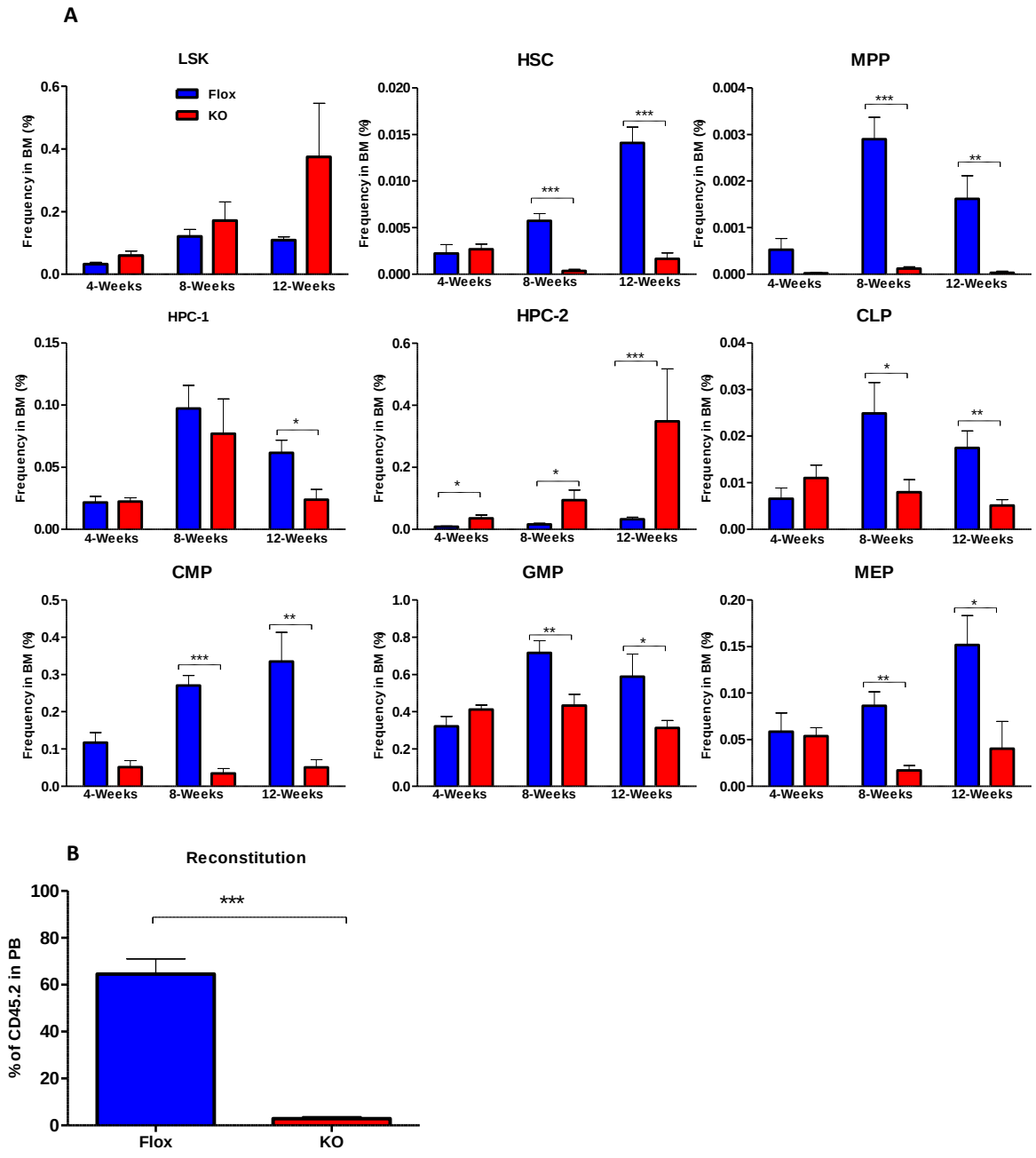


Figure 4-8 Deletion of Cbfb only in the haematopoietic cells resulted in HSCs and progenitors defects.

(A) Percentage of LSK and progenitors of the analysed mice at 4-, 8- and 12-weeks post TAM treatment. Error bars indicate mean ± SD of two independent experiments (n= 6 mice for each group at each time point). (F) Percentage of CD45.2 in PB of the secondary recipient mice at 4 weeks post transplantation (Error bars indicate mean ± SD of data generated from 5 mice).

### 4.2.3 Targeting Cbfb only in the microenvironment doesn't affect HSC and progenitor cells.

In the third approach, we decided to study the impact of Cbfb deletion in the microenvironments on development of haematopoietic stem and progenitor cells. To this end, two groups of CD45.2 mice (Cbfbfl/fl Rosa 26 Cre ER and cbfbfl/fl) were irradiated and transplanted with $1x10^6$ MNC cells harvested from a WT mouse (CD45.1). After achieving good reconstitutions, the two groups were subjected to TAM treatment (IP: 5 consecutive days 120µL of 10mg/ml) to delete Cbfb in the environment and then a tail vein bleeding was carried out to study the impact of this deletion on normal haematopoiesis (figure 4.9).

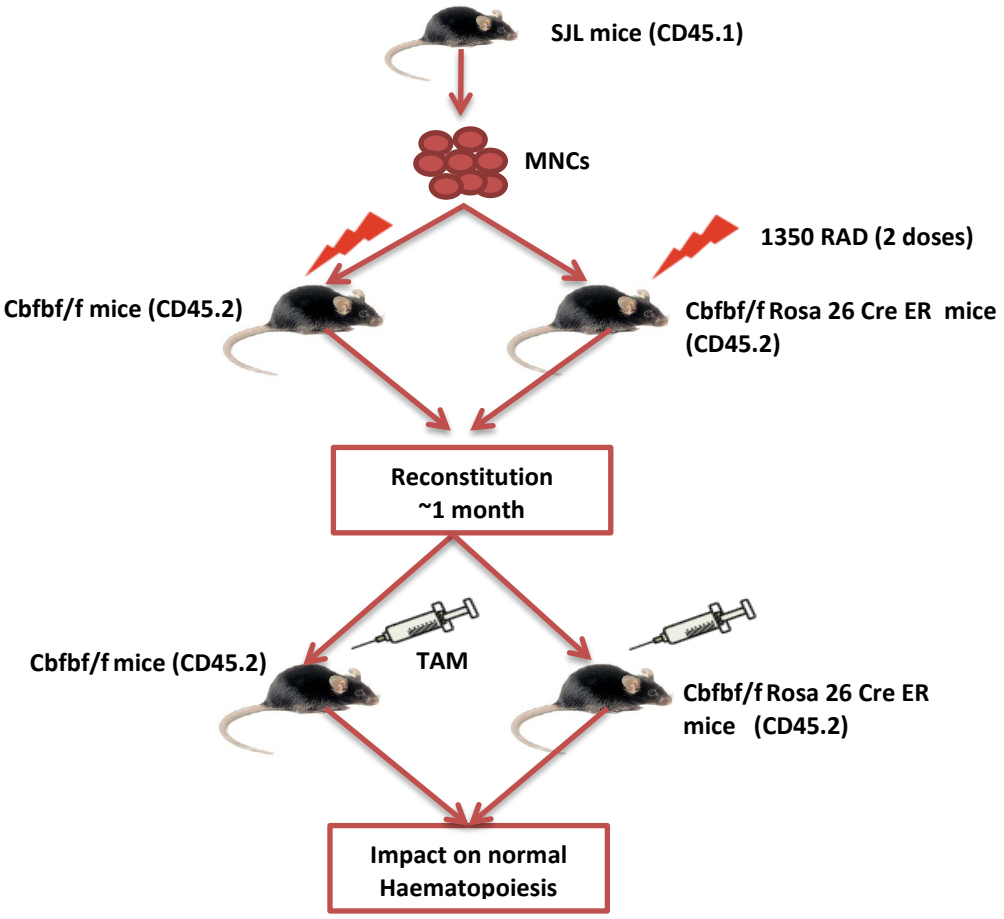


Figure 4-9 our in vivo approach to target Cbfb only in the microenvironment.

We managed to achieve a good reconstitution after 4-weeks post transplantation with similar distribution of myeloid and lymphoid cell in the PB (figure 4.10 A and C). TAM treatment was then carried out for 5 consultative days. Surprisingly, deletion of Cbfb from the microenvironment had no effect on the percentage of reconstitution at 4-weeks post TAM treatment as compared to the control group (figure 4.10 B). Moreover, myeloid and lymphoid FACS analysis of PB at 4-, 8- and 16- weeks post TAM treatment revealed no differences between the KO and floxed groups (figure 4.10 D-F). However, the KO mice started to get sick at around 20-weeks post TAM treatment, therefore these mice were sacrificed together with the control one and subjected to HSCs analysis. To see if the deletion of Cbfb was maintained, ear biopsies were taken from the analysed mice and PCR genotyping was conducted. It was clear that completed deletion of Cbfb was maintained in the KO mice even after 20-weeks (figure 4.10 G). On the other hand, as it was expected, genotyping of the BM cells showed only the WT band (figure 4.10 H). Similar to the PB, FACS analysis of the BM cells showed no differences in the distribution of myeloid and lymphoid cells between the two groups (figure 4.10 I). In addition, no significant difference was observed in the number of CD45.1 BM MNCs of the KO mice comparing to the flox one (figure 4.10 J). The phenotypic analysis of haematopoietic stem and progenitors cells revealed no significant differences between the two groups (figure 4.10 K). LSK populations of the KO mice were very similar to the floxed one with the exception of a slight expansion in HPC-2 in some of the KO mice but it was not statistically significant (figure 4.10 K). HSC

of the KO mice was slightly reduced comparing to the flox one but it was also not statistically significant. Finally, there were almost no differences observed in the progenitor populations between two groups (figure 4.10 K).

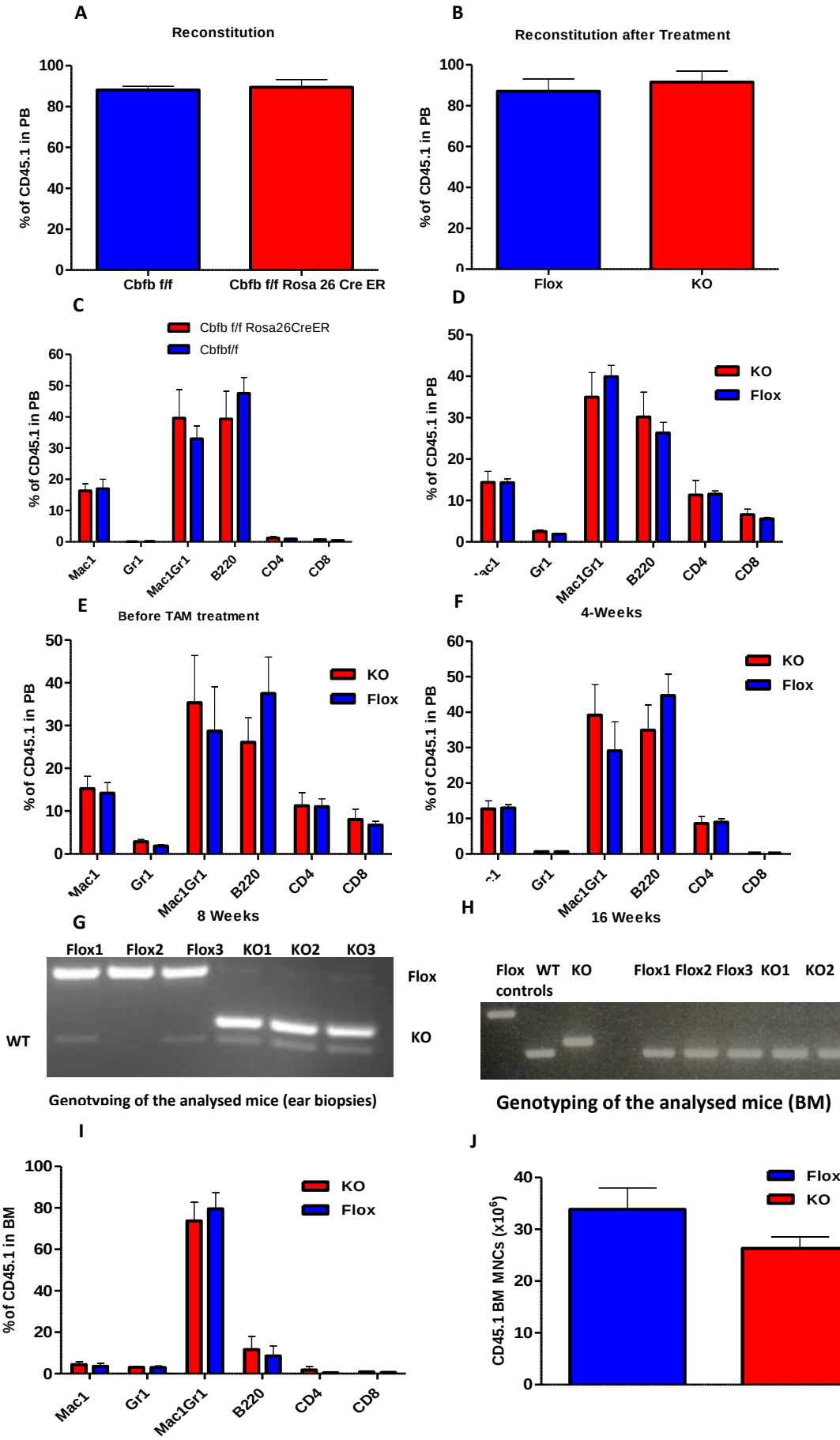
A
Reconstitution
% of CD45.1 in PB
Cbfb f/f
Cbfb f/f Rosa 26 Cre ER
B
Reconstitution after Treatment
% of CD45.1 in PB
Flox
KO
C
Cbfb f/f Rosa26CreER
Cbfbf/f
% of CD45.1 in PB
Mac1
Gr1
Mac1Gr1
B220
CD4
CD8
D
KO
Flox
% of CD45.1 in PB
Mac1Gr1
B220
CD4
CD8
E
Before TAM treatment
KO
Flox
% of CD45.1 in PB
Mac1
Gr1
Mac1Gr1
B220
CD4
CD8
8 Weeks
F
4-Weeks
KO
Flox
% of CD45.1 in PB
Gr1
Mac1Gr1
B220
CD4
CD8
16 Weeks
G
Flox1 Flox2 Flox3 KO1 KO2 KO3
Flox
WT
KO
Genotyping of the analysed mice (ear biopsies)
H
Flox WT KO
controls
Flox1 Flox2 Flox3 KO1 KO2 KO3
Genotyping of the analysed mice (BM)
I
KO
Flox
% of CD45.1 in BM
Mac1
Gr1
Mac1Gr1
B220
CD4
CD8
J
Flox
KO
CD45.1 BM MNCs (x10^6)

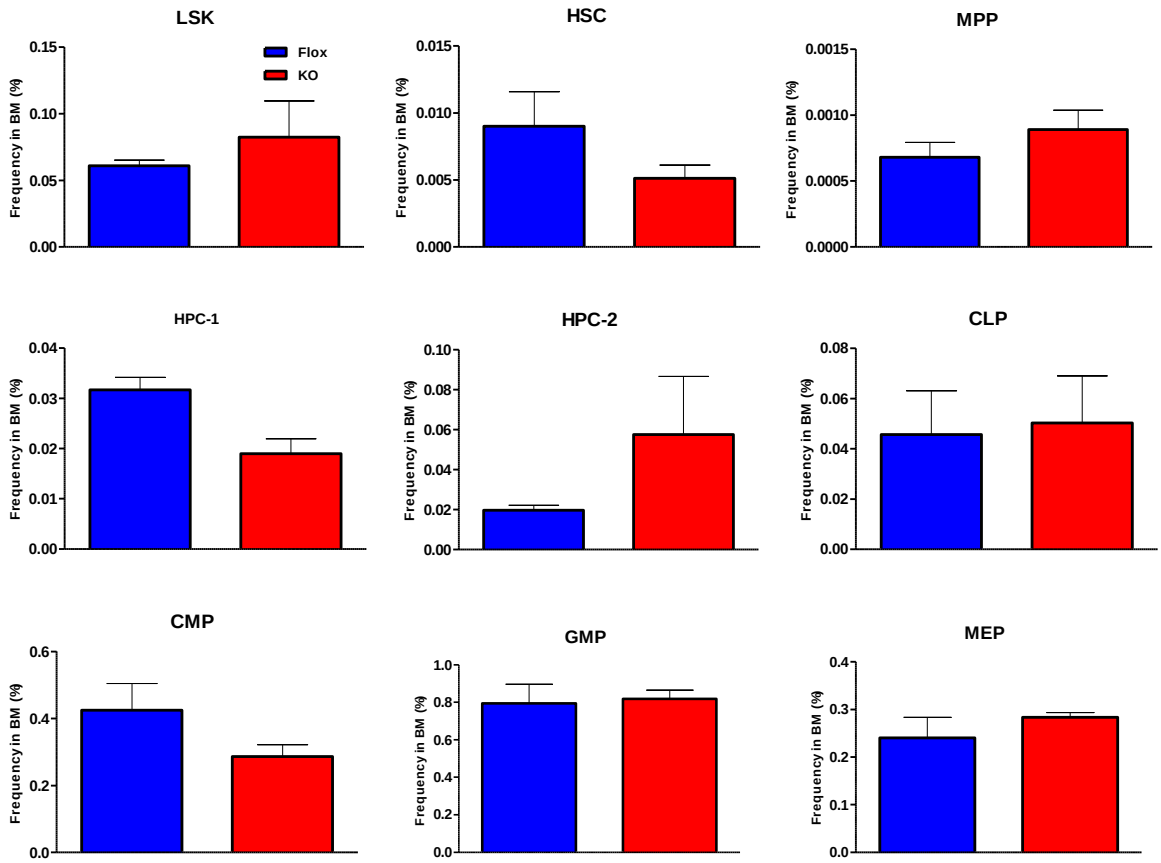


Figure 4-10 Deletion of Cbfb only in microenvironment had no effect on HSC and progenitor cells.

(A and B) Percentage of blood reconstitution (CD45.1 in PB) before (A) and after (B) TAM treatments. (C-F) FACs analysis of PB cells before TAM treatment (C) and post treatment at 4-, 8- and 16- weeks. (G) Genotyping of ear biopsies of the analysed mice (representative samples). (H) Genotyping of BM cells of the analysed mice (representative samples). (I) FACs analysis of BM cells of the analysed mice. (J) CD45.1 BM MNCs cell count of the analysed KO and flox mice. (K) Percentage of LSK and progenitor cells of the analysed mice. Error bars indicate mean ± SD of data generated from 5 mice of each group.

## 4.3 Discussion

To gain insight into the role of Cbfb in normal adult haematopoiesis, in particular in HSC and progenitor development, I used SLAM markers and employed three different experimental settings to study the effects of loss of Cbfb on haematopoietic development in the whole animal, in haematopoietic cells or in the microenvirnoment only. Firstly, to delete Cbfb in the whole animal, Cbfbfl/fl Cre-ER mice as well as the control group (Cbfbfl/fl) were treated with tamoxifen (100µl of 10mg/ml of 4-OHT) for four consecutive days. Analysis of their haematopoiesis was carried out at different time points (4-, 8-, and 12- weeks post treatment). In this experimental setting, deletion of Cbfb resulted in elevation of LSK populations with severe reduction in CMP. Interestingly, more refined gating within the LSK populations showed this elevation was due a specific increase of HPC-1 and HPC-2 at the expense of HSC and MPP. On the other hand CLP, GMP and MEP progenitors were comparable to the control group. However, complete Cbfb deletion was not maintained for the 8- and 12- weeks as a result of strong selection for the Cbfb undeleted cells. Therefore, the time as well as the tamoxifen dose were increased (120µl of 10mg/ml of 4-OHT) for five consecutive days. Surprisingly, the KO mice started to get sick within 1-2 weeks post tamoxifen treatment, and were consequently sacrificed and subjected to HSCs analysis. These mice had low count for WBC, RBC, HGB and PLT counts with reduced B220 and CD8 cells but with high proportion of Mac1 expressing cells, similar to what have been reported recently by Wang and colleagues using Cbfbf/f Mx1-Cre mice despite the lack of achieving complete Cbfb deletion in their study (Wang, Chin et al. 2015). Contradictory to their study, HSCs and MPPs were significantly reduced in our mouse model whereas

the Cbfbf/f Mx1-Cre and Cbfbf/f Vav-iCre mice had more ST-HSC and MPP after Cbfb was targeted but not completely ablated. Using different Cre models (Mx1-Cre and Vav-iCre) and especially using different markers to phenotypically define the stem cells such as flt3, CD34 or SLAM markers (CD150 and CD48) might explain these differences. Nonetheless, my study together with their finding demonstrate that CMP cells required Cbfb for their maintenance as the three mice models showed drastic reduction in CMP after Cbfb deletion (Wang, Chin et al. 2015). Interestingly, deletion of Cbfb in the microenvironment resulted in no major effect on the normal haematopoiesis and the distribution and numbers of stem and progenitor cells were similar to controls. However, the KO mice started to be sick at around 20-weeks post tamoxifen treatment and the reason of this still not clear.

To delineate the effect of Cbfb deletion in haematopoietic cells from non-haematopoietic cells, I used a different experimental setting in which Cbfbfl/fl Rosa Cre ER cells (or Cbfbfl/fl as controls) were transplanted into WT recipient mice allowing specific deletion of Cbfb only in haematopoietic cells. Engraftment levels of greater than 60% were considered as a starting point of having “good seeds in good soil”. To study the effect of Cbfb deletion (only in haematopoietic cells) on HSC and progenitor development, the experimental mice were treated with tamoxifen and analysed at different time points (4-, 8- and 12- weeks). The data the percentage of CD45.2 transplanted cells in the peripheral blood was drastically reduced after Cbfb deletion and also the MNC numbers were reduced in the KO mice throughout the time of analysis (4-12 weeks). Moreover, we also observed a severe reduction of stem/progenitor cells especially HSCs and MPPs when Cbfb was

deleted similar to what was observed in the whole animal suggesting that the effect of Cbfb ablation on normal haematopoiesis might be in a cell-autonomous manner.

It is interesting to note that our conditional mice still express the truncated Cbfb protein with defective Runx1 interaction ability, and it might rescue some of the haematopoietic defects especially when Cbfb was ablated in the whole animal. Indeed, ectopic expression of the Cbfb short form in Cbfb KO ES cells has been shown to rescue the definitive haematopoiesis defects (Miller, Stacy et al. 2001). Therefore the residual activity of this protein in the Cbfb KO embryos might explain the presence of having few definitive haematopoietic precursors (Wang, Stacy et al. 1996; Miller, Stacy et al. 2001).

To test the ability of Cbfb KO cells reconstituting secondary recipient, CD45.2 + cells (1x106) were sorted at 12-weeks post tamoxifen treatment and transplanted into secondary irradiated mice. The data demonstrated that the Cbfb KO cells failed to reconstitute secondary recipient mice comparing the WT cells suggesting a lack of HSC in the KO group. it has been demonstrated that Gata2 has a fundamental role for HSC generation and survival (de Pater, Kaimakis et al. 2013) and its expression was suppressed in the Cbfb KO cells (Wang, Chin et al. 2015). It is also possible that the homing properties of the Cbfb KO cells were severely compromised and which then failed to reconstitute secondary recipients. However further experiments are needed to test these possibilities.

# 5 Conclusion

Over the past years, there has been a huge interest in developing protein-protein interaction inhibitors that might hold the promise to eliminate cancers including haematological malignancies by disrupting alleged key protein interactions of the leukaemia initiating events. While in mixed lineage leukaemia inhibitors targeting the Menin-MLL interaction have been shown great promise in several models (Grembecka, He et al. 2012; Cao, Townsend et al. 2014; He, Senter et al. 2014), disrupting the interaction between AML1 and CBFB has also been proposed as a promising way to treat CBF leukaemia and inhibitors are being developed (Gorczynski, Grembecka et al. 2007; Cunningham, Finckbeiner et al. 2012). At the start of my PhD, the role of Cbfb in AE activity was not fully understood and the main aim was to use a Cbfb conditional knock out mouse model to clarify this by conducting *in vitro* experiments and also establishing an *in vivo* mouse model. My study clearly demonstrated that Cbfb is crucial for initiating of AE9a leukaemogenesis and also for the maintenance of this disease. However it was clear that different experimental strategies might lead to slightly different observations. For instance, AE9a *in vitro* activity was severely compromised in the fetal liver comparing to the adult BM cells. In addition, AE9a transformed LSK cells showed more Cbfb requirement comparing to CMP and GMP cells suggesting the cell of origin might have an impact and should be considered for the future studies. Although the *in vitro* data showed that Cbfb ablation had slightly higher effect on AE9a activity comparing to the full length (AE), future experiments are required to

further test the relevance of this observation. One possible approach will be sorting of stem and progenitor cells from the BM and fetal liver cells of the Cbfb conditional KO mice and then transduce them either with AE9 or AE in the absence or presence of cooperative mutants such as NRAS. Then, the transduced cells should be subjected to direct injections in which the ablation of Cbfb will be carried out using tamoxifen. This approach will provide useful hints about the cell origin and requirement of Cbfb in AE9a leukaemogenesis versus the full length (AE), although the effect of cooperative mutations must be carefully evaluated.

On the other hand, little was known about the role of Cbfb in adult haematopoiesis and I was able to show the importance of Cbfb in development of normal adult haematopoiesis during my PhD. The data clearly demonstrated the crucial function of Cbfb in maintaining stem and progenitor haematopoietic cells in a cell-autonomous manner. Together, the results of this PhD revealed an important function of Cbfb in both normal and malignant haematopoiesis. Thus, treating AE leukaemia by direct inhibition of the interaction between AML1 and CBFB with small molecule inhibitors should be considered carefully. Further studies investigating the effect of these inhibitors on AE leukaemogenesis and normal haematopoiesis in parallel and also in details using relevant *in vivo* models should reveal the existence of potential therapeutic window that allow maximum effect AE leukemia with minimum effects on normal haematopoiesis. Additionally, the current AE9a leukaemia model should be used to generate RNA/ChIP-sequencing data that will help to shed light into the underlying mechanisms for the function of Cbfb which hopefully leads to the development of novel therapeutic targets for AE leukaemia that have no or minimum effect on normal haematopoiesis.

# Appendix

Table A1 (List1): Gene differentially downregulated in AE9a transformed cells with Cbfb flox versus Cbfb KO (P-value <0.05).

| Gene | log2FoldChange |
|---|---|
| Sp100 | -0.92441 |
| Glipr1 | -0.9281 |
| R3hdm4 | -0.93907 |
| Mapk7 | -0.95655 |
| Aldoa | -0.97175 |
| Eid1 | -0.99577 |
| Upp1 | -1.00251 |
| Pde7a | -1.00354 |
| Gm16194 | -1.00357 |
| Gyg | -1.01819 |
| Rnf169 | -1.02093 |
| Pnkp | -1.02379 |
| Mapk8ip3 | -1.03301 |
| Hif1a | -1.03752 |
| Wipi1 | -1.04016 |
| Atp8b4 | -1.05197 |
| Bsg | -1.05227 |
| Prkd2 | -1.05347 |
| Gcnt1 | -1.05592 |
| Dgat1 | -1.06669 |
| Gm24407 | -1.06761 |
| Mdm4 | -1.07155 |
| Csgalnact2 | -1.07331 |
| Abtb1 | -1.07797 |
| Trappc6a | -1.10192 |
| Sil1 | -1.10282 |
| Crispld2 | -1.10863 |
| Tmsb10 | -1.10973 |
| AC157822.1 | -1.11124 |
| Gm15283 | -1.12365 |
| Dvl1 | -1.126 |
| Lamb3 | -1.1265 |
| Gstm4 | -1.13312 |
| Rlf | -1.13478 |
| Gadd45a | -1.13564 |

| | |
|---|---|
| Impdh1 | -1.13921 |
| Mocos | -1.13997 |
| BC037034 | -1.14042 |
| Zfp141 | -1.14357 |
| Sec24a | -1.15053 |
| P4ha1 | -1.15511 |
| Zfand4 | -1.15534 |
| E230016M11Rik | -1.15859 |
| Rin3 | -1.16778 |
| Hopx | -1.17041 |
| Rell1 | -1.18081 |
| Gda | -1.18454 |
| Dynlt1-ps1 | -1.18663 |
| Ero1l | -1.19806 |
| Arhgef4 | -1.20158 |
| Cdkn1a | -1.20184 |
| Jun | -1.20286 |
| Cul9 | -1.21178 |
| Glb1 | -1.21433 |
| Perp | -1.21918 |
| Mcu | -1.21972 |
| 1700037H04Rik | -1.2274 |
| Dstn | -1.22903 |
| Pold4 | -1.23218 |
| Clec2d | -1.2345 |
| Map1lc3a | -1.23665 |
| Azin2 | -1.23682 |
| Ift122 | -1.24119 |
| Cxcr4 | -1.25755 |
| Kdm7a | -1.25928 |
| Lama5 | -1.25951 |
| Trp53inp1 | -1.26316 |
| Fbxl2 | -1.26369 |
| Asnsd1 | -1.26417 |
| Gm28551 | -1.26957 |
| Shc4 | -1.27308 |
| Sesn2 | -1.27724 |
| Ccrn4l | -1.27878 |
| Nhsl2 | -1.28422 |
| Fam46a | -1.28926 |
| Ppp1r3b | -1.29022 |
| Tinagl1 | -1.29877 |

| | |
|---|---|
| Kif7 | -1.30669 |
| C8g | -1.30841 |
| Tesc | -1.31582 |
| Rras | -1.31991 |
| Dynlt1f | -1.32076 |
| Gca | -1.32105 |
| Srgn | -1.3224 |
| Acss2 | -1.32618 |
| Il18r1 | -1.32718 |
| Rab37 | -1.33088 |
| Cystm1 | -1.33102 |
| Tbc1d8 | -1.33169 |
| Fgd4 | -1.33275 |
| Nt5dc2 | -1.33353 |
| Zfp819 | -1.33931 |
| Rab34 | -1.34507 |
| Spry2 | -1.3542 |
| Pdia5 | -1.35615 |
| Trim24 | -1.3615 |
| Adamts10 | -1.36476 |
| Pcbp4 | -1.36968 |
| Selenbp1 | -1.3701 |
| Eif4a2 | -1.37219 |
| Fahd2a | -1.37256 |
| Ly6g | -1.3916 |
| Trib1 | -1.39454 |
| Zfp36 | -1.39895 |
| Fam162a | -1.41469 |
| Padi4 | -1.42648 |
| Bcl2l14 | -1.42764 |
| Fam101b | -1.4321 |
| Clu | -1.44244 |
| Fam114a1 | -1.44498 |
| Stx11 | -1.44583 |
| Cdc42bpg | -1.44655 |
| Csrnp2 | -1.45171 |
| RP24-394C15.7 | -1.45188 |
| Tmed3 | -1.45345 |
| Kcnh7 | -1.45731 |
| Neat1 | -1.45993 |
| Gpx3 | -1.4616 |
| Gab3 | -1.46184 |

| | |
|---|---|
| Ptpn3 | -1.46845 |
| Bmpr1a | -1.47577 |
| Itgb7 | -1.47663 |
| Gm1673 | -1.47682 |
| 0610009E02Rik | -1.47863 |
| Nfil3 | -1.48079 |
| Ptprv | -1.49274 |
| Nlrp12 | -1.49287 |
| Ahrr | -1.4957 |
| Mapk13 | -1.4963 |
| Cd69 | -1.49674 |
| Cxcl3 | -1.50421 |
| 9330159M07Rik | -1.50505 |
| Pvrl4 | -1.50708 |
| Mgst2 | -1.51017 |
| Hgf | -1.51078 |
| Mib2 | -1.51814 |
| Oxld1 | -1.5189 |
| Alox5 | -1.52703 |
| Scd1 | -1.53479 |
| 2310015A10Rik | -1.54404 |
| Olfm4 | -1.54578 |
| Sp140 | -1.5464 |
| Ak1 | -1.56702 |
| Atp2b4 | -1.56948 |
| Amigo2 | -1.57449 |
| Itgb4 | -1.57708 |
| Gnb5 | -1.57711 |
| Ms4a2 | -1.57982 |
| Isg20 | -1.58153 |
| Paqr8 | -1.58311 |
| Alox8 | -1.58325 |
| Mst1 | -1.58374 |
| Gm14636 | -1.58674 |
| Prune2 | -1.58743 |
| Tiam2 | -1.59179 |
| Abca13 | -1.59542 |
| Trim46 | -1.59679 |
| Arhgap28 | -1.60228 |
| Grik5 | -1.60294 |
| Ddit4 | -1.60447 |
| Fosl1 | -1.61008 |

| | |
|---|---|
| Smim24 | -1.61736 |
| Lpin1 | -1.62424 |
| Itga1 | -1.6249 |
| Apc2 | -1.62767 |
| Cecr2 | -1.62875 |
| Ngp | -1.62913 |
| Sned1 | -1.63115 |
| Pknox2 | -1.63862 |
| Pmaip1 | -1.64526 |
| Errfi1 | -1.64615 |
| Gm24270 | -1.64639 |
| Dock6 | -1.64754 |
| Igf1r | -1.64874 |
| Bcl2 | -1.65124 |
| Hspa2 | -1.6557 |
| Thbs3 | -1.66288 |
| Pcgf2 | -1.66551 |
| Il6 | -1.6678 |
| Thy1 | -1.67162 |
| Dhtkd1 | -1.67728 |
| Sec31b | -1.67797 |
| Rnd3 | -1.68046 |
| Tex2 | -1.68309 |
| Chrm3 | -1.68986 |
| Ptprs | -1.69299 |
| Lrg1 | -1.69838 |
| Gata2 | -1.70626 |
| Fignl2 | -1.70738 |
| Slco4a1 | -1.70791 |
| Car9 | -1.71118 |
| Prnp | -1.71626 |
| Faah | -1.718 |
| Syt3 | -1.7244 |
| Gm26669 | -1.72465 |
| Sh3pxd2a | -1.72834 |
| Adssl1 | -1.72964 |
| Gatm | -1.73051 |
| Mctp2 | -1.73537 |
| Gm5873 | -1.7378 |
| RP24-295A5.2 | -1.74192 |
| Gpr171 | -1.74355 |
| Gm3571 | -1.7442 |

| | |
|---|---|
| Lgals4 | -1.74615 |
| Wdr54 | -1.75427 |
| Gm17017 | -1.7559 |
| Clec2i | -1.7599 |
| Fads2 | -1.76543 |
| Cebpa | -1.77298 |
| Ets1 | -1.77442 |
| Ccdc40 | -1.7765 |
| Rdm1 | -1.77709 |
| Acacb | -1.78388 |
| Clec2g | -1.79757 |
| Aldoc | -1.8067 |
| Tcp11 | -1.80831 |
| Wfdc12 | -1.80887 |
| Adgrl2 | -1.80988 |
| Ccl27a | -1.82174 |
| Epha7 | -1.82715 |
| Crip1 | -1.82797 |
| Hyi | -1.82833 |
| Txnip | -1.82992 |
| Six5 | -1.83157 |
| Dbp | -1.83184 |
| Pik3ip1 | -1.83458 |
| Zfp36l1 | -1.83754 |
| Hid1 | -1.83978 |
| Zcchc14 | -1.84065 |
| Ablim2 | -1.84351 |
| Copz2 | -1.84634 |
| Per2 | -1.85132 |
| Gm15396 | -1.85541 |
| Slc30a2 | -1.85568 |
| H2-Ob | -1.85621 |
| Fam213b | -1.86271 |
| Gm15441 | -1.86402 |
| RP24-481E4.4 | -1.86487 |
| P3h3 | -1.86808 |
| Gm12031 | -1.86889 |
| Klrb1f | -1.86951 |
| Serpine1 | -1.87252 |
| B4galt6 | -1.87803 |
| Napsa | -1.88163 |
| Trpm6 | -1.88508 |

| | |
|---|---|
| Gpr34 | -1.88991 |
| Ak4 | -1.89347 |
| Klk1b1 | -1.89962 |
| Slc7a4 | -1.90046 |
| Reep6 | -1.90416 |
| Shf | -1.90506 |
| Fdps | -1.90523 |
| Sorl1 | -1.9144 |
| Btg2 | -1.92753 |
| Adamtsl4 | -1.92833 |
| Mir7678 | -1.93669 |
| Rasa4 | -1.94536 |
| Efemp2 | -1.94609 |
| Slpi | -1.94744 |
| Smpd5 | -1.95012 |
| Zfp827 | -1.95308 |
| Osm | -1.95414 |
| Cep170b | -1.95454 |
| Ptpru | -1.95499 |
| Islr2 | -1.96878 |
| Mar-09 | -1.96886 |
| Cyb561 | -1.96894 |
| Bahcc1 | -1.97038 |
| Per3 | -1.97295 |
| Il13 | -1.98075 |
| Spint2 | -1.98843 |
| Syne4 | -1.99807 |
| Gm15440 | -1.99836 |
| Scube3 | -1.99931 |
| Gp1bb | -2.0006 |
| Pycr1 | -2.00553 |
| Rnu3b3 | -2.00559 |
| Krba1 | -2.01202 |
| Notch1 | -2.01408 |
| Ndrg2 | -2.01521 |
| Gm12454 | -2.01779 |
| Esr2 | -2.01812 |
| Fam169b | -2.02085 |
| Scnn1a | -2.02205 |
| Rnf144a | -2.02321 |
| B3gnt5 | -2.03955 |
| U3 | -2.0424 |

| | |
|---|---|
| Ace | -2.04265 |
| Inhbb | -2.04397 |
| Cldn1 | -2.04468 |
| 9530077C05Rik | -2.05389 |
| Gm13031 | -2.05436 |
| Gm16214 | -2.05572 |
| Ttc21a | -2.06397 |
| Dlg2 | -2.07135 |
| Celsr1 | -2.074 |
| Col5a1 | -2.07439 |
| Dbn1 | -2.08245 |
| Flywch2 | -2.0841 |
| Plin5 | -2.08424 |
| Bcl6 | -2.08835 |
| 4930562C15Rik | -2.09336 |
| Cpa6 | -2.09389 |
| Cacnb1 | -2.10585 |
| Nupr1l | -2.10927 |
| Ctf2 | -2.11018 |
| 4931406G06Rik | -2.11635 |
| Ces1d | -2.1313 |
| Gm37188 | -2.15724 |
| Nlgn2 | -2.15863 |
| Neurl1b | -2.15936 |
| Cyp2s1 | -2.16292 |
| Dennd2a | -2.1682 |
| Tnnc1 | -2.16869 |
| Sep-05 | -2.1738 |
| Fosb | -2.17604 |
| Gm17048 | -2.17821 |
| Radil | -2.19079 |
| Bzrap1 | -2.20758 |
| Arfgef3 | -2.21369 |
| Heph | -2.22077 |
| Gatsl3 | -2.22814 |
| Garnl3 | -2.22899 |
| Tmem8b | -2.23084 |
| Ccno | -2.23243 |
| Cacna1h | -2.23525 |
| Rgs11 | -2.23709 |
| Hspa1b | -2.23736 |
| Sema4f | -2.23769 |

| | |
|---|---|
| I830127L07Rik | -2.24741 |
| Hdac11 | -2.24747 |
| Nos1ap | -2.2552 |
| Osbpl3 | -2.2614 |
| Ccr2 | -2.26188 |
| Ccdc106 | -2.26253 |
| Gpc2 | -2.26416 |
| P4ha2 | -2.26461 |
| Tifab | -2.26841 |
| Tpsg1 | -2.27187 |
| Lmntd2 | -2.28279 |
| Aldh1a3 | -2.28877 |
| Kdelr3 | -2.29685 |
| Rph3al | -2.29699 |
| Cd28 | -2.3014 |
| Lif | -2.308 |
| Tmem132b | -2.31894 |
| Ccbl1 | -2.31992 |
| 2010107G23Rik | -2.32205 |
| Lpar1 | -2.32286 |
| Nlrp6 | -2.33279 |
| Arhgef17 | -2.33336 |
| Padi2 | -2.334 |
| Tex15 | -2.34389 |
| Fam83h | -2.36161 |
| Usp17ld | -2.36251 |
| Ighv1-23 | -2.36339 |
| Gm20481 | -2.36447 |
| Lmtk3 | -2.36483 |
| Haao | -2.38019 |
| Celf5 | -2.38676 |
| Gm7694 | -2.3962 |
| Acaa1b | -2.40549 |
| Kcnc3 | -2.41188 |
| F730016J06Rik | -2.42146 |
| Myo18b | -2.42371 |
| Baiap3 | -2.43743 |
| Arap2 | -2.44532 |
| Pax8 | -2.46827 |
| Col20a1 | -2.4685 |
| Tnfaip6 | -2.46862 |
| Il2ra | -2.47417 |

| | |
|---|---|
| Ppfia3 | -2.48161 |
| Lipg | -2.48755 |
| Entpd3 | -2.49574 |
| Bend4 | -2.49656 |
| Agrn | -2.49752 |
| Lppr2 | -2.49876 |
| Catsperg1 | -2.49882 |
| Nrbp2 | -2.50388 |
| Gpr141 | -2.51112 |
| Hal | -2.51462 |
| Hspa1a | -2.52566 |
| Irf6 | -2.52996 |
| Mefv | -2.5399 |
| Prl2c5 | -2.54056 |
| Vldlr | -2.57752 |
| Pygm | -2.58315 |
| Bcas1 | -2.61977 |
| Mmp8 | -2.62717 |
| 4931406B18Rik | -2.6401 |
| Eps8l2 | -2.64306 |
| Skap1 | -2.65299 |
| Chst13 | -2.66193 |
| Gm15663 | -2.67076 |
| Cpa5 | -2.67159 |
| Mfsd2a | -2.67524 |
| Dnm1 | -2.68217 |
| 5430421N21Rik | -2.68229 |
| Col5a3 | -2.6841 |
| H2-Q7 | -2.68763 |
| Ptk7 | -2.69478 |
| Itih5 | -2.69873 |
| Zfp711 | -2.72382 |
| Epx | -2.7242 |
| 4932438H23Rik | -2.72767 |
| Satb1 | -2.73928 |
| Egr1 | -2.74134 |
| Gm29233 | -2.74461 |
| Cercam | -2.74601 |
| Tgfbr3 | -2.79178 |
| Dixdc1 | -2.80661 |
| Npr2 | -2.83996 |
| Txk | -2.85463 |

| | |
|---|---|
| Thbs1 | -2.86206 |
| Ect2l | -2.86451 |
| Gpc1 | -2.86645 |
| Cd226 | -2.8896 |
| Serpinb10 | -2.94301 |
| Cdh17 | -2.95158 |
| Crisp1 | -2.96098 |
| Zfr2 | -2.97064 |
| Csrp3 | -2.98134 |
| Mcpt2 | -2.99356 |
| Serpinb10 | -2.99417 |
| Kif17 | -3.00243 |
| Rnase12 | -3.06138 |
| Dsp | -3.08557 |
| Ptprf | -3.11213 |
| Serpine2 | -3.14995 |
| Sytl3 | -3.15262 |
| Hsf4 | -3.15913 |
| Dkkl1 | -3.17092 |
| Npdc1 | -3.17489 |
| Mef2b | -3.2159 |
| Aqp8 | -3.22621 |
| Vegfa | -3.33183 |
| Epcam | -3.3398 |
| Klk1b11 | -3.36996 |
| Mcpt4 | -3.41604 |
| Muc15 | -3.48267 |
| Eno2 | -3.4846 |
| Rcn3 | -3.49117 |
| Fcer1a | -3.58445 |
| Tmtc2 | -3.69437 |
| Avil | -3.75542 |
| Nt5e | -3.84749 |
| Pcsk9 | -3.87601 |
| Htra1 | -3.92831 |
| Pcdh1 | -3.99308 |
| Ptprg | -4.08647 |
| Acpp | -4.15683 |
| Cyp2b10 | -4.32886 |
| Scin | -4.45291 |
| Tpsb2 | -5.17158 |
| Tnfrsf9 | -5.90866 |

Table A2 List2: Gene differentially upregulated in AE9a transformed cells with Cbfb flox versus Cbfb KO (P-value <0.05).

| Gene | log2FoldChange |
|---|---|
| Bank1 | 5.361398 |
| Fcrls | 4.826186 |
| Hmga2 | 4.062039 |
| Nptx1 | 3.925574 |
| Htr1b | 3.633823 |
| Frmpd1 | 3.535109 |
| Tspan7 | 3.370843 |
| Chn2 | 3.332652 |
| Trim2 | 3.1411 |
| Igf2r | 3.126366 |
| Dcstamp | 3.123838 |
| Ly6a | 3.071798 |
| Scimp | 3.041859 |
| Ptk2 | 3.02991 |
| Rab15 | 2.977383 |
| Adgre4 | 2.97447 |
| Cyp1b1 | 2.925665 |
| Akap6 | 2.898708 |
| Cmklr1 | 2.876541 |
| Serpinb9b | 2.867189 |
| Fcgr1 | 2.856493 |
| Iqsec3 | 2.832567 |
| Ccl2 | 2.791345 |
| Gbp9 | 2.763548 |
| Npy | 2.64609 |
| Siglecg | 2.622247 |
| 4930447F24Rik | 2.617297 |
| Rbp4 | 2.610802 |
| 9130019P16Rik | 2.599713 |
| Ccl7 | 2.577576 |
| Bcl6b | 2.572248 |
| Sardh | 2.541796 |
| Luzp1 | 2.515121 |
| Lzts1 | 2.508307 |
| Ivl | 2.50817 |
| Edn1 | 2.501269 |
| Gpr65 | 2.495559 |

| | |
|---|---|
| Nbea | 2.471024 |
| Loxl2 | 2.457332 |
| Cd209a | 2.434148 |
| Slc12a2 | 2.399891 |
| Unc5c | 2.394732 |
| BC035044 | 2.394217 |
| Slc11a1 | 2.390897 |
| AC125099.2 | 2.388658 |
| Adarb1 | 2.381331 |
| Magi1 | 2.340872 |
| Bcl2a1d | 2.337664 |
| Peg10 | 2.331357 |
| Tmem144 | 2.311993 |
| Alox15 | 2.308573 |
| Treml4 | 2.303279 |
| Tnfsf4 | 2.3024 |
| Rab3il1 | 2.289997 |
| Nrxn1 | 2.288961 |
| Hist2h2ac | 2.281646 |
| Gata3 | 2.275575 |
| Mamdc2 | 2.273965 |
| Dlc1 | 2.244543 |
| Cdh2 | 2.225486 |
| Tulp3 | 2.219393 |
| Myct1 | 2.205433 |
| Fam49a | 2.199807 |
| Lrrc49 | 2.198308 |
| Grb10 | 2.188786 |
| Cd48 | 2.181731 |
| Ggact | 2.181227 |
| Gja5 | 2.173401 |
| Fam198b | 2.170923 |
| Bicd1 | 2.164356 |
| S100a4 | 2.163174 |
| Gimap4 | 2.161184 |
| Gpr84 | 2.15531 |
| RP23-326D6.5 | 2.148916 |
| Fzd6 | 2.148739 |
| Camk1d | 2.147589 |
| Hist1h2an | 2.137323 |
| Lrrc16a | 2.132127 |
| Apol11b | 2.111125 |

| | |
|---|---|
| Ighm | 2.111079 |
| D430036J16Rik | 2.107294 |
| Jph1 | 2.106944 |
| Gm21451 | 2.101159 |
| Flrt2 | 2.092365 |
| Cck | 2.08425 |
| Adam33 | 2.067121 |
| AL589651.4 | 2.057191 |
| Hmgn3 | 2.049403 |
| Hist1h3g | 2.041956 |
| Cobl | 2.037205 |
| Slc28a3 | 2.035086 |
| Gm36569 | 2.030204 |
| Eef1a2 | 2.027017 |
| Ccser1 | 2.006553 |
| Hist1h2bj | 2.004268 |
| Mylk3 | 1.997643 |
| Cltb | 1.997351 |
| F3 | 1.995551 |
| Bcl2a1b | 1.988814 |
| Tmem26 | 1.987928 |
| Pla2g5 | 1.98466 |
| Aven | 1.970341 |
| Lifr | 1.967926 |
| Hist1h2bp | 1.964391 |
| Trim10 | 1.963999 |
| Raet1d | 1.95595 |
| Gpatch4 | 1.952292 |
| Scml4 | 1.948642 |
| Gm13546 | 1.948424 |
| Rasgef1b | 1.940909 |
| Slc5a11 | 1.925801 |
| Pmp22 | 1.925484 |
| Hist1h2ah | 1.913995 |
| Awat1 | 1.903889 |
| Afp | 1.887257 |
| Nlrp1a | 1.883419 |
| Camk2a | 1.879884 |
| Rasal2 | 1.874883 |
| Fut10 | 1.868575 |
| Flt1 | 1.863536 |
| Bex1 | 1.859507 |

| | |
|---|---|
| Cd34 | 1.857398 |
| Hist1h1b | 1.848851 |
| Hist1h2bh | 1.845708 |
| Msrb2 | 1.838149 |
| AL590614.1 | 1.83198 |
| AL590614.2 | 1.829486 |
| Gm29094 | 1.827703 |
| Hist4h4 | 1.823051 |
| Shank3 | 1.820766 |
| Ms4a6d | 1.820372 |
| Nmi | 1.820196 |
| Slc25a13 | 1.819741 |
| Plekha8 | 1.817922 |
| Ctsk | 1.816888 |
| Eya1 | 1.815151 |
| Hist1h2ag | 1.812355 |
| Slc35a1 | 1.80628 |
| Batf3 | 1.80549 |
| S1pr1 | 1.80235 |
| Matk | 1.80018 |
| Gm15564 | 1.792027 |
| Nckap1 | 1.790327 |
| Dnmt3b | 1.780446 |
| Mcoln2 | 1.77488 |
| Trim30b | 1.773932 |
| Plet1 | 1.76814 |
| Hist2h4 | 1.761824 |
| Nefh | 1.761096 |
| Rgs9 | 1.75707 |
| Slc18a1 | 1.755352 |
| Apbb2 | 1.743882 |
| 4930558J22Rik | 1.734821 |
| P2ry13 | 1.732526 |
| Mfsd6 | 1.732193 |
| Qpct | 1.727921 |
| Hist2h3b | 1.722253 |
| Ttc28 | 1.717434 |
| Kcne3 | 1.716274 |
| Hist1h3h | 1.715408 |
| Bmp7 | 1.714756 |
| Hist1h4b | 1.713488 |
| AL662809.1 | 1.706427 |

| | |
|---|---|
| Nr1h3 | 1.701232 |
| Pop1 | 1.699207 |
| Ttc8 | 1.698726 |
| Ctla2b | 1.694796 |
| Myo1e | 1.6933 |
| Siglecf | 1.688342 |
| Gm16897 | 1.687423 |
| Mmp9 | 1.68108 |
| Hist1h2ai | 1.679953 |
| Ptgfrn | 1.671728 |
| Cpq | 1.670055 |
| Hist1h1a | 1.66677 |
| Hist1h3a | 1.664051 |
| Wdpcp | 1.660424 |
| Atp8b5 | 1.658256 |
| Lpcat1 | 1.656279 |
| Tie1 | 1.652326 |
| Trim17 | 1.643736 |
| Oas1a | 1.639519 |
| Sgsh | 1.635488 |
| Il1r1 | 1.62685 |
| AL589651.1 | 1.626707 |
| Il1a | 1.626015 |
| Hist1h2ac | 1.618375 |
| Hist1h3i | 1.618047 |
| Gm20628 | 1.61604 |
| Hist1h3b | 1.614954 |
| Lars2 | 1.605457 |
| Pde7b | 1.603687 |
| Hist1h2ad | 1.602105 |
| Hist2h2bb | 1.598626 |
| Hist3h2a | 1.597051 |
| Batf | 1.596295 |
| Gm7901 | 1.587326 |
| Hist1h1d | 1.583296 |
| Hist2h2bb | 1.578508 |
| Phgdh | 1.570857 |
| Slc26a11 | 1.56794 |
| Phb | 1.562829 |
| Klf8 | 1.55019 |
| Tns3 | 1.541964 |
| Card14 | 1.54149 |

| | |
|---|---|
| Hist1h2bk | 1.541244 |
| Hist1h3f | 1.534618 |
| Kazald1 | 1.5327 |
| Extl3 | 1.526492 |
| Atp13a2 | 1.523738 |
| Gm12141 | 1.518397 |
| Ftsj3 | 1.51722 |
| Hist1h2ab | 1.512188 |
| Grap | 1.507485 |
| Hist1h4j | 1.5054 |
| Dlg3 | 1.501753 |
| Grwd1 | 1.500109 |
| Hist1h4a | 1.499957 |
| Il17ra | 1.498386 |
| Tnfsf13 | 1.495998 |
| Hist1h4f | 1.494946 |
| Nup85 | 1.486842 |
| Tns1 | 1.476284 |
| Tgfbr1 | 1.47415 |
| Rgs3 | 1.473894 |
| Tnfrsf8 | 1.471137 |
| Ift27 | 1.468462 |
| Dkc1 | 1.463371 |
| Havcr2 | 1.461222 |
| Mical2 | 1.453348 |
| Dip2c | 1.448157 |
| Ndst1 | 1.446933 |
| Wdr4 | 1.444206 |
| Kti12 | 1.440308 |
| Mmp12 | 1.439458 |
| Tamm41 | 1.43391 |
| AC034285.3 | 1.427143 |
| Dscc1 | 1.425948 |
| Hspd1 | 1.42263 |
| Ly9 | 1.422438 |
| St6gal1 | 1.411556 |
| Cdk14 | 1.408278 |
| Sf3b3 | 1.40661 |
| Ank | 1.406408 |
| Mrpl20 | 1.405627 |
| Prkca | 1.404077 |
| 2810025M15Rik | 1.399921 |

| | |
|---|---|
| Bcl2a1a | 1.39983 |
| Hspbp1 | 1.394571 |
| Commd9 | 1.393705 |
| Bcat1 | 1.38368 |
| Dph2 | 1.383195 |
| Apex1 | 1.379895 |
| Bdh1 | 1.37959 |
| Ranbp1 | 1.378952 |
| Cpeb1 | 1.369313 |
| 4932441J04Rik | 1.357098 |
| Nme1 | 1.357094 |
| Dok2 | 1.354107 |
| Tpst1 | 1.352565 |
| Ppm1e | 1.352195 |
| Akr1c12 | 1.351497 |
| Tmco4 | 1.349587 |
| Xpo5 | 1.349208 |
| Oxct1 | 1.346979 |
| Polr1b | 1.341531 |
| Nolc1 | 1.333536 |
| Tyms | 1.333496 |
| Ccdc88a | 1.325036 |
| Pitpnm2 | 1.323488 |
| Pcdh7 | 1.322029 |
| Mcm5 | 1.3211 |
| Rpgrip1l | 1.309784 |
| Lrrcc1 | 1.303262 |
| Tomm40 | 1.30231 |
| Tnfsfm13 | 1.301278 |
| Hnrnpab | 1.29443 |
| Cyb5a | 1.277367 |
| Rai14 | 1.276962 |
| Mef2c | 1.270717 |
| Ddx21 | 1.261725 |
| Icam1 | 1.254893 |
| Srsf1 | 1.249754 |
| P2rx1 | 1.24869 |
| Socs2 | 1.246821 |
| Mybbp1a | 1.246046 |
| Gtf2h3 | 1.244438 |
| Parvb | 1.243945 |
| Set | 1.243503 |

| | |
|---|---|
| Zdhhc2 | 1.224832 |
| Ddx39 | 1.223539 |
| Fastkd2 | 1.219812 |
| Mcm2 | 1.218554 |
| Tomm5 | 1.218404 |
| Gusb | 1.209003 |
| Dok7 | 1.207914 |
| Tjp2 | 1.207102 |
| Psmb10 | 1.206627 |
| Heatr3 | 1.202548 |
| Fam173b | 1.200276 |
| Mettl16 | 1.199643 |
| Psmc5 | 1.189857 |
| Nudt1 | 1.184981 |
| Gimap6 | 1.180899 |
| Prkrir | 1.174107 |
| Prkd3 | 1.169306 |
| Gm13461 | 1.164033 |
| Mpdu1 | 1.162957 |
| Psmc4 | 1.160184 |
| Nasp | 1.150716 |
| Cct3 | 1.147133 |
| B230118H07Rik | 1.14638 |
| Slc16a10 | 1.139828 |
| Tfec | 1.132379 |
| Cluh | 1.129682 |
| Lmna | 1.126731 |
| Fyn | 1.121853 |
| Heatr1 | 1.119035 |
| Calm1 | 1.118357 |
| Cct6a | 1.115772 |
| Slc28a2 | 1.115097 |
| Spred1 | 1.10999 |
| Eif5a | 1.101954 |
| Psmd6 | 1.089937 |
| Sgce | 1.077804 |
| Cyth4 | 1.071849 |
| Rapgef1 | 1.071407 |
| Eif4g2 | 1.070621 |
| Slco3a1 | 1.066893 |
| Pkp4 | 1.065608 |
| Galk2 | 1.044772 |

| | |
|---|---|
| Tarbp2 | 1.037321 |
| Eif5al3-ps | 1.022213 |
| Polq | 1.020927 |
| Bcl2l1 | 1.020526 |
| Eif4a-ps4 | 1.004968 |
| Rab35 | 0.994987 |
| Atp10a | 0.987266 |
| Pip4k2a | 0.966403 |

Table A3: List of differentially expressed genes that were overlapped between Lo's study and our study. List 3= AE9a dysregulated gene in Lo's study vs our List 1. List 4= AE9a dysregulated gene in Lo's study vs our list2.

| **List 3** | **List 4** |
|---|---|
| Adamts10 | atp10a |
| Adssl1 | bc035044 |
| Alox5 | cyb5a |
| Atp8b4 | dlg3 |
| B4galt6 | fam198b |
| Bahcc1 | fyn |
| Ccr2 | grap |
| Cdkn1a | hist1h4b |
| Cebpa | hmga2 |
| Crip1 | hmgn3 |
| Csrnp2 | ighm |
| Cxcr4 | il17ra |
| Epx | kazald1 |
| Ero1l | lmna |
| Ets1 | lrrc16a |
| Gadd45a | luzp1 |
| Gatm | mef2c |
| Gatsl3 | nbea |
| Glipr1 | oxct1 |
| Gpc1 | phb |
| Gpr171 | pkp4 |
| Haao | plekha8 |
| Irf6 | pmp22 |
| Kif17 | prkca |
| Klrb1f | prkd3 |
| Mefv | slc12a2 |
| Ms4a2 | slc25a13 |
| Napsa | slc28a2 |
| Ndrg2 | slco3a1 |
| Nlgn2 | socs2 |
| Prnp | tfec |
| Ptprs | tie1 |
| Rasa4 | tnfsf13 |
| Rnf144a | tns1 |
| Rras | wdr4 |
| Satb1 | |

| | |
|---|---|
| Scin | |
| Serpine2 | |
| Slc30a2 | |
| Slco4a1 | |
| Slpi | |
| Sorl1 | |
| Spint2 | |
| Tifab | |

# References

Adolfsson, J., O. J. Borge, et al. (2001). "Upregulation of Flt3 expression within the bone marrow Lin(-)Sca1(+)c-kit(+) stem cell compartment is accompanied by loss of self-renewal capacity." Immunity **15**(4): 659-669.

Adolfsson, J., R. Mansson, et al. (2005). "Identification of Flt3+ lympho-myeloid stem cells lacking erythro-megakaryocytic potential a revised road map for adult blood lineage commitment." Cell **121**(2): 295-306.

Akashi, K., D. Traver, et al. (2000). "A clonogenic common myeloid progenitor that gives rise to all myeloid lineages." Nature **404**(6774): 193-197.

Banerji, S., K. Cibulskis, et al. (2012). "Sequence analysis of mutations and translocations across breast cancer subtypes." Nature **486**(7403): 405-409.

Basecke, J., M. Feuring-Buske, et al. (2002). "Transcription of AML1 in hematopoietic subfractions of normal adults." Ann Hematol **81**(5): 254-257.

Basecke, J., M. Schwieger, et al. (2005). "AML1/ETO promotes the maintenance of early hematopoietic progenitors in NOD/SCID mice but does not abrogate their lineage specific differentiation." Leuk Lymphoma **46**(2): 265-272.

Becker, A. J., C. E. Mc, et al. (1963). "Cytological demonstration of the clonal nature of spleen colonies derived from transplanted mouse marrow cells." Nature **197**: 452-454.

Bee, T., G. Swiers, et al. (2010). "Nonredundant roles for Runx1 alternative promoters reflect their activity at discrete stages of developmental hematopoiesis." Blood **115**(15): 3042-3050.

Bejar, R., K. Stevenson, et al. (2011). "Clinical effect of point mutations in myelodysplastic syndromes." N Engl J Med **364**(26): 2496-2506.

Blyth, K., E. R. Cameron, et al. (2005). "The RUNX genes: gain or loss of function in cancer." Nat Rev Cancer **5**(5): 376-387.

Bonnet, D. and J. E. Dick (1997). "Human acute myeloid leukemia is organized as a hierarchy that originates from a primitive hematopoietic cell." Nat Med **3**(7): 730-737.

Cai, X., J. J. Gaudet, et al. (2011). "Runx1 loss minimally impacts long-term hematopoietic stem cells." PLoS One **6**(12): e28430.

Cao, F., E. C. Townsend, et al. (2014). "Targeting MLL1 H3K4 methyltransferase activity in mixed-lineage leukemia." Mol Cell **53**(2): 247-261.

Chen, Y., Y. Hu, et al. (2009). "Loss of the Alox5 gene impairs leukemia stem cells and prevents chronic myeloid leukemia." Nat Genet **41**(7): 783-792.

Chou, F. S. and J. C. Mulloy (2011). "The thrombopoietin/MPL pathway in hematopoiesis and leukemogenesis." J Cell Biochem **112**(6): 1491-1498.

Christensen, J. L. and I. L. Weissman (2001). "Flk-2 is a marker in hematopoietic stem cell differentiation: a simple method to isolate long-term stem cells." Proc Natl Acad Sci U S A **98**(25): 14541-14546.

Cozzio, A., E. Passegue, et al. (2003). "Similar MLL-associated leukemias arising from self-renewing stem cells and short-lived myeloid progenitors." Genes Dev **17**(24): 3029-3035.

Cunningham, L., S. Finckbeiner, et al. (2012). "Identification of benzodiazepine Ro5-3335 as an inhibitor of CBF leukemia through quantitative high throughput screen against RUNX1-CBFbeta interaction." Proc Natl Acad Sci U S A **109**(36): 14592-14597.

Dakic, A., D. Metcalf, et al. (2005). "PU.1 regulates the commitment of adult hematopoietic progenitors and restricts granulopoiesis." J Exp Med **201**(9): 1487-1502.

Davis, J. N., D. Rogers, et al. (2010). "Association of core-binding factor beta with the malignant phenotype of prostate and ovarian cancer cells." J Cell Physiol **225**(3): 875-887.

de Bruijn, M. F. and N. A. Speck (2004). "Core-binding factors in hematopoiesis and immune function." Oncogene **23**(24): 4238-4248.

de Guzman, C. G., A. J. Warren, et al. (2002). "Hematopoietic stem cell expansion and distinct myeloid developmental abnormalities in a murine model of the AML1-ETO translocation." Mol Cell Biol **22**(15): 5506-5517.

de Pater, E., P. Kaimakis, et al. (2013). "Gata2 is required for HSC generation and survival." J Exp Med **210**(13): 2843-2850.

DeKelver, R. C., B. Lewin, et al. (2013). "Cooperation between RUNX1-ETO9a and novel transcriptional partner KLF6 in upregulation of Alox5 in acute myeloid leukemia." PLoS Genet **9**(10): e1003765.

Doulatov, S., F. Notta, et al. (2012). "Hematopoiesis: a human perspective." Cell Stem Cell **10**(2): 120-136.

Dulak, A. M., S. E. Schumacher, et al. (2012). "Gastrointestinal adenocarcinomas of the esophagus, stomach, and colon exhibit distinct patterns of genome instability and oncogenesis." Cancer Res **72**(17): 4383-4393.

Ellis, M. J., L. Ding, et al. (2012). "Whole-genome analysis informs breast cancer response to aromatase inhibition." Nature **486**(7403): 353-360.

Forsberg, E. C., S. S. Prohaska, et al. (2005). "Differential expression of novel potential regulators in hematopoietic stem cells." PLoS Genet **1**(3): e28.

Galloway, J. L., R. A. Wingert, et al. (2005). "Loss of gata1 but not gata2 converts erythropoiesis to myelopoiesis in zebrafish embryos." Dev Cell **8**(1): 109-116.

Gekas, C., F. Dieterlen-Lievre, et al. (2005). "The placenta is a niche for hematopoietic stem cells." Dev Cell **8**(3): 365-375.

Gorczynski, M. J., J. Grembecka, et al. (2007). "Allosteric inhibition of the protein-protein interaction between the leukemia-associated proteins Runx1 and CBFbeta." Chem Biol **14**(10): 1186-1197.

Grembecka, J., S. He, et al. (2012). "Menin-MLL inhibitors reverse oncogenic activity of MLL fusion proteins in leukemia." Nat Chem Biol **8**(3): 277-284.

Grisolano, J. L., J. O'Neal, et al. (2003). "An activated receptor tyrosine kinase, TEL/PDGFbetaR, cooperates with AML1/ETO to induce acute myeloid leukemia in mice." Proc Natl Acad Sci U S A **100**(16): 9506-9511.

Growney, J. D., H. Shigematsu, et al. (2005). "Loss of Runx1 perturbs adult hematopoiesis and is associated with a myeloproliferative phenotype." Blood **106**(2): 494-504.

Guan, Y., B. Gerhard, et al. (2003). "Detection, isolation, and stimulation of quiescent primitive leukemic progenitor cells from patients with acute myeloid leukemia (AML)." Blood **101**(8): 3142-3149.

Hamburger, A. W. and S. E. Salmon (1977). "Primary bioassay of human tumor stem cells." Science **197**(4302): 461-463.

Hart, S. M. and L. Foroni (2002). "Core binding factor genes and human leukemia." Haematologica **87**(12): 1307-1323.

He, S., T. J. Senter, et al. (2014). "High-affinity small-molecule inhibitors of the menin-mixed lineage leukemia (MLL) interaction closely mimic a natural protein-protein interaction." J Med Chem **57**(4): 1543-1556.

Heuser, M., H. Yun, et al. (2011). "Cell of origin in AML: susceptibility to MN1-induced transformation is regulated by the MEIS1/AbdB-like HOX protein complex." Cancer Cell **20**(1): 39-52.

Higuchi, M., D. O'Brien, et al. (2002). "Expression of a conditional AML1-ETO oncogene bypasses embryonic lethality and establishes a murine model of human t(8;21) acute myeloid leukemia." Cancer Cell **1**(1): 63-74.

Hock, H., M. J. Hamblen, et al. (2003). "Intrinsic requirement for zinc finger transcription factor Gfi-1 in neutrophil differentiation." Immunity **18**(1): 109-120.

Holtschke, T., J. Lohler, et al. (1996). "Immunodeficiency and chronic myelogenous leukemia-like syndrome in mice with a targeted mutation of the ICSBP gene." Cell **87**(2): 307-317.

Hu, Y. and G. K. Smyth (2009). "ELDA: extreme limiting dilution analysis for comparing depleted and enriched populations in stem cell and other assays." J Immunol Methods **347**(1-2): 70-78.

Huang, G., K. Shigesada, et al. (2001). "Dimerization with PEBP2beta protects RUNX1/AML1 from ubiquitin-proteasome-mediated degradation." EMBO J **20**(4): 723-733.

Huang, X., J. W. Peng, et al. (1999). "Solution structure of core binding factor beta and map of the CBF alpha binding site." Nat Struct Biol **6**(7): 624-627.

Ichikawa, M., T. Asai, et al. (2004). "AML-1 is required for megakaryocytic maturation and lymphocytic differentiation, but not for maintenance of hematopoietic stem cells in adult hematopoiesis." Nat Med **10**(3): 299-304.

Ichikawa, M., S. Goyama, et al. (2008). "AML1/Runx1 negatively regulates quiescent hematopoietic stem cells in adult hematopoiesis." J Immunol **180**(7): 4402-4408.

Irie-Sasaki, J., T. Sasaki, et al. (2001). "CD45 is a JAK phosphatase and negatively regulates cytokine receptor signalling." Nature **409**(6818): 349-354.

Ishikawa, F., S. Yoshida, et al. (2007). "Chemotherapy-resistant human AML stem cells home to and engraft within the bone-marrow endosteal region." Nat Biotechnol **25**(11): 1315-1321.

Jacob, B., M. Osato, et al. (2010). "Stem cell exhaustion due to Runx1 deficiency is prevented by Evi5 activation in leukemogenesis." Blood **115**(8): 1610-1620.

Kagoshima, H., Y. Akamatsu, et al. (1996). "Functional dissection of the alpha and beta subunits of transcription factor PEBP2 and the redox susceptibility of its DNA binding activity." J Biol Chem **271**(51): 33074-33082.

Kamikubo, Y., L. Zhao, et al. (2010). "Accelerated leukemogenesis by truncated CBF beta-SMMHC defective in high-affinity binding with RUNX1." Cancer Cell **17**(5): 455-468.

Kiel, M. J., O. H. Yilmaz, et al. (2005). "SLAM family receptors distinguish hematopoietic stem and progenitor cells and reveal endothelial niches for stem cells." Cell **121**(7): 1109-1121.

Kiel, M. J., O. H. Yilmaz, et al. (2008). "CD150- cells are transiently reconstituting multipotent progenitors with little or no stem cell activity." Blood **111**(8): 4413-4414; author reply 4414-4415.

Kim, W. Y., M. Sieweke, et al. (1999). "Mutual activation of Ets-1 and AML1 DNA binding by direct interaction of their autoinhibitory domains." EMBO J **18**(6): 1609-1620.

Kondo, M., I. L. Weissman, et al. (1997). "Identification of clonogenic common lymphoid progenitors in mouse bone marrow." Cell **91**(5): 661-672.

Kumaravelu, P., L. Hook, et al. (2002). "Quantitative developmental anatomy of definitive haematopoietic stem cells/long-term repopulating units (HSC/RUs): role of the aorta-gonad-mesonephros (AGM) region and the yolk sac in colonisation of the mouse embryonic liver." Development **129**(21): 4891-4899.

Kundu, M., A. Chen, et al. (2002). "Role of Cbfb in hematopoiesis and perturbations resulting from expression of the leukemogenic fusion gene Cbfb-MYH11." Blood **100**(7): 2449-2456.

Kwok, C., B. B. Zeisig, et al. (2010). "The role of CBFbeta in AML1-ETO's activity." Blood **115**(15): 3176-3177.

Kwok, C., B. B. Zeisig, et al. (2009). "Transforming activity of AML1-ETO is independent of CBFbeta and ETO interaction but requires formation of homo-oligomeric complexes." Proc Natl Acad Sci U S A **106**(8): 2853-2858.

Lam, K. and D. E. Zhang (2012). "RUNX1 and RUNX1-ETO: roles in hematopoiesis and leukemogenesis." Front Biosci (Landmark Ed) **17**: 1120-1139.

Latchman, D. S. (1997). "Transcription factors: an overview." Int J Biochem Cell Biol **29**(12): 1305-1312.

Li, Z., S. M. Lukasik, et al. (2006). "A mutation in the S-switch region of the Runt domain alters the dynamics of an allosteric network responsible for CBFbeta regulation." J Mol Biol **364**(5): 1073-1083.

Link, K. A., F. S. Chou, et al. (2010). "Core binding factor at the crossroads: determining the fate of the HSC." J Cell Physiol **222**(1): 50-56.

Liu, X., Q. Zhang, et al. (2009). "Overexpression of an isoform of AML1 in acute leukemia and its potential role in leukemogenesis." Leukemia **23**(4): 739-745.

Lo, M. C. and L. F. Peterson (2013). "Combined gene expression and DNA occupancy profiling as a strategy to identify therapeutic target(s) in t(8;21) acute myeloid leukemia." Crit Rev Eukaryot Gene Expr **23**(2): 103-113.

Lorenz, E., D. Uphoff, et al. (1951). "Modification of irradiation injury in mice and guinea pigs by bone marrow injections." J Natl Cancer Inst **12**(1): 197-201.

Lorsbach, R. B., J. Moore, et al. (2004). "Role of RUNX1 in adult hematopoiesis: analysis of RUNX1-IRES-GFP knock-in mice reveals differential lineage expression." Blood **103**(7): 2522-2529.

Lutterbach, B., J. J. Westendorf, et al. (1998). "ETO, a target of t(8;21) in acute leukemia, interacts with the N-CoR and mSin3 corepressors." Mol Cell Biol **18**(12): 7176-7184.

Makino, S. (1959). "The role of tumor stem-cells in regrowth of the tumor following drastic applications." Acta Unio Int Contra Cancrum **15(Suppl 1)**: 196-198.

McGrath, K. E., A. D. Koniski, et al. (2003). "Circulation is established in a stepwise pattern in the mammalian embryo." Blood **101**(5): 1669-1676.

Medvinsky, A. and E. Dzierzak (1996). "Definitive hematopoiesis is autonomously initiated by the AGM region." Cell **86**(6): 897-906.

Medvinsky, A., S. Rybtsov, et al. (2011). "Embryonic origin of the adult hematopoietic system: advances and questions." Development **138**(6): 1017-1031.

Medvinsky, A. L., N. L. Samoylina, et al. (1993). "An early pre-liver intraembryonic source of CFU-S in the developing mouse." Nature **364**(6432): 64-67.

Mendoza-Villanueva, D., W. Deng, et al. (2010). "The Runx transcriptional co-activator, CBFbeta, is essential for invasion of breast cancer cells." Mol Cancer **9**: 171.

Metcalf, D. (2007). "Concise review: hematopoietic stem cells and tissue stem cells: current concepts and unanswered questions." Stem Cells **25**(10): 2390-2395.

Mikkola, H. K., J. Klintman, et al. (2003). "Haematopoietic stem cells retain long-term repopulating activity and multipotency in the absence of stem-cell leukaemia SCL/tal-1 gene." Nature **421**(6922): 547-551.

Miller, J. D., T. Stacy, et al. (2001). "Core-binding factor beta (CBFbeta), but not CBFbeta-smooth muscle myosin heavy chain, rescues definitive hematopoiesis in CBFbeta-deficient embryonic stem cells." Blood **97**(8): 2248-2256.

Miyoshi, H., K. Shimizu, et al. (1991). "t(8;21) breakpoints on chromosome 21 in acute myeloid leukemia are clustered within a limited region of a single gene, AML1." Proc Natl Acad Sci U S A **88**(23): 10431-10434.

Morrison, S. J., N. Uchida, et al. (1995). "The biology of hematopoietic stem cells." Annu Rev Cell Dev Biol **11**: 35-71.

Motoda, L., M. Osato, et al. (2007). "Runx1 protects hematopoietic stem/progenitor cells from oncogenic insult." Stem Cells **25**(12): 2976-2986.

Mulloy, J. C., J. Cammenga, et al. (2003). "Maintaining the self-renewal and differentiation potential of human CD34+ hematopoietic cells using a single genetic element." Blood **102**(13): 4369-4376.

Naoe, Y., R. Setoguchi, et al. (2007). "Repression of interleukin-4 in T helper type 1 cells by Runx/Cbf beta binding to the Il4 silencer." J Exp Med **204**(8): 1749-1755.

Niki, M., H. Okada, et al. (1997). "Hematopoiesis in the fetal liver is impaired by targeted mutagenesis of a gene encoding a non-DNA binding subunit of the transcription factor, polyomavirus enhancer binding protein 2/core binding factor." Proc Natl Acad Sci U S A **94**(11): 5697-5702.

North, T., T. L. Gu, et al. (1999). "Cbfa2 is required for the formation of intra-aortic hematopoietic clusters." Development **126**(11): 2563-2575.

North, T. E., T. Stacy, et al. (2004). "Runx1 is expressed in adult mouse hematopoietic stem cells and differentiating myeloid and lymphoid cells, but not in maturing erythroid cells." Stem Cells **22**(2): 158-168.

Ogawa, E., M. Inuzuka, et al. (1993). "Molecular cloning and characterization of PEBP2 beta, the heterodimeric partner of a novel Drosophila runt-related DNA binding protein PEBP2 alpha." Virology **194**(1): 314-331.

Oguro, H., L. Ding, et al. (2013). "SLAM family markers resolve functionally distinct subpopulations of hematopoietic stem cells and multipotent progenitors." Cell Stem Cell **13**(1): 102-116.

Okada, H., T. Watanabe, et al. (1998). "AML1(-/-) embryos do not express certain hematopoiesis-related gene transcripts including those of the PU.1 gene." Oncogene **17**(18): 2287-2293.

Okuda, T., Z. Cai, et al. (1998). "Expression of a knocked-in AML1-ETO leukemia gene inhibits the establishment of normal definitive hematopoiesis and directly generates dysplastic hematopoietic progenitors." Blood **91**(9): 3134-3143.

Okuda, T., J. van Deursen, et al. (1996). "AML1, the target of multiple chromosomal translocations in human leukemia, is essential for normal fetal liver hematopoiesis." Cell **84**(2): 321-330.

Orkin, S. H. and L. I. Zon (2008). "Hematopoiesis: an evolving paradigm for stem cell biology." Cell **132**(4): 631-644.

Osawa, M., K. Hanada, et al. (1996). "Long-term lymphohematopoietic reconstitution by a single CD34-low/negative hematopoietic stem cell." Science **273**(5272): 242-245.

Park, S., N. A. Speck, et al. (2009). "The role of CBFbeta in AML1-ETO's activity." Blood **114**(13): 2849-2850.

Penninger, J. M., J. Irie-Sasaki, et al. (2001). "CD45: new jobs for an old acquaintance." Nat Immunol **2**(5): 389-396.

Redondo, J. M., J. L. Pfohl, et al. (1992). "Indistinguishable nuclear factor binding to functional core sites of the T-cell receptor delta and murine leukemia virus enhancers." Mol Cell Biol **12**(11): 4817-4823.

Rhoades, K. L., C. J. Hetherington, et al. (2000). "Analysis of the role of AML1-ETO in leukemogenesis, using an inducible transgenic mouse model." Blood **96**(6): 2108-2115.

Rhodes, J., A. Hagen, et al. (2005). "Interplay of pu.1 and gata1 determines myelo-erythroid progenitor cell fate in zebrafish." Dev Cell **8**(1): 97-108.

Rosenbauer, F. and D. G. Tenen (2007). "Transcription factors in myeloid development: balancing differentiation with transformation." Nat Rev Immunol **7**(2): 105-117.

Roudaia, L., M. D. Cheney, et al. (2009). "CBFbeta is critical for AML1-ETO and TEL-AML1 activity." Blood **113**(13): 3070-3079.

Salmon, S. E., A. W. Hamburger, et al. (1978). "Quantitation of differential sensitivity of human-tumor stem cells to anticancer drugs." N Engl J Med **298**(24): 1321-1327.

Sasaki, K., H. Yagi, et al. (1996). "Absence of fetal liver hematopoiesis in mice deficient in transcriptional coactivator core binding factor beta." Proc Natl Acad Sci U S A **93**(22): 12359-12363.

Schindler, J. W., D. Van Buren, et al. (2009). "TEL-AML1 corrupts hematopoietic stem cells to persist in the bone marrow and initiate leukemia." Cell Stem Cell **5**(1): 43-53.

Schwieger, M., J. Lohler, et al. (2002). "AML1-ETO inhibits maturation of multiple lymphohematopoietic lineages and induces myeloblast transformation in synergy with ICSBP deficiency." J Exp Med **196**(9): 1227-1240.

Shivdasani, R. A., E. L. Mayer, et al. (1995). "Absence of blood formation in mice lacking the T-cell leukaemia oncoprotein tal-1/SCL." Nature **373**(6513): 432-434.

Shoemaker, S. G., R. Hromas, et al. (1990). "Transcriptional regulation of interleukin 3 gene expression in T lymphocytes." Proc Natl Acad Sci U S A **87**(24): 9650-9654.

Silver, D. P. and D. M. Livingston (2001). "Self-excising retroviral vectors encoding the Cre recombinase overcome Cre-mediated cellular toxicity." Mol Cell **8**(1): 233-243.

Smith, L. L., J. Yeung, et al. (2011). "Functional crosstalk between Bmi1 and MLL/Hoxa9 axis in establishment of normal hematopoietic and leukemic stem cells." Cell Stem Cell **8**(6): 649-662.

So, C. W., H. Karsunky, et al. (2003). "MLL-GAS7 transforms multipotent hematopoietic progenitors and induces mixed lineage leukemias in mice." Cancer Cell **3**(2): 161-171.

Sroczynska, P., C. Lancrin, et al. (2009). "The differential activities of Runx1 promoters define milestones during embryonic hematopoiesis." Blood **114**(26): 5279-5289.

Takahashi, A., M. Satake, et al. (1995). "Positive and negative regulation of granulocyte-macrophage colony-stimulating factor promoter activity by AML1-related transcription factor, PEBP2." Blood **86**(2): 607-616.

Talebian, L., Z. Li, et al. (2007). "T-lymphoid, megakaryocyte, and granulocyte development are sensitive to decreases in CBFbeta dosage." Blood **109**(1): 11-21.

Tang, Y. Y., B. E. Crute, et al. (2000). "Biophysical characterization of interactions between the core binding factor alpha and beta subunits and DNA." FEBS Lett **470**(2): 167-172.

Taniuchi, I., M. Osato, et al. (2002). "Differential requirements for Runx proteins in CD4 repression and epigenetic silencing during T lymphocyte development." Cell **111**(5): 621-633.

Tighe, J. E. and F. Calabi (1994). "Alternative, out-of-frame runt/MTG8 transcripts are encoded by the derivative (8) chromosome in the t(8;21) of acute myeloid leukemia M2." Blood **84**(7): 2115-2121.

Tighe, J. E. and F. Calabi (1995). "t(8;21) breakpoints are clustered between alternatively spliced exons of MTG8." Clin Sci (Lond) **89**(3): 215-218.

Till, J. E. and C. E. Mc (1961). "A direct measurement of the radiation sensitivity of normal mouse bone marrow cells." Radiat Res **14**: 213-222.

Tsuzuki, S., D. Hong, et al. (2007). "Isoform-specific potentiation of stem and progenitor cell engraftment by AML1/RUNX1." PLoS Med **4**(5): e172.

Wang, C. Q., D. W. Chin, et al. (2015). "Cbfb deficiency results in differentiation blocks and stem/progenitor cell expansion in hematopoiesis." Leukemia **29**(3): 753-757.

Wang, J., T. Hoshino, et al. (1998). "ETO, fusion partner in t(8;21) acute myeloid leukemia, represses transcription by interaction with the human N-CoR/mSin3/HDAC1 complex." Proc Natl Acad Sci U S A **95**(18): 10860-10865.

Wang, Q., T. Stacy, et al. (1996). "Disruption of the Cbfa2 gene causes necrosis and hemorrhaging in the central nervous system and blocks definitive hematopoiesis." Proc Natl Acad Sci U S A **93**(8): 3444-3449.

Wang, Q., T. Stacy, et al. (1996). "The CBFbeta subunit is essential for CBFalpha2 (AML1) function in vivo." Cell **87**(4): 697-708.

Wang, S., Q. Wang, et al. (1993). "Cloning and characterization of subunits of the T-cell receptor and murine leukemia virus enhancer core-binding factor." Mol Cell Biol **13**(6): 3324-3339.

Wang, Y. Y., L. J. Zhao, et al. (2011). "C-KIT mutation cooperates with full-length AML1-ETO to induce acute myeloid leukemia in mice." Proc Natl Acad Sci U S A **108**(6): 2450-2455.

Warren, A. J., J. Bravo, et al. (2000). "Structural basis for the heterodimeric interaction between the acute leukaemia-associated transcription factors AML1 and CBFbeta." EMBO J **19**(12): 3004-3015.

Weissman, I. L., D. J. Anderson, et al. (2001). "Stem and progenitor cells: origins, phenotypes, lineage commitments, and transdifferentiations." Annu Rev Cell Dev Biol **17**: 387-403.

Yamanaka, R., C. Barlow, et al. (1997). "Impaired granulopoiesis, myelodysplasia, and early lethality in CCAAT/enhancer binding protein epsilon-deficient mice." Proc Natl Acad Sci U S A **94**(24): 13187-13192.

Yan, J., Y. Liu, et al. (2004). "CBFbeta allosterically regulates the Runx1 Runt domain via a dynamic conformational equilibrium." Nat Struct Mol Biol **11**(9): 901-906.

Yan, M., S. A. Burel, et al. (2004). "Deletion of an AML1-ETO C-terminal NcoR/SMRT-interacting region strongly induces leukemia development." Proc Natl Acad Sci U S A **101**(49): 17186-17191.

Yan, M., E. Kanbe, et al. (2006). "A previously unidentified alternatively spliced isoform of t(8;21) transcript promotes leukemogenesis." Nat Med **12**(8): 945-949.

Yang, L., D. Bryder, et al. (2005). "Identification of Lin(-)Sca1(+)kit(+)CD34(+)Flt3- short-term hematopoietic stem cells capable of rapidly reconstituting and rescuing myeloablated transplant recipients." Blood **105**(7): 2717-2723.

Yeh, J. R., K. M. Munson, et al. (2008). "AML1-ETO reprograms hematopoietic cell fate by downregulating scl expression." Development **135**(2): 401-410.

Yergeau, D. A., C. J. Hetherington, et al. (1997). "Embryonic lethality and impairment of haematopoiesis in mice heterozygous for an AML1-ETO fusion gene." Nat Genet **15**(3): 303-306.

Yeung, J., M. T. Esposito, et al. (2010). "beta-Catenin mediates the establishment and drug resistance of MLL leukemic stem cells." Cancer Cell **18**(6): 606-618.

Yeung, J. and C. W. So (2009). "Identification and characterization of hematopoietic stem and progenitor cell populations in mouse bone marrow by flow cytometry." Methods Mol Biol **538**: 301-315.

Yuan, Y., L. Zhou, et al. (2001). "AML1-ETO expression is directly involved in the development of acute myeloid leukemia in the presence of additional mutations." Proc Natl Acad Sci U S A **98**(18): 10398-10403.

Zeisig, B. B., A. G. Kulasekararaj, et al. (2012). "SnapShot: Acute myeloid leukemia." Cancer Cell **22**(5): 698-698 e691.

Zeisig, B. B. and C. W. So (2009). "Retroviral/Lentiviral transduction and transformation assay." Methods Mol Biol **538**: 207-229.

Zhang, D. E., K. Fujioka, et al. (1994). "Identification of a region which directs the monocytic activity of the colony-stimulating factor 1 (macrophage colony-stimulating factor) receptor promoter and binds PEBP2/CBF (AML1)." Mol Cell Biol **14**(12): 8085-8095.

Zhang, D. E., P. Zhang, et al. (1997). "Absence of granulocyte colony-stimulating factor signaling and neutrophil development in CCAAT enhancer binding protein alpha-deficient mice." Proc Natl Acad Sci U S A **94**(2): 569-574.

Zhang, J., B. A. Hug, et al. (2001). "Oligomerization of ETO is obligatory for corepressor interaction." Mol Cell Biol **21**(1): 156-163.

Zhang, J., M. Kalkum, et al. (2004). "E protein silencing by the leukemogenic AML1-ETO fusion protein." Science **305**(5688): 1286-1289.

Zhang, L., S. M. Lukasik, et al. (2003). "Structural and functional characterization of Runx1, CBF beta, and CBF beta-SMMHC." Blood Cells Mol Dis **30**(2): 147-156.

Zhang, P., J. Iwasaki-Arai, et al. (2004). "Enhancement of hematopoietic stem cell repopulating capacity and self-renewal in the absence of the transcription factor C/EBP alpha." Immunity **21**(6): 853-863.

Zhang, Y., P. Strissel, et al. (2002). "Genomic DNA breakpoints in AML1/RUNX1 and ETO cluster with topoisomerase II DNA cleavage and DNase I hypersensitive sites in t(8;21) leukemia." Proc Natl Acad Sci U S A **99**(5): 3070-3075.

**References**

Zhao, S., Y. Zhang, et al. (2014). "KRAS (G12D) cooperates with AML1/ETO to initiate a mouse model mimicking human acute myeloid leukemia." Cell Physiol Biochem **33**(1): 78-87.